Safety Standards

of the
Nuclear Safety Standards Commission (KTA)

KTA 3206 (2014-11)

Break Preclusion Verifications for Pressure-Retaining Components in Nuclear Power Plants

(Nachweise zum Bruchausschluss für druckführende Komponenten in Kernkraftwerken)

This version includes the corrections from 11/2015 and 12/2019.

If there is any doubt regarding the information contained in this translation, the German wording shall apply.

Editor:

KTA-Geschaeftsstelle

c/o Bundesamt fuer kerntechnische Entsorgungssicherheit (BfE)

Willy-Brandt-Str. 5 • 38226 Salzgitter • Germany

Telephone +49 (0) 30 18333-1621 • Telefax +49 (0) 30 18333-1625

KTA SAFETY STANDARD

November 2014	**Break Preclusion Verifications for Pressure-Retaining Components in Nuclear Power Plants**	KTA 3206

Contents

PLEASE NOTE: Only the original German version of this safety standard represents the joint resolution of the 35-member Nuclear Safety Standards Commission (Kerntechnischer Ausschuss, KTA). The German version was made public in the Federal Gazette (Bundesanzeiger) on February 5, 2018. Copies of the German versions of the KTA safety standards may be mail-ordered through the Wolters Kluwer Deutschland GmbH (info@wolterskluwer.de). Downloads of the English translations are available at the KTA website (http://www.kta-gs.de).

All questions regarding this English translation should please be directed to the KTA office:
KTA-Geschaeftsstelle c/o BfE, Willy-Brandt-Strasse 5, D-38226 Salzgitter, Germany or kta-gs@bfe.bund.de

Comments by the editor:

Taking into account the meaning and usage of auxiliary verbs in the German language, in this translation the following agreements are effective:

shall	indicates a mandatory requirement,
shall basically	is used in the case of mandatory requirements to which specific exceptions (and only those!) are permitted. It is a requirement of the KTA that these exceptions - other than those in the case of **shall normally** - are specified in the text of the safety standard,
shall normally	indicates a requirement to which exceptions are allowed. However, the exceptions used, shall be substantiated during the licensing procedure,
should	indicates a recommendation or an example of good practice,
may	indicates an acceptable or permissible method within the scope of this safety standard.

Fundamentals

(1) The safety standards of the Nuclear Safety Standards Commission (KTA) have the objective to specify safety-related requirements, compliance of which provides the necessary precautions in accordance with the state of the art in science and technology against damage arising from the construction and operation of the facility (Sec. 7 para. 2 subpara. 3 Atomic Energy Act - AtG) in order to achieve the fundamental safety functions specified in the Atomic Energy Act and the Radiological Protection Ordinance (StrlSchV) and further detailed in the Safety Requirements for Nuclear Power Plants as well as in the Interpretations on the Safety Requirements for Nuclear Power Plants.

(2) As regards the design, fabrication, erection and inspection as well as operation and maintenance of the safety-relevant plant components, No. 3.1 (1) of the Safety Requirements for Nuclear Power Plants requires that such principles and procedures are applied which meet the special safety requirements of nuclear technology.

Safety requirement No. 3.4 (1) requires that the reactor coolant pressure boundary is constructed, arranged and operated such that the occurrence of rapidly extending cracks and of brittle fractures need not be assumed.

For the components of the primary circuit the requirements of the aforementioned safety requirements are comprehensively concretized by the following safety standards:

KTA 3201.1 Materials and Product Forms

KTA 3201.2 Design and Analysis

KTA 3201.3 Manufacture

KTA 3201.4 In-service Inspections and Operational Monitoring

as well as

KTA 3203 Surveillance of the Irradiation Behaviour of Reactor Pressure Vessel Materials of LWR Facilities

KTA 3205.1 Component-Support Structures with Non-Integral Connections;
Part 1: Component-Support Structures with Non-Integral Connections for Components of the Reactor Coolant Pressure Boundary of Light Water Reactors.

For systems outside the primary circuit the requirements are concretized in the following safety standards:

KTA 3211.1 Pressure- and activity-retaining components of systems outside the primary circuit;
Part 1: Materials

KTA 3211.2 Pressure- and activity-retaining components of systems outside the primary circuit;
Part 2: Design and Analysis

KTA 3211.3 Pressure- and activity-retaining components of systems outside the primary circuit;
Part 3: Manufacture

KTA 3211.4 Pressure- and activity-retaining components of systems outside the primary circuit;
Part 4: In-service Inspections and Operational Monitoring

KTA 3205.2 Component-Support Structures with Non-Integral Connections;
Part 2: Component-Support Structures with Non-Integral Connections for Pressure- and Activity-Retaining Components of Systems Outside the Primary Circuit

Note:
This KTA safety standard refers to both the standard series of KTA 3201 and the standard series of KTA 3211, where the KTA 3201 standard series shall apply to primary circuit components and KTA 3211 standard series to components outside the primary circuit respectively.

According to safety requirement No. 3.4 (4) restricted leak and break assumptions may be claimed for piping systems and components of the reactor coolant pressure boundary and for pressure-retaining walls of components outside the primary circuit for which, within the design concept, catastrophic failure need not be assumed during plant operation. For these piping systems and components a verification is required that defects to be assumed in pressure-retaining walls cannot lead to a leak or rupture of the piping system or component which put the restricted leak and break assumptions into question.

KTA safety standard 3206 “Break preclusion verifications for pressure-retaining components in nuclear power plants” is intended to concretize these measures and verifications within its range of application.

(3) The task of this safety standard is to determine the procedures for break preclusion verification and to include requirements for the:

a) assessment of quality upon design and manufacture
b) safeguarding of quality during operation
   ba) proof of quality ascertained during previous operation
   bb) safeguarding of the required quality for further operation
c) calculation process for evaluating postulated cracks and manufacturing defects.

(4) The general quality assurance requirements are laid down in KTA 1401. In addition, the specific quality-relevant requirements laid down in KTA safety standard series 3201 and 3211 shall be observed. Special quality assurance requirements which are to be observed for break preclusion verifications are laid down individually in this standard. KTA safety standard 1403 lays down technical and organisational measures for early identification of ageing phenomena relevant to nuclear power plant safety and for maintaining as-required quality conditions.

1 Scope

This safety standard shall be applied to pressure-retaining components and systems in nuclear power plants with light-water reactors for which restricted break and leak assumptions (break preclusion) are assumed, especially with reference to reaction and jet forces on pipes, components, component internals, electrical equipment inside the containment and parts of buildings.

2 Definitions

(1) Basis Safety

The basis safety of a plant part is subject to the following requirements:

a) high-quality material properties, especially toughness
b) conservative stress limitation
c) avoidance of peak stresses by optimum design
d) guarantee of application of optimized manufacturing and inspection technologies
e) knowledge and evaluation of defect conditions, if any
f) consideration of service fluid environmental conditions

Where the requirements laid down in KTA safety standards KTA 3201.1 to KTA 3201.3 and KTA 3211.1 to KTA 3211.3 respectively are observed, component basis safety will be obtained to exclude catastrophic failure of a plant part due to manufacturing defects.

(2) Basis safety concept

The basis safety concept lays down four further principles (so-called independent redundancies) in addition to the basis safety

a) multiple testing principle, e.g. independent quality assurance,
b) worst-case-principle, e.g. consideration of most unfavourable conditions according to the current state of knowledge,
c) principle of plant monitoring and documentation, e.g. monitoring of operational parameters relevant to component integrity, in-service inspections,
d) verification principle, e.g. experimental verification of the procedures applied.

These principles are technical requirements which justify the application of break preclusion (restricted leak and break assumptions for the leak postulate 0.1F covering such assumptions or for values less than 0.1F based on fracture-mechanical evaluations instead of the break postulate 2F).

(3) Break preclusion

Break preclusion means the preclusion of

a) instable failure and
b) excess of pre-determined leak size

of a pressure-retaining component under given boundary conditions over the total operational lifetime by means of deterministic procedures.

(4) Resistance to fracture

Resistance to fracture means the safety against failure by instable crack propagation.

(5) Integrity

Integrity is the condition of a component or barrier at which the safety requirements with regard to strength, resistance to fracture and leak tightness are met.

(6) Integrity concept

The integrity concept is the further development of the basis safety concept by concretizing the measures and verifications for safeguarding the quality required for the integrity of a component or system over its total operational lifetime. The integrity concept comprises the:

a) proof of the as-required quality upon design and manufacture (basis safety),
b) proof of the existing quality upon previous operation,
c) safeguarding of the required quality for further operation.

(7) Leak-before-break (LBB)

Leak-before-break means the property of a pressure-retaining system area which ensures that a through-thickness crack is sub-critical to instability under all operational and accident loadings and that a leak arising from such through-thickness crack is detected in time under the operational loadings of steady-state operation so that intervention of plant operation is ensured before global component failure occurs.

(8) Quality, required

Required quality means the condition of a part, component or system with respect to their capability of meeting the specified requirements.

(9) Damage mechanisms

Damage mechanisms are all physical, chemical and biological processes which may impair the integrity or function of a component.

3 Basic requirements for components with break preclusion

(1) Break preclusion is subject to the application of the integrity concept (**Figure 3-1**).

(2) Where the verifications are made and measures are taken required according to the integrity concept respectively, **Figure 3-1**, restricted break and leak assumptions can be utilized for the components and systems considered.

(3) The integrity of the components and systems of the reactor coolant pressure boundary and the systems outside the primary circuit for which restricted break and leak assumption are utilized shall be ensured by a complete concept (integrity concept) acc. to section 3 of KTA 3201.4 over the total operational lifetime.

Note:
This safety standard contains requirements and supplementary specifications in excess of the requirements laid down by KTA 3201.4.

(4) The requirements for basis safety are to be met.

(5) The toughness of ferritic steels shall meet the requirements of KTA 3201.1, subpara. 3.2.4.2 (6) or KTA 3211.1, para. 4.3.1 unless the criteria of A 1 (2) or A 1 (4) are to be applied.

(6) The relevant damage mechanisms determined to KTA 1403, para 4.1.2 and their effects on integrity shall be shown in relation to the respective component, be evaluated as regards their causes and consequences and be limited by taking suitable measures such that the quality is not inadmissibly affected.

(7) As regards operation, the design and construction shall ensure that corrosive damage mechanisms, especially crack-forming corrosion, such as stress corrosion cracking (SCC) or strain-induced corrosion (SIC), relevant vibration loads, (e.g. steady-state vibrations, resonant vibrations) need not be assumed. In addition, the design, manufacture and optimized operating mode shall ensure that no non-specified effects, especially short-time dynamic loadings (e.g. due to water hammer, transient condensation shocks) need be assumed.

The effectiveness of the measures taken shall be checked during manufacture, commissioning as well as operation.

(8) Where the state of knowledge as regards safeguarding of component integrity during operation is changed (see KTA 3201.4, Figure 3-1), the changes shall be evaluated with respect to the properties relevant to break preclusion and measures be taken, where required.

Note:
This may also be documented within a status report to be established acc. to KTA 1403.

(9) In case of service-induced relevant indications (consequences of operational damage mechanisms) one of the criteria mentioned under (6) and (7) is no more satisfied. In such a case it is required to

a) determine and eliminate the causes of the effective damage mechanisms,
b) establish anew the measures to be taken for meeting the requirements for break preclusion.

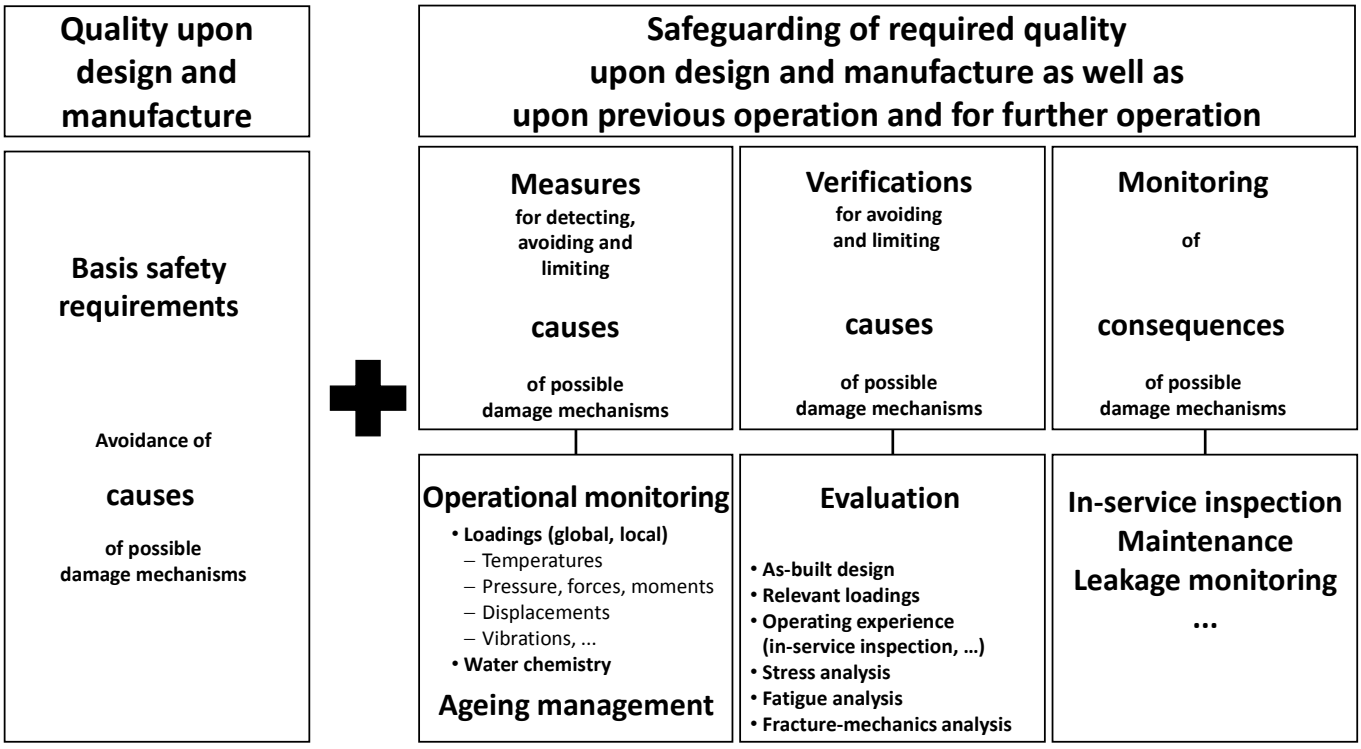

Figure 3-1: Essential elements of the integrity concept

4 Procedure for demonstration of break preclusion

4.1 Required demonstrations

The following shall be demonstrated:

a) Proof of quality upon design and manufacture (basis safety) to section 4.2,

b) Proof of existing quality upon previous operation to section 4.3,

c) Proof of safeguarding of the required quality for further operation to section 4.4.

4.2 Proof of quality upon design and manufacture

(1) The components and systems shall be described and it shall be demonstrated that they satisfy the general principles of Section 3. The records shall contain any data relevant to the verification objective and include at least:

a) design data sheets and pipe loading specifications acc. to KTA 3201.3, Table 4-2 or KTA 3211.3, Table 4-3,

b) water chemistry (chemical and physical values to be observed, type and extent of monitoring),

c) pipework isometric drawings, fabrication drawings,

d) manufacturing processes and product forms for the purpose of evaluating their possible influences on material properties or damage mechanisms,

e) location and type of welds,

f) material properties of product forms and welds (including heat treatment as well as results of welding procedure qualifications and production control tests),

g) design and location of component support structures,

h) stress, fatigue and fracture mechanics analyses,

i) information on non-destructive testing during fabrication (test methods applied incl. recording levels and evaluation threshold, extent of testing) and on in-service inspections (test methods applied incl. recording levels and evaluation threshold, extent of testing and inspection intervals),

j) information of operational monitoring

ja) type and extent of monitoring of loadings (e.g. temperature, pressure, displacements, vibrations),

jb) leakage monitoring.

k) system and component related representation of damage mechanisms possible during operation and the causes of these damage mechanisms.

(2) For the analyses mentioned under (1) h) the relevant loadings shall be determined on the basis of the current loading level specifications. These shall also cover reaction forces from postulated leak assumptions (≤ 0.1F) which are assumed to occur at any weld location and highly loaded base material areas (especially at bends). Highly loaded base material areas are areas where one of the following criteria applies:

a) the utilization of allowable stresses to KTA 3201.2 or KTA 3211.2 in one of the loading levels A, B, C or D exceeds 80%.

b) The usage factor exceeds the fatigue attention values determined by KTA 3201.4.

(3) Where during commissioning of the component or system indications for possible non-specified loadings are found, e.g. dynamic (vibration) loadings, temperature differentials, thermal stratification, temperature asymmetries, restraint to thermal expansion, they shall be analysed and measures shall be taken to record, to evaluate and - where necessary - to minimise such loadings during operation.

(4) The as-built design of components and systems shall be described (manufacturing documents). Deviations from data given in the design documents to (1) shall be described separately. In this case, the following shall specifically be documented:

a) repair work performed,

b) defect condition upon manufacture.

(5) The as-built design (existing quality) of the components and systems shall be evaluated by comparison with the design requirements (required quality).

(6) Although no cracks need be assumed when satisfying the general principles of section 3, a fracture-mechanics analysis acc. to **Annex A** shall basically be performed. Criteria which when satisfied do not require fracture-mechanics verifications are given in **Annex A**.

(7) Manufacturing defects are permitted without further verification if they are below the acceptance levels to KTA 3201.3 upon performance of the pertinent non-destructive examinations.

Crack-like defects due to manufacturing are not permitted.

For non-crack-like defects exceeding the acceptance levels to KTA 3201.3 which are detected during manufacture and are to be left as they are (tolerance), the following applies:

a) the defect shall be postulated a crack and it shall be demonstrated by fracture mechanics verifications per Annex A, section A 4, that its crack growth potential is limited and that sufficient safety margin is available as regards its load bearing capacity,
b) monitoring within in-service inspections shall be laid down to ensure that the defects are not capable of growing during plant service lifetime within the required accuracy specific to the NDT analysis method used during the in-service inspection.

(8) Where break preclusion is to be assumed at a later point in time of operation the proof of quality upon design and manufacture acc. to (1) to (7) shall be made for these components prior to first assumption of break preclusion.

4.3 Proof of existing quality upon previous operation

(1) The existing quality shall be proved

a) for the first time upon completion of commissioning or first assumption of break preclusion during service lifetime, or
b) in case of changed boundary conditions or state of knowledge for safeguarding component integrity during operation (see KTA 3201.4, Figure 3-1) with respect to the properties relevant to break preclusion verification.

(2) The proof shall at least include:

a) the description and evaluation of the changes occurred compared to the manufacturing condition, i.e. changes in
   aa) the as-built design e.g. due to repair measures, replacement measures or changes of supports and supporting structures,
   ab) material properties,
   ac) the relevant loadings of specified normal operation and the loadings from postulated accidents, e.g. due to changes in specified loadings based on the results of operational monitoring or due to new knowledge gained regarding specified accidents,
   ad) the status of relevant indications, e.g. based on the results from in-service inspections,
   ae) the damage mechanisms possible during operation and their causes, e.g. due to new knowledge gained,
   af) the water chemistry, e.g. due to results obtained from operational monitoring,
   ag) leakage monitoring,
b) an evaluation of the operating experience made with own plants or comparable plants of other utilities as well as on account of the current state of knowledge.

(3) It shall be demonstrated that

a) the causes of damage mechanisms possible during operation can be kept under control and
b) under the concrete operating conditions (temperature, loading, water chemistry) no inadmissible consequences of possible operational damage mechanisms need be expected.

(4) When evaluating the material properties, the following shall be considered:

a) material data representative for the area to be evaluated (including data from acceptance tests),
b) type and extent of tests and inspections and inspection certificates,
c) results from research projects,
d) results from examinations on disassembled parts as well as
e) operating experience as regards damage mechanisms for the areas of base material, weld metal and heat affected zone.

(5) For the evaluation of the loadings of specified normal operation as per (2) ac) the loadings shall be determined based on

a) process data and
b) the evaluation of operational monitoring (e.g. temperature transients and thermal stratification, displacements, vibrations).

In the case of specified loadings it shall be checked by evaluating the respective operational monitoring data whether these specified loadings really cover the actually occurring loadings.

(6) The evaluation of the status of relevant indications shall be based on

a) manufacturing inspections,
b) in-service inspections (WKP),
c) special inspections (e.g. on the cause of information notices),
d) results obtained from research projects transferrable to the plant (e.g. as regards inspection procedures, detectability) and
e) results, if any, from destructive tests on disassembled parts.

(7) Where the evaluations as per (2) to (6) lead to changes in boundary conditions with an expected safety-relevant effect on the results of the verification of existing quality to section 4.2, the unchanged validity of the analyses performed shall be confirmed.

4.4 Safeguarding of the required quality for further operation

To ensure plant integrity during further operation

a) the causes and consequences of possible operational damage mechanisms shall be monitored and evaluated in accordance with KTA 3201.4.
b) the requirements for ageing management of components of group M1 to KTA 1403 shall be met.

5 Documentation and reporting system

(1) The results of the demonstrations to be performed to section 4 shall be documented.

(2) The documentation of quality upon design and manufacture shall at least contain:

a) the design and manufacturing documents as per 4.2 (1) a) to i) including the boundary conditions for the existing design type (design, supports, supporting structures, material properties, welds and welding procedures, repair work performed, deviations from design documents, status of relevant indications) as per 4.2 (4) with evaluation as per 4.2 (5),

b) the documentation of the safeguarding of the existing design with respect to relevant loadings, stress analysis, fatigue analysis, fracture mechanics analysis as per **Annex A**, cf. 4.2 (6) and (7),

c) the description of possible operational damage mechanisms as per 3 (6) and 4.2 (1) k),

d) measures for controlling possible operational damage mechanisms and thus safeguarding the quality during operation in accordance with the integrity concept including measures for verification of the boundary conditions established as per 4.2 (3),

e) the operational monitoring concept as regards monitoring measures of the causes and consequences of possible operational damage mechanisms (determination of operational monitoring measures) as per 4.2 (1) j).

(3) The documentation of the existing quality upon previous operation shall at least contain:

a) the description and evaluation of the as-built design compared to the manufacturing condition in accordance with 4.3 (2) on the basis of the actual state of knowledge (results obtained from monitoring of the causes and consequences of possible operational damage mechanisms with due consideration of the status of relevant indications and operating experience),

b) the description and evaluation of the changes in possible operational damage mechanisms and their causes compared to the manufacturing condition.

(4) The documentation of tests and inspections and operational monitoring measures within the reporting period for safeguarding the required quality for further operation shall at least contain:

a) a summary of the results obtained from the monitoring of the causes of possible damage mechanisms (results obtained from the monitoring of mechanical and thermal loadings, monitoring of water quality),

b) an evaluation of the results obtained from the monitoring of causes in due consideration of applied optimization measures such as mode of plant operation,

c) a summary of the results obtained from the monitoring of the consequences of possible operational damage mechanisms (e.g. from non-destructive testing, monitoring of loose parts, leakage monitoring),

d) the evaluation of the results obtained from the monitoring of the consequences of possible damage mechanisms (here especially the confirmation of the previous status of relevant indications),

e) the documentation of the observation of state of knowledge (e.g. evaluation and assessment of planned and unplanned occurrences and events in the own plant and in other plants, change of safety standards requirements).

(5) The effectiveness of the measures taken shall be documented.

Note:
This may also be documented within a status report to be established according to KTA 1403.

Annex A (normative)

Performance of fracture mechanics analysis

A 1 General requirements

(1) A fracture mechanics analysis shall basically be performed

a) for piping to section A 2 and

b) for pressure vessels as well as valve bodies and pump casings to section A 3

where cracks (see **Figures A-1** and **A-2**) are to be postulated at locations resulting in the smallest critical crack size. The postulated defects shall be assumed to occur on the surface and in the direction subject to the greatest crack loading.

(2) A fracture mechanics analysis to section A 2 is not required for piping satisfying one of the following criteria:

a) at loading level A the operating pressure is equal to or less than 2.0 MPa and the operating temperature is equal to or less than 100 °C (low-energy systems), or

b) the utilization time is equal to or less than 2% of the plant service lifetime, or

c) the nominal stress during specified normal operation is equal to or less than 50 N/mm^2 and the usage factor is equal to or less than the attention values laid down in KTA 3201.4.

(3) A fracture mechanics analysis to section A 3 is not required for pressure vessels satisfying the following criteria a) to c):

a) The proof of quality upon design and manufacture to section 4.2 has been rendered.

b) It has been proved that brittle failure need not be assumed. To this end, the required component toughness shall be proved by experimental investigations that represent the loading and material conditions as well as the manufacturing process of the component. These investigations shall cover all relevant operating conditions and defect conditions to be assessed.

Note:
For pressure vessels fabricated to meet basis safety requirements investigation programs were performed with which the fulfilment of criteria b) was proved, e.g. research project 1500 304 B, component safety (Phase II), summarized evaluation of the project, final report. Staatliche Materialprüfungsanstalt (MPA) University of Stuttgart, May 1991.

c) The usage factor determined for the end of operational lifetime is equal to or less than the attention values laid down in KTA 3201.4.

(4) A fracture mechanics analysis to section A 3 is not even required for pressure vessels satisfying one of the following criteria:

a) at loading level A for pressure vessels filled with water the operating pressure is equal to or less than 2.0 MPa and the operating temperature is equal to or less than 100 °C (low-energy systems), or

b) the utilization time is equal to or less than 2% of the plant service lifetime, or

c) the nominal stress during specified normal operation is equal to or less than 50 N/mm^2 and the usage factor is equal to or less than the attention values laid down in KTA 3201.4.

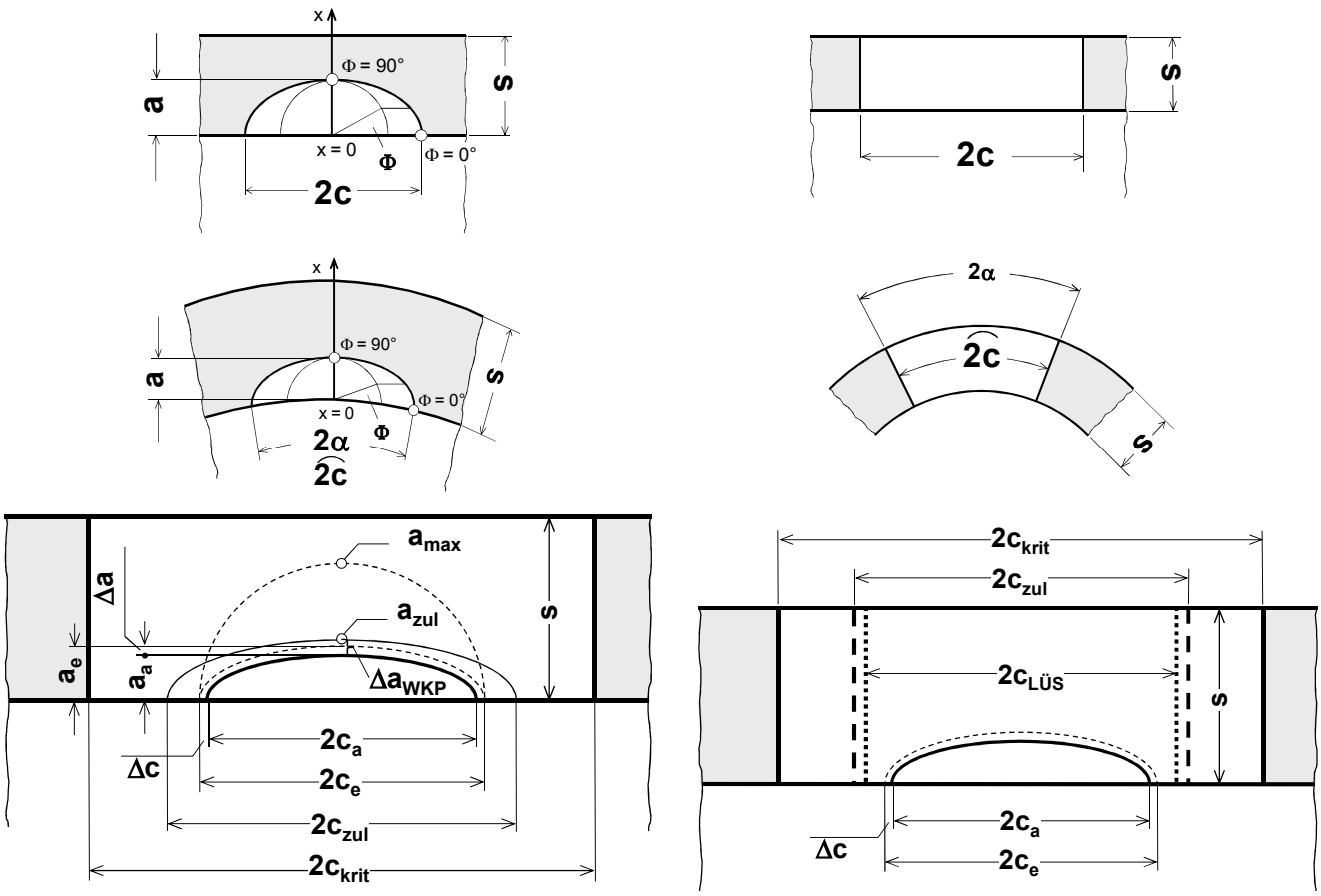

Figure A-1: Crack configurations and symbols for piping

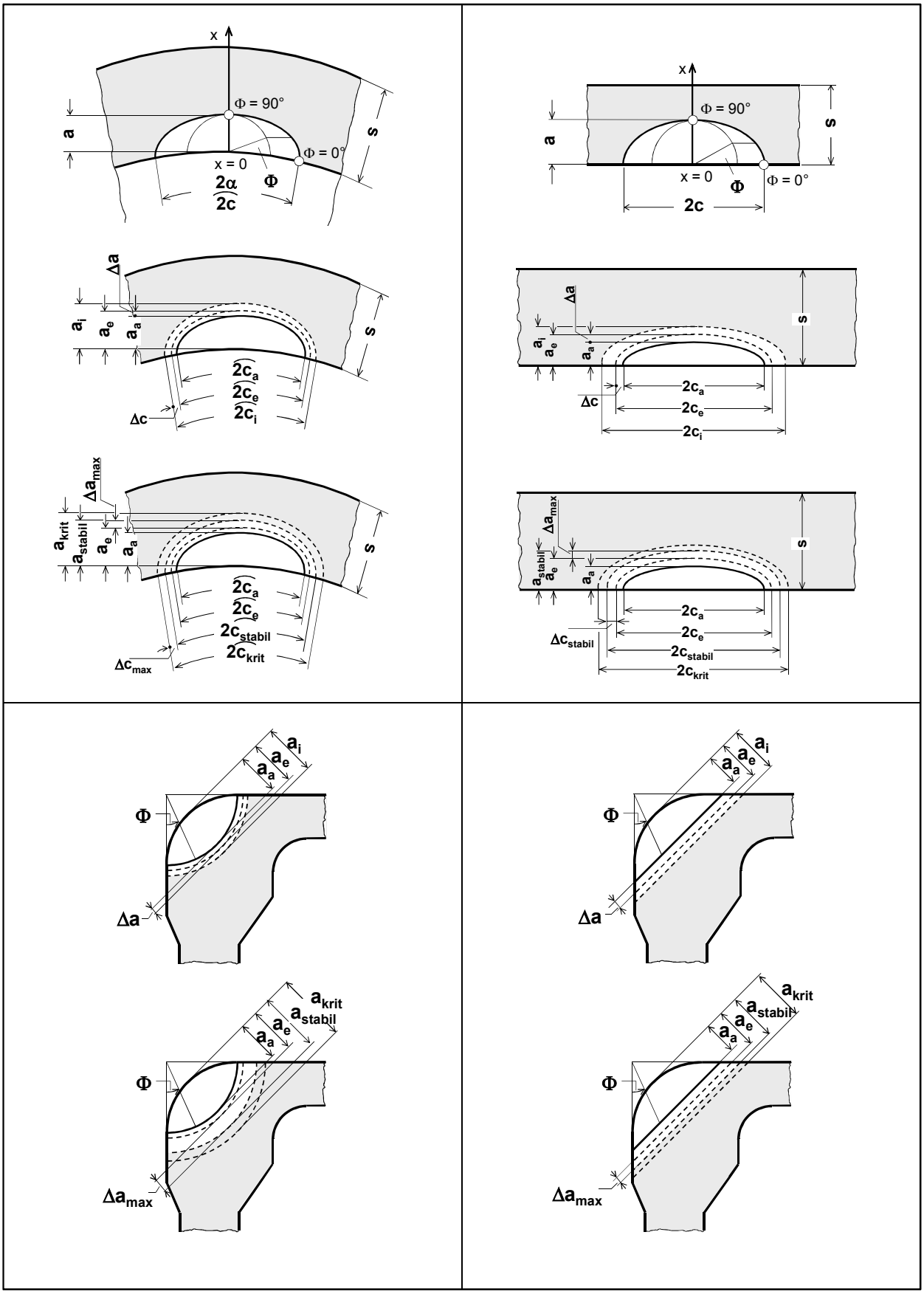

Figure A-2: Crack configurations and symbols for pressure vessels

(5) A fracture mechanics analysis is not required for pump casings if one of the criteria a) or b) is satisfied:

a) one of the criteria under (2) is satisfied by the connected piping,

b) it can be proved by means of an evaluation of the valve body or pump casing design that the crack growth potential of the connected piping is covering the crack growth potential of the valve body or pump casing.

(6) The evaluation as per (5) b) shall consider the following factors of influence:

a) loads occurring and the resulting stresses,

b) environmental conditions,

c) material and possible damage mechanisms,

d) defect sizes to be postulated.

(7) Where manufacturing defects above the acceptance level to KTA 3201.3 are present which were detected during manufacture or within in-service inspections and were clearly identified to be manufacturing defects and were left as they are (tolerance), they shall be evaluated by means of a fracture mechanics analysis to section A 4.

Note:
Operational defects arising from an active damage mechanism during operation or have developed from manufacturing defects, are covered by para. 3 (9) and shall not be subject to a fracture mechanics analysis.

(8) Crack-growth calculations shall be made by applying an appropriate equation to describe fatigue crack growth, e.g. the Paris-Erdogan equation.

Annex B, section B 2.5 describes the procedure to be applied for the purpose of this safety standard.

(9) The fracture mechanics analysis of the load bearing capacity of cracked piping may be made using the following procedures:

a) Analytical procedures to calculate the limit load (limit load analysis)

These analysis procedures make statements possible on the limit load capacity of cracked parts in which case the limits of application (due to geometry and material) and the resulting restrictions are to be considered. When using these procedures an effective evaluation is only possible if their applicability has been confirmed by experimental investigations. Here, distinction is principally made between

aa) flow stress concepts (local plastic yielding)

ab) plastic limit load concepts (global plastic yielding)

Annex B, section B 2.1 contains a description of the procedures to be applied for the purpose of this safety standard.

b) J-Integral/Tearing modulus procedure and Two-criteria method

J-Integral/Tearing modulus procedure and the two-criteria method make an evaluation possible as regards crack initiation and instability. Statements on the behaviour after onset of crack initiation are only possible if the J-R curves determined by means of laboratory samples can be considered to be representative of the component considered.

The fracture mechanics parameters may be determined both by analytical solutions and numerical methods (e.g. by the finite element method).

The description of the methods to be applied for the purpose of this safety standard is contained in Annex B, section B 2.2 (J-Integral/Tearing modulus procedure) and section B 2.3 (two-criteria method).

c) Damage mechanisms (local approach)

Local damage mechanism approaches make possible an evaluation of the total failure behaviour including global instability. The damage mechanic model parameters shall be determined in dependence of the material.

Annex B, section B 2.4 contains the description of the approach to be applied for the purpose of this safety standard.

(10) Fracture mechanics analysis for evaluating the integrity of cracked vessels may be performed by means of the approaches mentioned under (9) b) and c).

(11) As regards the determination of

a) leakage areas (crack opening areas)

b) leak flow rates

analytical and numerical methods may be applied (for the determination of the leakage areas e.g. Dugdale method, Irwin method, FEM; for the determination of the leak flow rates e.g. the flow rate models by Pana or by Moody)

Depending on the various problems a comparison with the leak area or leak rate detectable by leakage monitoring and the determination of the resulting jet forces is possible.

Depending on the objective of verification - minimum leak rate for determining the leak detection requirements or maximum leak rate for determining jet and reaction forces - conservative approaches shall be selected to define the leak rate.

The description of the methods to be applied for the purpose of this safety standard is contained in Annex B, section B 3.1 (calculation of leak opening area) and section B 3.2 (calculation of leak flow rate).

A 2 Evaluation of postulated cracks in piping

(1) For the postulated initial crack the following verifications shall be made by fracture mechanics evaluation for all relevant loadings as follows:

a) The crack growth potential is limited. Here, it shall be shown that the surface crack to be safeguarded (crack size to be used plus the calculated sub-critical fatigue crack growth during the operating time to be safeguarded) does not attain the value laid down in (2) f).

b) The crack length to be safeguarded (crack length to be used plus the calculated fatigue crack growth during the operating time to be safeguarded) is less than the length of a through-thickness crack permitted during operation and accidents.

c) The leakage crack length which is safely detected by the method used is less than the allowable length of a through-thickness crack, so that leak-before-break is given, or it is ensured that the criteria of (2) hb) are satisfied.

(2) To this end, the following calculation steps shall be taken, see **Figure A-3**:

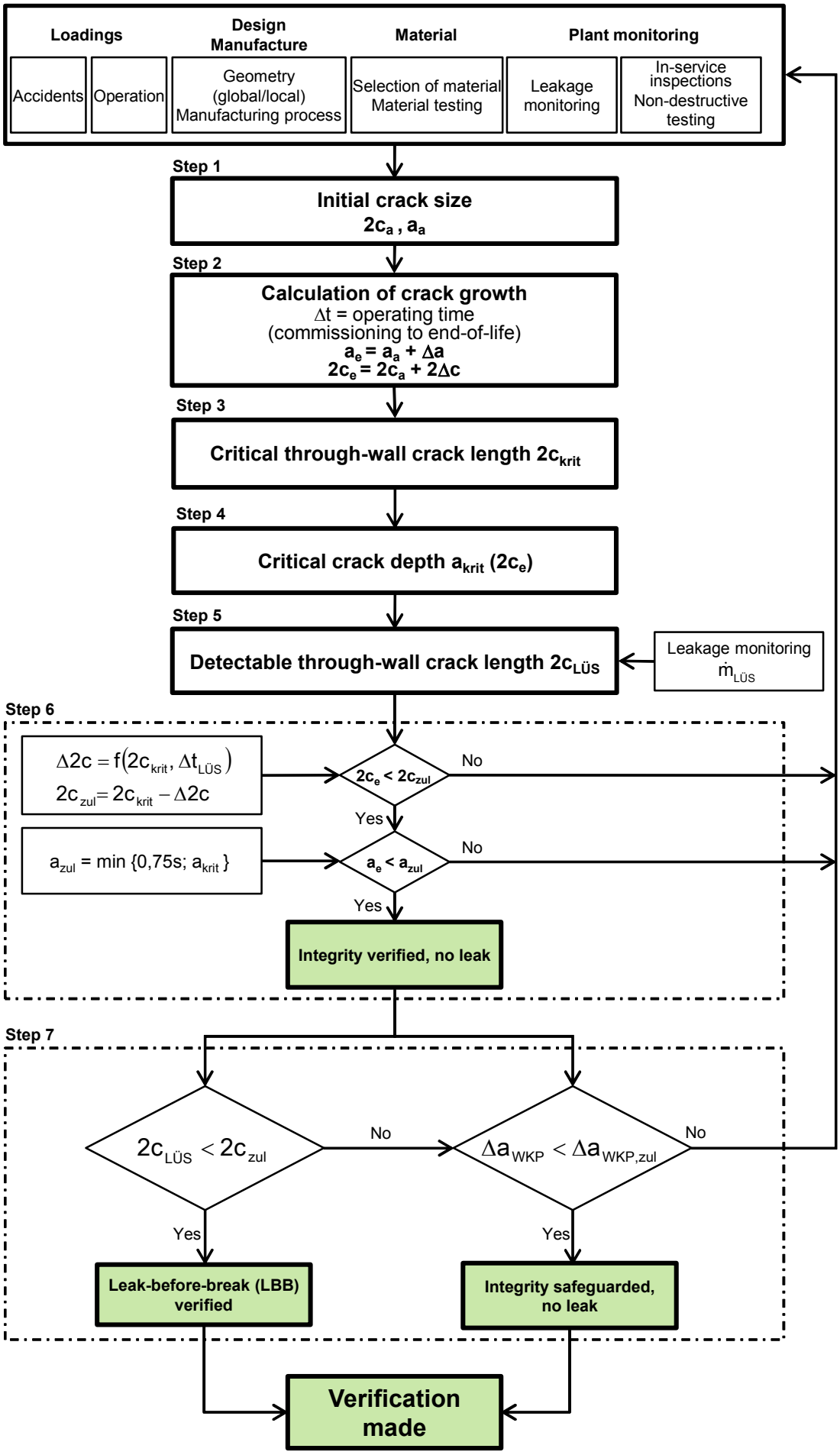

Figure A-3: Fracture mechanics analysis of postulated cracks in piping

a) Step 1: Determination of initial crack

The fracture-mechanics analyses shall either be made on the basis of any covering crack geometry or on the basis of component or system-related crack geometries.

aa) Covering crack geometries

Independently of the material a semi-elliptical crack with the following crack depth shall be assumed as initial crack:

$a_a = 0.3 \cdot s$ for $s < 25$ mm (A 2-1)

$a_a = 0.2 \cdot s$ for $s \geq 50$ mm (A 2-2)

In case of ferritic steels the following crack depth may be taken:

$a_a = 0.2 \cdot s$ for $s < 25$ mm (A 2-3)

$a_a = 0.1 \cdot s$ for $s \geq 50$ mm (A 2-4)

The crack depth may be interpolated for each value ranging between 25 mm < s < 50 mm.

The crack length shall be taken as follows:

$2c_a \geq 6 \cdot a_a$ (A 2-5)

ab) Component or system-related crack geometries

The size of the initial crack to be assumed with a depth a_a and a length $2c_a$ shall be determined such that it corresponds at least to the acceptance limit of the non-destructive test methods used as per KTA 3201.4.

b) Step 2: Calculation of crack growth Δa and Δ2c

The calculation shall be made on the basis of the initial crack (a_a and $2c_a$) with the specified loadings of specified normal operation in due consideration of the loadings determined by operational measurements and the pertinent load cycles. The crack growth shall be calculated as fatigue crack growth by using a fatigue growth law for the appropriate environment. The calculation shall be made for a period of time covering the total operational lifetime.

The final crack size at the end of the period considered shall be as follows:

Final crack depth $a_e = a_a + \Delta a$ (A 2-6)

Final crack length $2c_e = 2c_a + \Delta 2c$ (A 2-7)

The calculation shall be made to section A 1 (8).

For the calculation of the fatigue crack growth under LWR environment conditions the crack growth curves of ASME BPVC Section XI for ferritic steels and to NUREG/CR-6176 for austenitic steels may be used.

c) Step 3: Determination of the smallest critical length of a through-thickness crack $2c_{krit}$ from all load cases to be considered (operational load cases and specified accidents)

The calculation of the critical crack length shall be made to section A 1 (9).

d) Step 4: Determination of the critical depth a_{krit} of a surface crack with a length $2c_e$

The critical depth a_{krit} shall be the smallest critical depth of a surface crack with a length $2c_e$ to be determined from all load cases to be considered (operational load cases and specified accidents).

The calculation of the critical crack depth shall be made using the methods of section A 1 (9).

e) Step 5: Calculation of the detectable length $2c_{LÜS}$ of a through-thickness crack

The following steps shall be taken:

ea) Determination of the leak mass flow $\dot{m}_{LÜS,det}$ safely detectable by leakage monitoring

Note:
The safely detectable leak mass flow is subject to the sensitivity of leakage monitoring.

eb) Determination of the intervention mass flow $\dot{m}_{LÜS,BHB}$ which when being exceeded shall cause intervention measures to be taken (e.g. leak detection measures, plant shutdown) as laid down in the operating manual.

The intervention mass flow shall be laid down in due consideration of operational aspects such that its detectability is ensured

$\dot{m}_{LÜS,BHB} \geq \dot{m}_{LÜS,det}$

ec) Calculation of leak mass flow $\dot{m}_{Leck}$ in dependence of the crack length

The calculation of the leak mass flow shall be made by using the calculation methods described under section A 1 (11) for the crack opening area A_{Leck} and the flow resistance in connection with the prescriptions as per Annex B, sections B 3.1 and B 3.2 for the loadings of steady-state load operation.

ed) Determination of the length $2c_{LÜS,BHB}$ of a through-thickness crack to be safeguarded

The crack length $2c_{LÜS}$ to be safeguarded is that length at which the leak mass flow $\dot{m}_{Leck}$ is equal to the intervention mass flow $\dot{m}_{LÜS,BHB}$.

f) Step 6: Verification of limited operational crack growth

It shall be verified that the final crack size (a_e, $2c_e$) determined under step 2 meets the following requirements:

$a_e \leq a_{zul}$ (A 2-8)

and

$2c_e \leq 2c_{zul}$ (A 2-9)

The allowable depth a_{zul} of a surface crack with a length $2c_e$ shall be determined for the plant service lifetime as follows:

$a_{zul} = \min \{0.75 \cdot s; a_{krit}(2c_e)\}$ (A 2-10)

with a_{krit} taken from step 4.

Note:
The operational crack growth shall be limited such that no through-thickness crack occurs during the plant service lifetime. In crack growth calculations, e.g. in IIW document IIW-1823-07 ex XIII-2151r4-07/XV-1254r4-07 and in ASME BPVC Section XI a through-thickness crack is assumed to occur at a crack depth $0.75 \cdot s$ as well as where a_{krit} is reached.

The allowable crack length $2c_{zul}$ is the length of a through-thickness crack 2c at which due to crack growth over the period Δt_{WKP} the value $2c_{krit}$ is even reached (see **Figure A-4**).

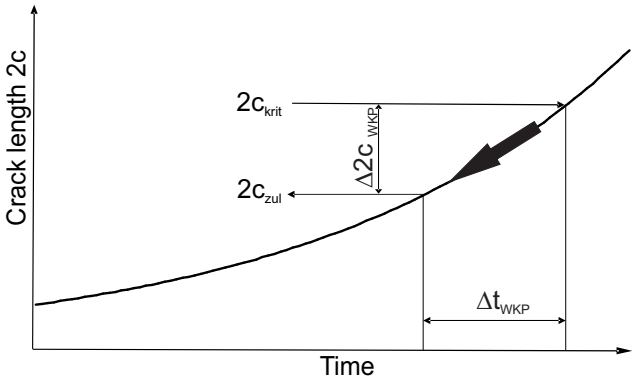

Figure A-4: Determination of the allowable crack length $2c_{zul}$ (schematic)

The allowable crack length $2c_{zul}$ shall be determined as follows:

Starting from a through-thickness crack length 2c, the crack growth shall be calculated to reach the value of $2c_{krit}$ under

the assumed specified loadings of specified normal operation in due consideration of the loadings and pertinent load cycles determined by operational measurements, in which case $2c < 2c_{krit}$ and $2c \leq 2c_{zul}$ shall be selected.

Here, the following equation applies:

$$2c_{zul} = 2c_{krit} - \Delta 2c_{WKP} (\Delta t_{WKP}) \quad \text{(A 2-11)}$$

The crack growth shall be calculated as fatigue crack growth by using a fatigue growth law for the appropriate environment. To this end, the crack growth curves of ASME BPVC Section XI for ferritic steels and to NUREG/CR-6176 for austenitic steels may be used.

The period for safe leak detection shall be taken as the in-service non-destructive testing interval Δt_{WKP} laid down for the respective component by KTA 3201.4 or KTA 3211.4.

g) Step 7: Verification of leak-before-break

The verification of leak-before-break shall show that the following requirement is met:

$$2c_{LÜS} < 2c_{zul} \quad \text{(A 2-12)}$$

with $2c_{zul}$ taken from step 6 and $2c_{LÜS}$ taken from step 4.

h) The fracture mechanics verification is made if

ha) the requirements of steps 6 and 7 have been met,

hb) the leak flow rate from a through-thickness crack cannot be determined with the required accuracy (e.g. in case of low operational stress level and thus resulting low leak rate), but the requirements of step 6 have been met, and appropriate measures of the integrity concept (especially operational monitoring measures for continuous recording of all relevant loadings and their timely evaluation as well as intervals of in-service inspections adapted thereto) are taken over the total operational lifetime to ensure that the sub-critical fatigue crack growth of the initial crack to be safeguarded (see step 1) meets the requirement shown hereafter within the in-service non-destructive testing interval laid down for the respective component by KTA 3201.4 or KTA 3211.4:

$$\Delta a_{WKP} \leq 0.125 \times (a_{zul} - a_a) \quad \text{(A 2-13)}$$

Note:
The factor 0.125 results from the ratio of a usual inspection interval of 5 years to a total service lifetime of 40 years.

A 3 Evaluation of postulated cracks in pressure vessels as well as in valve bodies and pump casings

A 3.1 Pressure vessels

(1) The fracture mechanics evaluation shall show for the postulated initial crack that its crack growth potential is limited. For the surface cack to be safeguarded (crack dimensions to be assumed plus the calculated sub-critical fatigue crack growth during the operating time to be safeguarded) it shall be shown that under operational loadings no crack initiation takes place and under accident loadings only a limited stable crack extension can occur.

(2) To this end, the following calculation steps shall be taken, see **Figure A-5**:

a) Step 1: Determination of relevant pressure vessel areas

By means of the following criteria those pressure vessel areas with the most unfavourable properties regarding loading, material and defect conditions shall be determined such that by means of the fracture mechanics analysis of these areas the vessel is safeguarded in total:

aa) stress utilization for operational loading each (levels A and B) and for accident loading (levels C and D),

ab) usage factor over the total service lifetime,

ac) material toughness (e.g. by means of the impact energy in notched-bar impact testing) of base materials, weld filler metals and heat-affected zones,

ad) crack size as per acceptance limit of the non-destructive test methods and techniques used.

For each of the vessel areas thus determined the following steps shall be performed:

b) Step 2: Determination of the initial crack

The size of the initial crack to be assumed with a depth a_a and a length $2c_a$ shall be determined such that it corresponds at least to the acceptance limit of the non-destructive test methods used as per KTA 3201.4.

c) Step 3: Calculation of crack growth Δa and Δ2c

The calculation shall be made on the basis of the initial crack (a_a and $2c_a$) with the specified loadings of specified normal operation in due consideration of the loadings determined by operational measurements and the pertinent load cycles. The crack growth shall be calculated as fatigue crack growth by using a fatigue growth law for the appropriate environment. The calculation shall be made for a period of time covering the total operational lifetime.

The final crack size at the end of the period considered shall be as follows:

$$\text{Final crack depth } a_e = a_a + \Delta a \quad \text{(A 3-1)}$$

$$\text{Final crack length } 2c_e = 2c_a + \Delta 2c \quad \text{(A 3-2)}$$

The calculation shall be made to section A 1 (8).

For the calculation of the fatigue crack growth under LWR environment conditions the crack growth curves of ASME BPVC Section XI for ferritic steels and to NUREG/CR-6176 for austenitic steels may be used.

d) Step 4: Determination of the smallest crack initiation size from the load cases of level A and B loadings

The calculation shall be made by using the procedures as per section A 1 (10).

e) Step 5: Determination of the ductile crack extension to be expected for the load cases of level C and D loadings

The calculation shall be made by using the procedures as per section A 1 (10).

Here, the influence of the multi-axial stress condition on the crack resistance of the material shall be considered.

f) Step 6: Fracture mechanics evaluation

The fracture mechanics verification is made if

fa) for loading levels A and B the final crack size is less than the initiation crack size and

fb) it was shown for loading levels C and D that only stable crack extension can occur.

Where the crack extension to be expected exceeds the J-R curve safeguarded by tests, the stable crack extension criteria is not satisfied. Instead of a J-R curve safeguarded by tests a conservative assessment of J-R curves may be used on the basis of the upper shelf impact energy obtained from a notched-bar impact test, e.g. according to US NRC Reg. Guide 1.161, where, in this case, the crack extension shall be limited to the application limits of ASTM-E 1820-11.

A 3.2 Valve bodies and pump casings

Where the evaluation of postulated cracks in valve bodies and pump casings is required (see section A 1 (5)), the procedure for pressure vessels described in A 3.1 shall apply analogously.

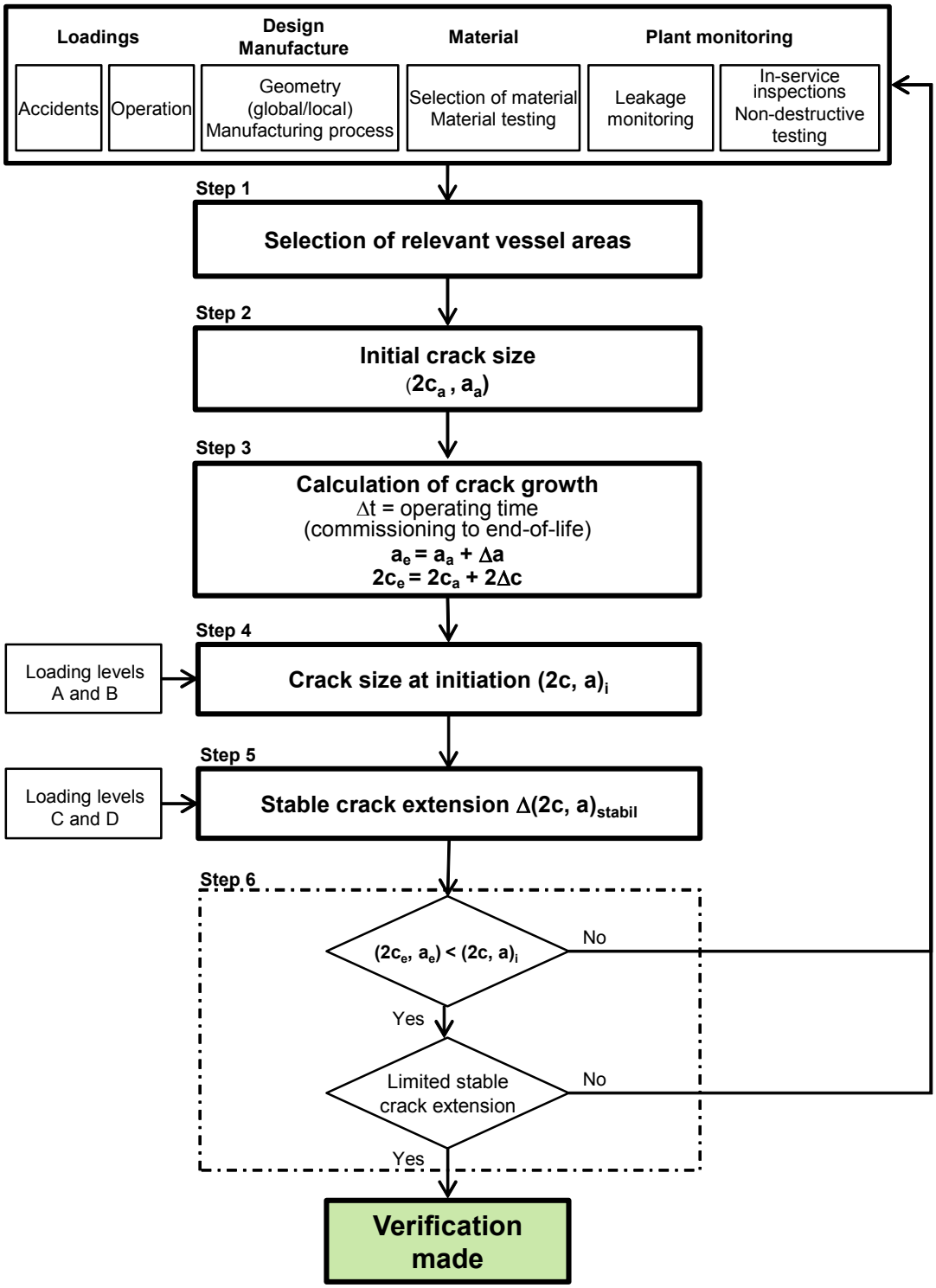

Figure A-5: Fracture mechanics analysis of postulated cracks in pressure vessels

A 4 Evaluation of manufacturing defects

(1) A fracture mechanics evaluation shall be made to prove that

a) the crack growth potential is limited,

b) sufficient safety margins are available as regards load bearing capacity.

(2) To this end, the following calculation steps shall be made at first for both piping and pressure vessels, see **Figures A-6 and A-7**:

a) Step 1: The manufacturing defect shall be described as crack using an envelope of crack length and depth.

Note:
A description of an envelope of crack length and depth of manufacturing defects for use in fracture mechanics evaluation is e.g. contained in the "ASME Boiler and Pressure Vessel Code, Section XI, 2010, Article IWA-3300 Flaw Characterization".

b) Step 2: Calculation of crack growth Δa and Δ2c

The crack growth shall be calculated to section A 2 (2) b) for the period concerning the interval for periodic non-destructive testing determined for the respective component.

(3) For piping the following calculation steps shall be taken upon performance of steps 1 and 2:

a) Step 3: Verification of limited operational crack growth

The crack growth calculated in step 2 of the initial crack to be safeguarded (see step 1) shall satisfy the condition of equation A 2-13.

b) Step 4: Verification of load bearing capacity

A fracture-mechanics evaluation shall be made to verify the load bearing capacity of the defect-containing component by using the safety factors for the respective loadings laid down for loading levels A, B, C and D in **Table A-1**.

The verification of load bearing capacity shall be made according to A 1 (9).

c) The fracture mechanics verification is made if the requirements in a) and b) have been met.

(4) For pressure vessels the following calculation steps shall be taken upon performance of steps 1 and 2:

a) Step 3: determination of the smallest crack initiation size for the load cases of loading levels A, B, C and D

The calculation shall be made using the procedures laid down in A 1 (10).

b) Step 4: Verification as regards crack initiation

The fracture mechanics verification is made if it can be proved for all load cases of loading levels A, B, C and D that at the final crack size calculated in step 2 no crack initiation will occur.

Loading level	Safety factor for circumferential flaws		Safety factor for longitudinal flaws
	Membrane stress	Bending stress	Membrane stress
A	2.7	2.3	2.7
B	2.4	2.0	2.4
C	1.8	1.6	1.8
D	1.3	1.4	1.3

Table A-1: Safety factors for primary stresses on components containing manufacturing flaws

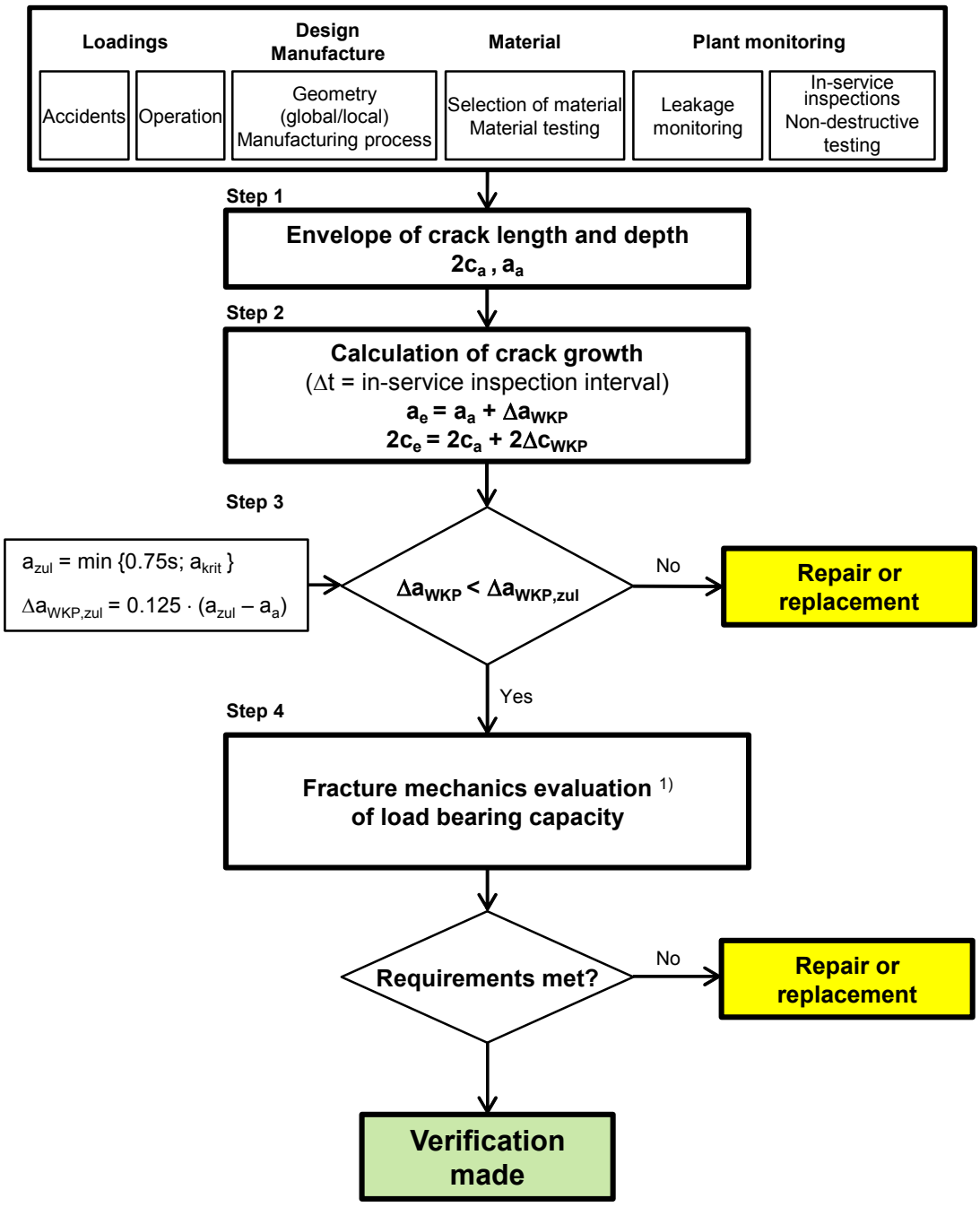

1) The fracture mechanics evaluation of the load bearing capacity shall be made using the safety factors to be applied on the loadings as per **Table A-1**

Figure A-6: Fracture mechanics analysis of manufacturing defects in piping

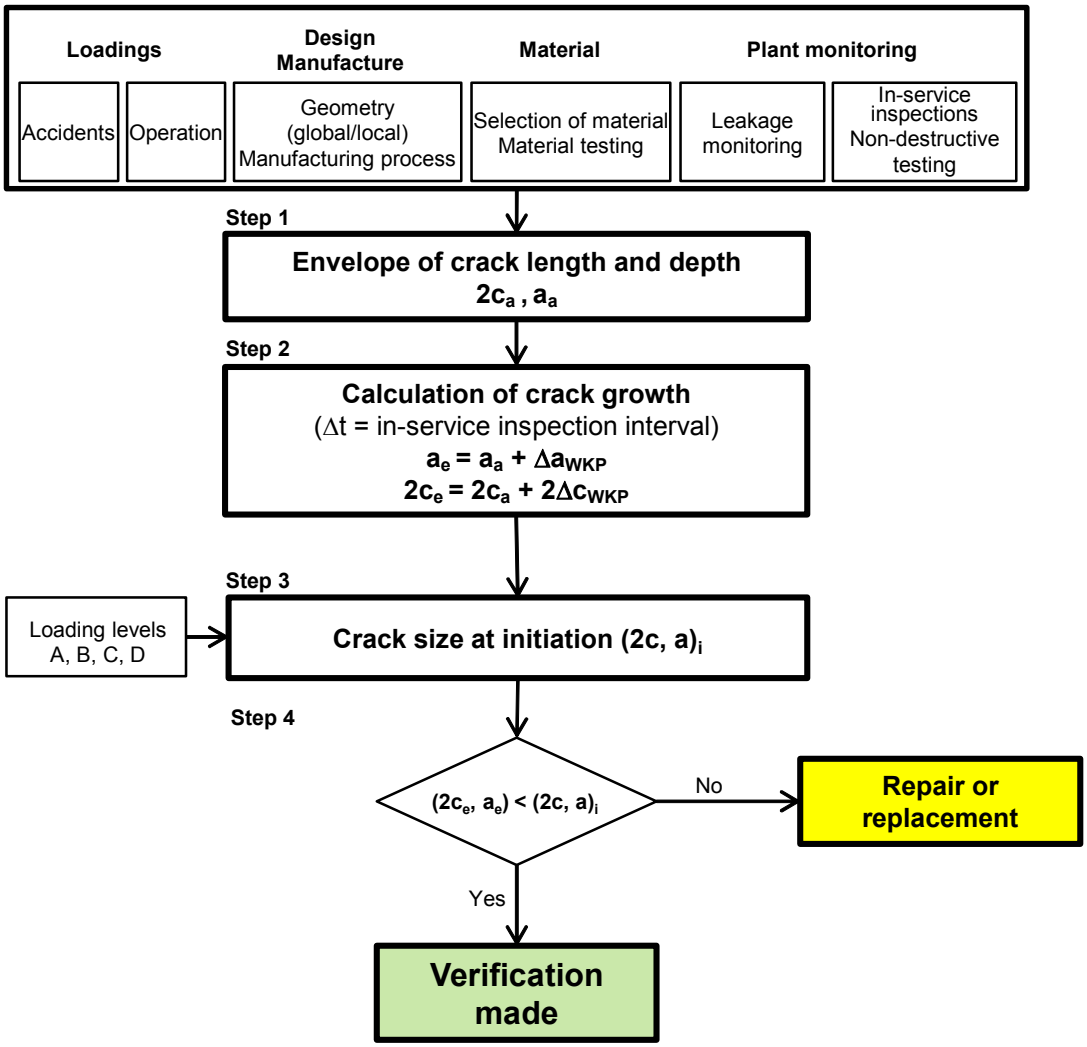

Figure A-7: Fracture mechanics analysis of manufacturing defects in pressure vessels

Annex B (normative)

Fracture mechanics analysis procedures

B 1 General requirements

(1) The application of the procedures described in sections B 2.1 to B 3.2 shall be based on the following data:

a) the minimum design strength values laid down by KTA 3201.1, KTA 3211.1 or specification approved,

b) the characteristic fracture mechanics values given under Annex C or from other sources as far as their suitability has been proved for the respective component,

c) in case of analyses of postulated cracks: nominal dimensions of the respective component (wall thickness, inside radius),

d) in case of evaluation of manufacturing defects: as-built dimensions of the respective component.

Note:
The procedures described in sections B 2.1 to B 3.2 have been validated and lead to conservative results for the materials according to KTA 3201.1 and KTA 3211.1.

(2) It is permitted to use

a) other solutions than indicated in sections B 2.1 to B 3.2,

b) the actual data (e.g. dimensions, material property values) of the part to be assessed

if their suitability has been proved in the licensing or supervision procedure.

(3) In the case of clad components the fracture mechanics analysis is conservative if

a) the postulated crack, crack growth calculations and critical crack sizes exclusively refer to the base material,

b) the cladding is considered when determining the leakage area and the leak rate.

B 2 Fracture mechanics procedures

B 2.1 Limit load analysis

B 2.1.1 Fundamentals

(1) Limit load analyses are a simple-to-handle tool for determining critical crack sizes and critical loadings (limit load). The available analytical procedures make it possible, with comparably little expenditure, to make statements on the limit load of cracked piping in which case the geometry and material-relevant limits of application and the related restrictions are to be considered.

(2) The available procedures for limit load calculation are distinguished according to the failure criteria used:

a) flow stress concepts (FSC, local plastic yielding),

b) plastic limit load concepts (PLL, global plastic yielding).

(3) The essential input value for these procedures is the flow stress σ_f. The flow stress is an operand derived specifically from experimental investigations on piping components for the purpose of limit load calculations [1], [2]. This operand is determined such that the limit load (maximum loading) determined by the experiments is calculated to form a conservative value. The flow stress value is determined using he design strength values $R_{p0.2}$ and R_m where $R_{p0.2} \le \sigma_f \le R_m$. The flow stress to be used depends on the procedure applied (flow stress concept, plastic limit load concept), the material, component dimensions and crack configuration (e.g. axial or circumferential cracks). When evaluating cracks in welds between ferritic steels, in welds between austenitic steels and in dissimilar welds between ferritic and austenitic steels with buttering and nickel-alloy weld metal [3], the use of the material properties of the base material, in case of dissimilar welds the use of the austenitic base material instead of the material properties of the weld metal or heat-affected zone is conservative, i.e. it will lead to the determination of the smallest critical crack size.

B 2.1.2 Longitudinal crack under internal pressure loading

B 2.1.2.1 Straight pipe

(1) The calculation method for straight pipes with longitudinal cracks is based on semi-empirical approaches, such as described in [4], [5], [6], [7], [8], [9], [10].

(2) With this method the failure of a pipe with a surface crack and a through-thickness crack is calculated exclusively in consideration of primary stresses (P_m) from internal pressure loading.

(3) The failure of a surface crack with a length 2c and a depth a means the rupture of the residual wall thickness so that a through-thickness crack with a length 2c occurs (leak). The failure of a through-thickness crack with a length 2c means instable crack extension (rupture).

(4) The nominal circumferential stress at failure is calculated from the following relation:

$$\sigma_u = \sigma_f \cdot M^{-1} \qquad \text{(B 2.1-1)}$$

with σ_f as per [2]:

$$\sigma_f = (1.7 - 1.2 \cdot R_{p0.2}/R_m) \cdot R_{p0.2} \qquad \text{(B 2.1-2)}$$

$M = M_t$ for through-thickness cracks

$$M_t = \sqrt{1 + 1.61 \cdot \left(\frac{c^2}{r_m \cdot s} \right)} \qquad \text{(B 2.1-3)}$$

and $$0 \le \frac{2c}{\sqrt{r_m \cdot s}} \le 10 \qquad \text{(B 2.1-4)}$$

$M = M_p$ for surface cracks

$$M_p = \frac{1 - \left(\frac{a}{s \cdot M_t} \right)}{1 - \left(\frac{a}{s} \right)} \qquad \text{(B 2.1-5)}$$

where

2c : crack length

a : crack depth

r_m : mean radius

s : wall thickness

D_i : inside diameter

M : correction factor

σ_u : circumferential stress

The pressure at failure p_V for through-thickness cracks in the pipe is calculated with

$$\sigma_{u,Rohr} = \frac{p \cdot D_i}{2 \cdot s} \qquad \text{(B 2.1-6)}$$

to obtain

$$p_V = \frac{2 \cdot s}{D_i} \cdot \frac{\sigma_f}{M_t} \qquad \text{(B 2.1-7)}$$

and for surface cracks to obtain

$$p_V = \frac{2 \cdot s}{D_i} \cdot \frac{\sigma_f}{M_p} \qquad \text{(B 2.1-8)}$$

B 2.1.2.2 Pipe bends

The procedures described in cl. B 2.1.2.1 are applicable to pipe bends with longitudinal cracks under internal pressure. Here, the maximum circumferential stress σ_u for the crack located on the pipe circumference (e.g. intrados, extrados or straight portion of bend) shall be determined to cl. 8.4.8.2 of KTA 3201.2 or by means of a finite element analysis and be considered in equation B 2.1-1 with $M = M_t$ for through-thickness cracks and with $M = M_p$ for surface cracks.

B 2.1.3 Circumferential crack in straight pipe under internal pressure and external bending moment

B 2.1.3.1 General

(1) To evaluate circumferential defects the following concepts may be applied:

a) Plastic Limit Load (PLL) [11], [12]

b) Flow Stress Concept (FSC) [2], [13] - [16].

(2) The models on which the methods are based assume ductile material behaviour. Both methods use the material property values obtained from tensile tests to determine the flow stress σ_f. Fracture mechanics values will not be used. The calculated values for the critical flaw size or limit load are directly influenced by the amount of flow stress.

(3) The flow stress to be used is given in **Table B 2.1-1**.

Material and dimensions		Flow stress σ_f		
		PLL	FSC/MPA	FSC/KWU
Austenitic materials	DN 300 up to DN 400	$R_{p0,2}$ or $(R_{p0.2}+R_m)/2.4$ [1]	R_m	$(R_{p0.2}+R_m)/2$ or $0.6\cdot(R_{p0.2}+R_m)$ [2]
	DN 80 up to DN 250		$(R_{p0.2}+R_m)/2$	
	DN 50 up to DN 65		R_m	
Ferritic materials	DN 200 up to DN 800	$R_{p0.2}$	R_m [3] or $(R_{p0.2}+R_m)/2$	R_m
	DN 60 up to DN 150			

1) For materials 1.4541 and 1.4550 and dimensions DN 50 up to DN 300
2) For materials 1.4541 and 1.4550
3) For cracks in base material

Table B 2.1-1: Range of application and flow stresses to be used for plastic limit load (PLL) and flow stress concept (FSC)

B 2.1.3.2 Plastic Limit Load (PLL concept)

(1) The PLL concept is based on the minimum value solution for plastic limit load of pipes with circumferential flaws. Here, it is assumed that at sufficiently high material ductility a fully plastic stress condition is obtained across the pipe cross-section. This is based on a linear-elastic - ideal plastic material behaviour where a constant flaw geometry is assumed and possible crack initiation and crack extension are not considered. No statement on the progress of failure is possible.

Under bending load and superimposed internal pressure the failure moment is calculated from considerations of equilibrium conditions as follows:

a) for the case $\alpha + \beta \le \pi$:

$$M_V = 2\cdot\sigma_f\cdot {r_m}^2\cdot s\cdot\left[2\cdot\sin\beta-\left(\frac{a}{s}\right)\cdot\sin\alpha\right] \qquad \text{(B 2.1-9)}$$

The location of the neutral fibre is thus calculated to obtain

$$\beta = \frac{\pi-\left(\frac{a}{s}\right)\cdot\alpha}{2} - \frac{\pi\cdot r_i^2\cdot p_i}{4\cdot r_m\cdot s\cdot\sigma_f} \qquad \text{(B 2.1-10)}$$

b) for the case $\alpha + \beta > \pi$:

$$M_V = 2\cdot\sigma_f\cdot {r_m}^2\cdot s\cdot\left[2-\left(\frac{a}{s}\right)\right]\cdot\sin\beta \qquad \text{(B 2.1-11)}$$

The location of the neutral fibre is thus calculated to obtain

$$\beta = \frac{\pi}{\left(2-\frac{a}{s}\right)}\cdot\left[1-\left(\frac{a}{s}\right)-\frac{r_i^2\cdot p_i}{2\cdot r_m\cdot s\cdot\sigma_f}\right] \text{ and } b \ge 0 \qquad \text{(B 2.1-12)}$$

This method is based on a constant stress distribution in the defective pipe cross-section at the pertinent flow stress σ_f, see **Figures B 2.1-1** and **B 2.1-2**.

(2) The pipe failure at given internal pressure and bending moment loading is calculated to obtain:

$$\frac{\pi}{4}\cdot\frac{\sigma_{ax,M}}{\sigma_f}-\cos\left(\frac{a}{s}\cdot\frac{\alpha}{2}+\frac{\pi}{2}\cdot\frac{\sigma_{ax,p}}{\sigma_f}\right)+\frac{1}{2}\cdot\frac{a}{s}\cdot\sin\alpha = 0 \qquad \text{(B 2.1-13)}$$

with

$$\sigma_{ax,p} = \frac{p}{(D_a/D_i)^2-1} \qquad \text{(B 2.1-14)}$$

$$\sigma_{ax,M} = \frac{M}{W} \qquad \text{(B 2.1-15)}$$

and

$$W = \frac{\pi}{32}\cdot\frac{{D_a}^4-{D_i}^4}{D_a} \qquad \text{(B 2.1-16)}$$

where:

W : pipe resistance moment

D_a : external diameter

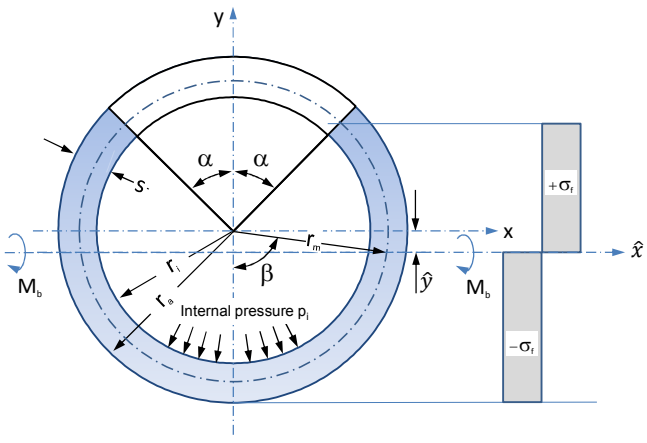

Figure B 2.1-1: PLL – through-thickness crack in circumferential direction

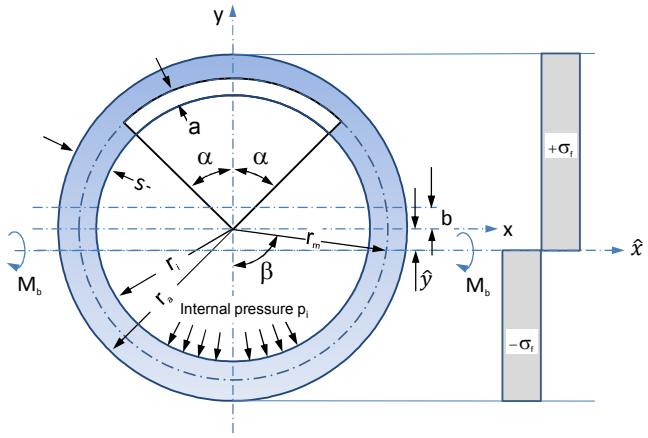

Figure B 2.1-2: PLL - surface crack in circumferential direction

B 2.1.3.3 Flow stress concept (FSC)

(1) Within the flow stress concept, the calculation of the failure due to loadings and the determination of critical flaw sizes is derived from the classical beam bending theory to Bernoulli. With this method, the inertia moments of the defective pipe cross-section are exactly determined in consideration of the displacement of the neutral fibre. Failure is assumed to occur if at the location of highest loading the stress assumed to be linearly distributed over the defective cross-section has attained a limit value (see **Figures B 2.1-3** and **B 2.1-4**). To this end the flow stress σ_f is used. Here, it is not assumed that the total defective pipe cross-section is subject to plastic deformation. The flaw geometry is assumed to be constant. Crack initiation and crack extension possibly occurring are not considered. No statement can be made as to the course of failure.

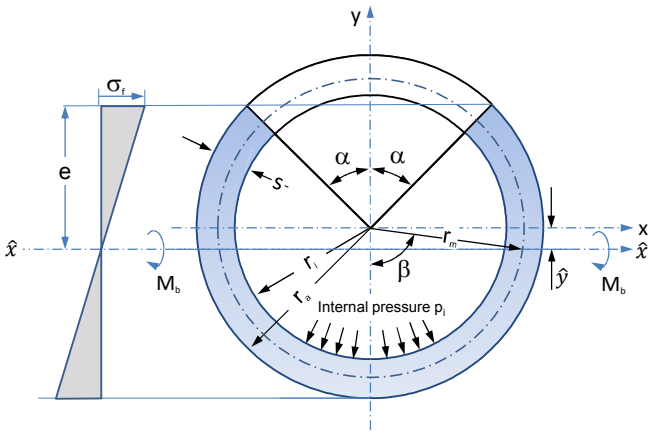

Figure B 2.1-3: FSC/MPA – through-thickness crack in circumferential direction

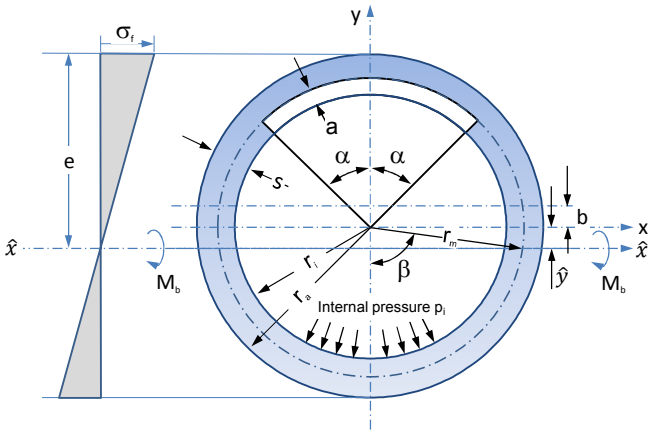

Figure B 2.1-4: FSC/MPA – Surface crack in circumferential direction

(2) Where the range of application is observed, the MPA method (FSC/MPA) [1] or alternatively the Siemens-KWU method (now AREVA) (FSC/KWU) [2] may be used.

a) Calculation to MPA (FSC/MPA)

In due consideration of the exact inertia moments and displacement of centroids the failure moment for a through-thickness crack is calculated as follows:

$$M_V = \frac{I_{\hat{x}}}{e} \cdot \left[\sigma_f - \frac{A_0}{A_q - A_f} \cdot p_i \right] - \hat{y} \cdot A_o \cdot p_i \qquad \text{(B 2.1-17)}$$

and for a circumferential crack at the internal surface as follows:

$$M_V = \frac{I_{\hat{x}}}{e} \cdot \left[\sigma_f - \frac{A_w}{A_q - A_f} \cdot p_i \right] - (\hat{y} + b) \cdot A_w \cdot p_i \qquad \text{(B 2.1-18)}$$

The calculation factors are shown in **Table B 2.1-2**.

Surface crack	Through-thickness crack	
$A_0 = \pi \cdot r_i^2$		
$Aq = \pi \cdot (r_a^2 - r_i^2)$		
$A_f = \text{arc}\,\alpha \cdot (R^2 - r_i^2)$	$A_f = \text{arc}\,\alpha \cdot (r_a^2 - r_i^2)$	
$A_w = A_0 + A_f$	$A_w = A_0$	
$A_n = A_q - A_f$	$A_n = A_q - A_f$	
$R = (r_i + a)$	$R = r_a$	
$e = \hat{y} + r_a$	for $\alpha \le 90°$	$e = \hat{y} + r_a \cdot \cos\alpha$
	for $\alpha > 90°$	$e = \hat{y} + r_i \cdot \cos\alpha$
$\hat{y} = \frac{2 \cdot (R^3 - r_i^3) \cdot \sin\alpha}{3 \cdot A_n}$	$\hat{y} = \frac{2 \cdot (R^3 - r_i^3) \cdot \sin\alpha}{3 \cdot A_n}$	
$b = \frac{2 \cdot (R^3 - r_i^3) \cdot \sin\alpha}{3 \cdot A_w}$	$b = 0$	
$I_x = \pi \cdot \frac{(r_a^4 - r_i^4)}{4}$	$I_x = \pi \cdot \frac{(r_a^4 - r_i^4)}{4}$	
$I_{\underset{x}{\wedge}} = I_x - \hat{y}^2 \cdot A_n - \left[A_f + \frac{\sin 2\alpha}{2} \cdot (R^2 - r_i^2) \right] \cdot \frac{R^2 + r_i^2}{4}$		

Table B 2.1-2: Definition of the calculation factors used in the flow stress concept according to MPA

b) Calculation to Siemens-KWU (now AREVA) (FSC/KWU)

Failure is assumed to occur if the locally acting effective stress attains the flow stress:

$$\sigma_{eff} = \sigma_f \qquad \text{(B 2.1-19)}$$

The loading leading to failure σ_{eff} for point A of a surface defect and B of a through-thickness crack (**Figure B 2.1-5**) is calculated from

$$\sigma_{eff(A)} = k_{a(A)} \cdot \sigma_{ax,p} + k_{b(A)} \cdot \sigma_{ax,M} \qquad \text{(B 2.1-20)}$$

$$\sigma_{eff(B)} = k_{a(B)} \cdot \sigma_{ax,p} + k_{b(B)} \cdot \sigma_{ax,M} \qquad \text{(B 2.1-21)}$$

with the stresses from internal pressure and moment as per equations B 2.1-14 and B 2.1-15.

and with the stress intensification factors

$$k_{a(A),(B)} = \frac{1-\frac{a}{s}\cdot\left(\frac{\alpha}{\pi}+\frac{\sin 2\alpha}{2\cdot\pi}-2\cdot\frac{\sin\alpha}{\pi}\cdot\cos\varphi\right)}{\left(1-\frac{a}{s}\cdot\frac{\alpha}{\pi}\right)\cdot\left[1-\frac{a}{s}\cdot\left(\frac{\alpha}{\pi}+\frac{\sin 2\alpha}{2\cdot\pi}\right)\right]-2\cdot\left(\frac{a}{s}\right)^2\cdot\frac{\sin^2\alpha}{\pi^2}} \quad \text{(B 2.1-22)}$$

$$k_{b(A),(B)} = \frac{\left(1-\frac{a}{s}\cdot\frac{\alpha}{\pi}\right)\cdot\cos\varphi+\frac{a}{s}\cdot\frac{\sin\alpha}{\pi}}{\left(1-\frac{a}{s}\cdot\frac{\alpha}{\pi}\right)\cdot\left[1-\frac{a}{s}\cdot\left(\frac{\alpha}{\pi}+\frac{\sin 2\alpha}{2\cdot\pi}\right)\right]-2\cdot\left(\frac{a}{s}\right)^2\cdot\frac{\sin^2\alpha}{\pi^2}} \quad \text{(B 2.1-23)}$$

as well as $\varphi = 0$ for point A and $\varphi = \alpha$ for point B

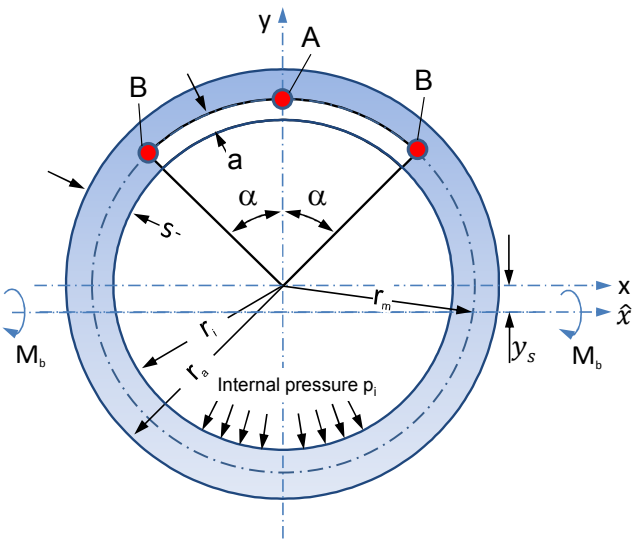

Figure B 2.1-5: FSC/KWU - Notations

B 2.1.4 Limits of application

(1) The methods presume large plastic deformations at the crack tip. They shall only be applied at upper-shelf energy level in notched-bar impact testing and only to materials which meet the requirements for upper-shelf energy level in impact testing to KTA 3201.1 and KTA 3211.1.

(2) The flow stresses σ_f to be used were derived from a large number of experimental investigations in dependence of pipe and defect geometry as well material toughness. The range of application is shown in **Table B 2.1-1**.

B 2.2 J-T procedure

B 2.2.1 Fundamentals

(1) The J-T procedure is based on the J-integral, in short J, and the Tearing Modulus, in short T.

The crack-driving force in the linear-elastic and elastic-plastic material range is measured and calculated by the parameter J. J is defined as the work performed under the stress applied in proximity of a crack in an elastic or elastic-plastic stress and strain field. J depends on the geometry of the component, the stress applied, the crack size and the elastic-plastic stress-strain curve of the material.

In its simplest form, the material resistance is measured by the elastic-plastic fracture toughness J_{Ic}. Due to the ductile property of the material in its elastic-plastic range considerable stable crack growth may occur.

Normally the material resistance is, however, determined by means of the J-R curve. This property shown by the J-R material curve represents the material resistance against stable crack growth (Tearing).

(2) The original definition of the J-integral is the path-independent line integral according to Rice [17] which is defined for the elastic and elastic-plastic material range as follows:

$$J = \int_{\Gamma}\left(Wdy - \vec{T}\cdot\frac{\partial\vec{u}}{\partial x}\right)ds \quad \text{(B 2.2-1)}$$

For elastic material behaviour J means the strain energy release rate and is correlated to the stress intensity factor K. Thus it is possible to compare J with exact methods:

$$J = -\frac{\partial U}{\partial A} \quad \text{(B 2.2-2)}$$

In the elastic case the following applies:

$$J = G = \frac{K^2}{E} \quad \text{(B 2.2-3)}$$

Strictly speaking the J-integral has not been defined for three-dimensional cases. According to Parks [18] it is possible, at least for the elastic case, to determine the J-integral alongside the crack front via the change in potential energy. In Finite Element Codes this is also implemented for elastic-plastic cases by means of the calculation of the change in potential energy as a consequence of the small displacements of knot points along the crack front.

(3) If all parameters of the solution equation have been specified, the J-integral can be determined as a function of the stress applied and in dependence of the crack size a. In general, the curves look like those shown in **Figure B 2.2-1**. It is recognizable that the sizes have been correlated non-linearly.

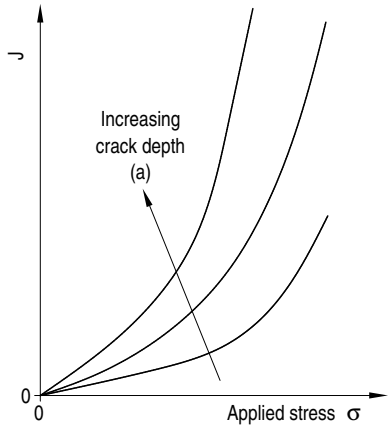

Figure B 2.2-1 Correlation of J and the applied stress [19]

(4) For better clarity the correlation of J and the crack size a at an applied loading s can be converted into a J versus Tearing Modulus ratio, where the Tearing Modulus T is defined as follows:

$$T = \left(\frac{dJ}{da}\right)\cdot\frac{E}{\sigma_0^2} \quad \text{(B 2.2-4)}$$

where:

E : modulus of elasticity

σ_0 : yield point.

From this correlation the so-called crack-resistance curve (J-R curve) is obtained to describe the material resistance against stable crack growth. The comparison of an applied J-integral with the J-R curve enables the determination of the crack size or stress at which unstable crack propagation occurs, see **Figure B 2.2-2**.

The intersection of the curve defining the applied load with the J-R curve of the material results in the point of instability. The stable ductile crack growth Δa is determined from the crack initial length and its growth to attain instability.

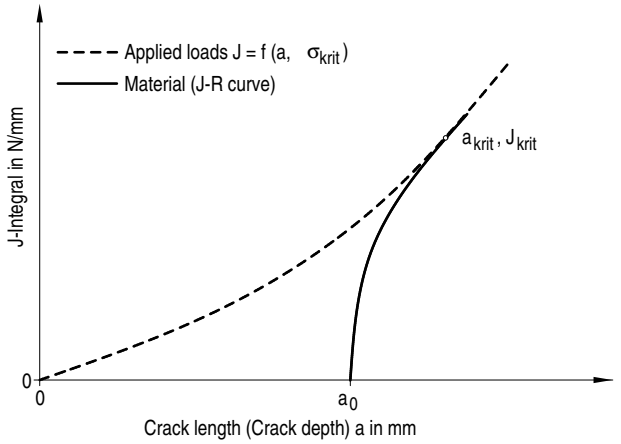

Figure B 2.2-2: Determination of crack instability in the J - Δa - loading diagram

(5) The behaviour of the J-R curve upon J_i (physical crack initiation value) is shown schematically in **Figure B 2.2-3**. Where for a given material with a crack the loading is increased, the J applied will increase and the crack tip will be rounded (blunting). At a certain value of J (depending on the material) the crack starts to propagate in a stable and ductile manner. This point in time is commonly called J_i and may conservatively be used as measure for ductile fracture toughness. Where the load and thus the J applied further increases, the crack will also grow in a stable manner. This correlation is called the J-R curve.

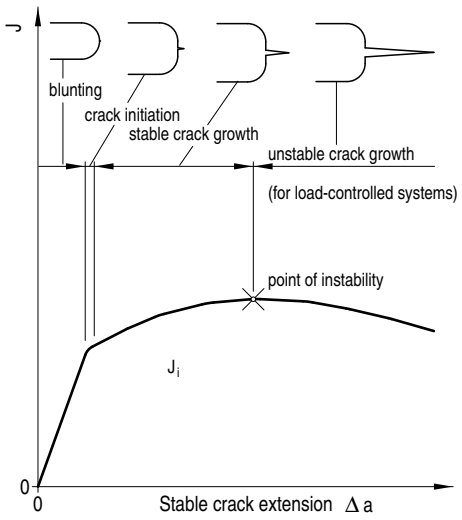

Figure B 2.2-3: Typical crack growth behaviour of ductile materials [19]

(6) Similarly to the J over crack length "a" curve the J-R curve describing the correlation of J and stable crack growth may be entered in a J-T diagram. To determine the point of instability in **Figure B 2.2-3** the J-T curve for the applied load is compared to the J-T curve for the material as shown in **Figure B 2.2-4**. The point of intersection is the point where instability commences, and the respective crack size over the applied J-integral can be determined from the diagram.

Depending on the material and the loadings of the structure the applied J-integral may exceed the material property value, and the crack would become unstable (fast ductile fracture). This behaviour is generally called the tearing instability concept. If the material resistance is high and the applied J-integral is small the crack may continue to grow in a stable manner until the limit load of the structure is attained.

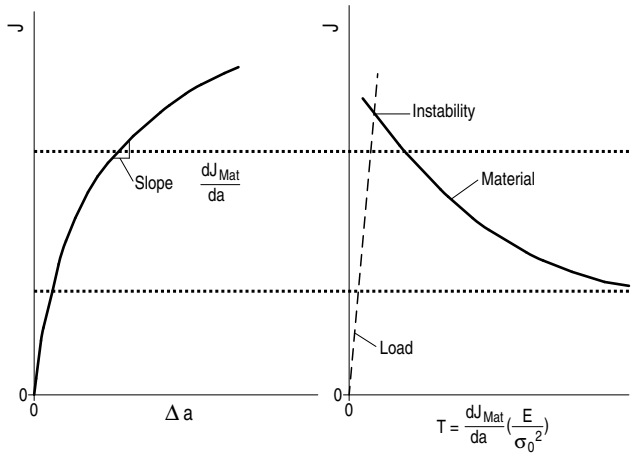

Figure B 2.2-4: Tearing Modulus – Concept for stable crack growth [19]

B 2.2.2 Formula to be applied

(1) The following is suited for fracture-mechanics analyses to the J-T approach:

a) numerical solutions using finite element calculations for cracked components,

b) handbook solutions using the Ramberg-Osgood equation for describing the stress-strain curve [19] – [27],

c) handbook solutions based on finite-element calculations for cracked components [28].

In the following, the formula to be used acc. to b) for handbook solutions are shown as example:

(2) Handbook solutions using the Ramberg-Osgood equation are generally written as follows [19]:

$$J = f(G, a, \sigma, \alpha, n) \qquad \text{(B 2.2-5)}$$

where:

G : geometry parameter of the structure (specimen)

a : crack size

σ : stress

α, n : parameter for the Ramberg-Osgood equation for describing the stress-strain curve.

(3) For fracture mechanics analyses to the J-T approach as per (1) b) the following solutions may be applied:

a) Surface crack in axial direction in a cylinder under internal pressure (infinitely long defect to [22]):

$$J = J^{elastic}(a,P) + J^{plastic}(a,P) \qquad \text{(B 2.2-6)}$$

Note:

(1) $J^{elastic}$ is the elastic contribution, $J^{plastic}$ represents the fully plastic portion.

(2) A solution for finite length flaws is contained in [23].

where

$$J^{elastic}(a,P) = \frac{4 \cdot P^2 \cdot R_0^4 \cdot \pi \cdot a}{E' \cdot (R_0^2 - R_i^2)^2} \cdot F^2\left(\frac{a}{s}, \frac{R_i}{R_0}\right) \qquad \text{(B 2.2-7)}$$

$$E' = E \text{ for plane stress} \qquad \text{(B 2.2-8)}$$

$$E' = \frac{E}{1-\nu^2} \text{ für plane strain} \qquad \text{(B 2.2-9)}$$

$$J^{plastic}(a,P) = \alpha \cdot \sigma_0 \cdot \varepsilon_0 \cdot (s-a) \cdot \frac{a}{s} \cdot h_1\left(\frac{a}{s}, n, \frac{R_i}{R_0}\right) \cdot \left(\frac{P}{P_0}\right)^{n+1} \qquad \text{(B 2.2-10)}$$

with the limit load:

$$P_0 = \frac{2}{\sqrt{3}} \cdot \frac{(s-a)\cdot \sigma_0}{R_c} \qquad \text{(B 2.2-11)}$$

where

$$R_c = R_i + a \qquad \text{(B 2.2-12)}$$

F : functional values as per **Table B 2.2-1**

h_1 : function values as per **Tables B 2.2-2** to **Table B 2.2-4**

F	a/s=1/8	a/s=1/4	a/s=1/2	a/s=3/4
s/R_i=1/5	1.19	1.38	2.1	3.3
s/R_i=1/10	1.20	1.44	2.36	4.23
s/R_i=1/20	1.20	1.45	2.51	5.25

Table B 2.2-1: Function values F

s/R_i=1/5	n=1	n=2	n=3	n=5	n=7	n=10
a/s=1/8	6.32	7.93	9.32	11.5	13.12	14.94
a/s=1/4	7.00	8.34	9.03	9.59	9.71	9.45
a/s=1/2	9.79	10.37	9.07	5.61	3.52	2.11
a/s=3/4	11.00	5.54	2.84	1.24	0.83	0.493

Table B 2.2-2: Function values h_1 for s/R_i=1/5

s/R_i=1/10	n=1	n=2	n=3	n=5	n=7	n=10
a/s=1/8	5.22	6.64	7.59	8.76	9.34	9.55
a/s=1/4	6.16	7.49	7.96	8.08	7.78	6.98
a/s=1/2	10.5	11.6	10.7	6.47	3.95	2.27
a/s=3/4	16.1	8.19	3.87	1.46	1.05	0.787

Table B 2.2-3: Function values h_1 for s/R_i=1/10

s/R_i=1/20	n=1	n=2	n=3	n=5	n=7	n=10
a/s=1/8	4.50	5.79	6.62	7.65	8.07	7.75
a/s=1/4	5.57	6.91	7.37	7.47	7.21	6.53
a/s=1/2	10.8	12.8	12.8	8.16	4.88	2.62
a/s=3/4	23.1	13.1	5.87	1.90	1.23	0.883

Table B 2.2-4: Function values h_1 for s/R_i=1/20

b) Through-thickness crack in axial direction in a cylinder under internal pressure [24]:

$$J = \frac{8\cdot c\cdot \sigma_{fJ}^{\,2}}{\pi \cdot E} \ln\left[\sec\left(\frac{M_{Jax}\cdot \pi \cdot \frac{p\cdot r_m}{s}}{2\cdot \sigma_{fJ}}\right)\right] \qquad \text{(B 2.2-13)}$$

where $r_m = R_i + 0.5\cdot s$ (B 2.2-14)

$$M_{Jax} = \sqrt{1 + 1.2987\cdot \lambda_{ax}^2 - 0.026905\cdot \lambda_{ax}^4 + 5.3549\cdot 10^{-4}\cdot \lambda_{ax}^6} \qquad \text{(B 2.2-15)}$$

$$\sigma_{fJ} = 0.5\cdot\left(R_{p_{0.2}} + R_m\right) \qquad \text{(B 2.2-16)}$$

and the dimensionless parameter:

$$\lambda_{ax} = \frac{c}{\sqrt{r_m \cdot s}} \qquad \text{(B 2.2-17)}$$

Range of application:

Dugdale model, $0 < \lambda_{Ax} \le 5$; $\frac{p\cdot r_m}{s} < \frac{\sigma_{fJ}}{M_{Jax}}$

c) Surface crack in circumferential direction of a cylinder under tension and bending [29]:

$$J = J^{elastic}(a_e, N, M) + J^{plastic}(a, N, M) \qquad \text{(B 2.2-18)}$$

where

$$J^{elastic}(a_e, N, M) = \frac{K_{I,ae}^2}{E'} \qquad \text{(B 2.2-19)}$$

$$E' = E \text{ for plane stress} \qquad \text{(B 2.2-20)}$$

$$E' = \frac{E}{1-\nu^2} \text{ for plane strain} \qquad \text{(B 2.2-21)}$$

$$K_{I,ae} = K_{I,ae}^{tension} + K_{I,ae}^{bending} \qquad \text{(B 2.2-22)}$$

$$K_{I,ae}^{bendng} = \sqrt{\frac{M^2\cdot r_m^{\,2}}{I^2}\cdot \pi \cdot a_e \cdot F_B^2\left(\frac{r_m}{s}, \frac{a_e}{s}, \gamma\right)} \qquad \text{(B 2.2-23)}$$

$$\text{mit } I = \frac{\pi\cdot(R_0^4 - R_i^4)}{4} \qquad \text{(B 2.2-24)}$$

$$K_{I,ae}^{tension} = \sqrt{N^2 \cdot \frac{a_e}{4\cdot \pi \cdot r_m^{\,2}\cdot s^2}\cdot F_T^2\left(\frac{r_m}{s}, \frac{a_e}{s}, \gamma\right)} \qquad \text{(B 2.2-25)}$$

$$a_e = a + \phi \cdot r_y \qquad \text{(B 2.2-26)}$$

$$\text{where } r_y = \frac{1}{\beta\cdot\pi}\cdot\left(\frac{n-1}{n+1}\right)\cdot\left(\frac{K_{I,a}}{\sigma_0}\right)^2 \qquad \text{(B 2.2-27)}$$

$$\phi = \frac{1}{1+\left(\frac{N}{N_0}\right)^2} \qquad \text{(B 2.2-28)}$$

$$J^{plastic}(a, N, M) =$$

$$\alpha\cdot\sigma_0\cdot\varepsilon_0\cdot(s-a)\cdot\frac{a}{s}\cdot h_1\left(\frac{r_m}{s}, \frac{a}{s}, \gamma, \lambda, n\right)\cdot\left(\frac{A}{A_{NC}}\right)^{n+1}\left(\frac{N}{N_0'}\right)^{n+1} \qquad \text{(B 2.2-29)}$$

$$N_0 = \pi\cdot\sigma_0\cdot(R_0^2 - R_i^2) \qquad \text{(B 2.2-30)}$$

$$M_0 = 2\cdot\sigma_0\cdot s\cdot(R_0^2 - R_i^2) \qquad \text{(B 2.2-31)}$$

$$N_0' = \frac{1}{2}\cdot\left[-\frac{N_0^2\cdot r_m\cdot\lambda}{M_0} + \sqrt{\left(\frac{N_0^2\cdot r_m\cdot\lambda}{M_0}\right)^2 + 4\cdot N_0^2}\right] \qquad \text{(B 2.2-32)}$$

the dimensionless parameter:

$$\lambda = \frac{M}{N\cdot r_m} \qquad \text{(B 2.2-33)}$$

$$A = \pi\cdot(R_0^2 - R_i^2) \qquad \text{(B 2.2-34)}$$

$$A_{NC} = \pi\cdot\left[(R_0^2 - R_c^2) + \frac{\pi-\gamma}{\pi}\cdot(R_c^2 - R_i^2)\right] \qquad \text{(B 2.2-35)}$$

$$\text{where } R_c = R_i + a \qquad \text{(B 2.2-36)}$$

Note:
J^e means the adapted elastic portion
J^p represents the fully plastic portion
$K_I = K_{I,tension} + K_{I,bending}$ calculated with
$\beta = 2$ for plane stress

β = 6 for plane strain

F : Function values for $r_m/s = 10$ as per **Table B 2.2-5**

F for $r_m/s = 10$	a/s	$2 \cdot \gamma$					
		27.5°	45°	90°	180°	270°	360°
F_T Tension	0.50	1.446	1.607	1.749	1.815	1.818	1.82
	0.55	—	1.662	1.852	1.908	1.911	1.896
	0.75	1.472	1.793	2.245	2.468	—	2.443
F_B Bending	0.50	1.684					
	0.75	2.159					

Table B 2.2-5: Function values for $r_m/s = 10$

h_1 : Function values for $r_m/s = 10$ as per **Table B 2.2-6**

a/s	n	$2 \cdot \gamma$	h_1		
			$\lambda = 0$	$\lambda = 0.5$	$\lambda = \infty$
0.50	2	45°	17.8	—	—
0.50	2	90°	18.2	32.8	25.5
0.50	2	180°	13.0	—	—
0.50	5	45°	28.8	—	—
0.50	5	90°	33.1	59.4	38.7
0.50	5	180°	20.3	—	—
0.50	10	45°	43.5	—	—
0.50	10	90°	57.2	104.9	51.9
0.50	10	180°	31.2	—	—
0.75	2	45°	48.2	—	—
0.75	2	90°	64.9	113.0	85.9
0.75	2	180°	45.1	—	—
0.75	5	45°	72.3	—	—
0.75	5	90°	110.8	178.1	110.9
0.75	5	180°	63.3	—	—
0.75	10	45°	93.6	—	—
0.75	10	90°	145.4	249.7	103.3
0.75	10	180°	53.5	—	—

Table B 2.2-6: Function values h_1 for $r_m/s = 10$

d) Through-thickness crack in straight pipe under tension and bending [29]

$$J = J^{elastic}(c_e, N, M) + J^{plastic}(c, N, M) \qquad \text{(B 2.2-37)}$$

Note:
$J^{elastic}$ is the elastic contribution, $J^{plastic}$ represents the fully plastic portion, c represents half the crack length (referred to r_m).

where

$$J^{elastic}(c_e, N, M) = \frac{K_{I,ce}^2}{E'} \qquad \text{(B 2.2-38)}$$

$$E' = E \text{ for plane stress} \qquad \text{(B 2.2-39)}$$

$$E' = \frac{E}{1-\nu^2} \text{ for plane strain} \qquad \text{(B 2.2-40)}$$

$$K_{I,ce} = K_{I,ce}^{tension} + K_{I,ce}^{bending} \qquad \text{(B 2.2-41)}$$

$$K_{I,ce}^{tension} = \sqrt{N^2 \cdot \frac{c_e \cdot F_T^2\left(\frac{c_e}{b}, \frac{r_m}{s}\right)}{4 \cdot \pi \cdot r_m^2 \cdot s^2}} \qquad \text{(B 2.2-42)}$$

$$K_{I,ce}^{bending} = \sqrt{M^2 \cdot \pi \cdot c_e \cdot \left(\frac{r_m}{l}\right)^2 \cdot F_B^2\left(\frac{c_e}{b}, \frac{r_m}{s}\right)} \qquad \text{(B 2.2-43)}$$

With plasticity correction factor

$$c_e = c + \phi \cdot r_y \qquad \text{(B 2.2-44)}$$

F_T : Function values as per **Table B 2.2-7**

F_B : Function values as per **Table B 2.2-8**

F_T	c/b=1/16	c/b=1/8	c/b=1/4	c/b=1/2
s/r_m=1/5	1.049	1.176	1.607	3.745
s/r_m=1/10	1.077	1.259	1.802	4.208
s/r_m=1/20	1.127	1.387	2.059	4.811

Table B 2.2-7: Function values F_T

F_B	c/b=1/16	c/b=1/8	c/b=1/4	c/b=1/2
s/r_m=1/5	1.046	1.143	1.423	2.555
s/r_m=1/10	1.070	1.219	1.599	2.896
s/r_m=1/20	1.118	1.343	1.836	3.337

Table B 2.2-8: Function values F_B

$$J_{plastic} = \alpha \cdot \sigma_0 \cdot \varepsilon_0 \cdot c_{Lig.} \cdot \frac{c}{b} \cdot h_1\left(\frac{c}{b}, n, \lambda, \frac{r_m}{s}\right) \cdot \left[\frac{N}{N_0'}\right]^{n+1} \qquad \text{(B 2.2-45)}$$

N_0' in the above equation is obtained from:

$$N_0' = \frac{1}{2} \cdot \left[-\frac{N_0^2 \cdot r_m \cdot \lambda}{M_0} + \sqrt{\left(\frac{N_0^2 \cdot r_m \cdot \lambda}{M_0}\right)^2 + 4 \cdot N_0^2}\right] \qquad \text{(B 2.2-46)}$$

With the limit load:

$$N_0 = 2 \cdot \sigma_0 \cdot r_m \cdot s \cdot \left[\pi - \gamma - 2\arcsin\left(\frac{1}{2}\sin\gamma\right)\right] \qquad \text{(B 2.2-47)}$$

and the limit moment:

$$M_0 = 4 \cdot \sigma_0 \cdot r_m^2 \cdot s \cdot \left[\cos\left(\frac{\gamma}{2}\right) - \frac{1}{2}\sin\gamma\right] \qquad \text{(B 2.2-48)}$$

and the uninterrupted ligament:

$$2c_{Lig} = 2 \cdot r_m \cdot (\pi - \gamma) = 2 \cdot (b\text{-}c) \qquad \text{(B 2.2-49)}$$

the dimensionless parameter:

$$\lambda = \frac{M}{N \cdot r_m} \qquad \text{(B 2.2-50)}$$

h_1 : functional values for through-thickness crack under tension and bending as per **Table B 2.2-9** and **B 2.2-10**

λ	c/b	n=2	n=5	n=10
0.5	1/8	7.222	8.631	9.421
	1/4	6.506	6.063	6.123
1.0	1/8	7.925	9.604	10.958
	1/4	7.363	7.333	8.242
2.0	1/8	7.970	9.335	9.985
	1/4	7.438	7.156	7.519

Table B 2.2-9: Function values h_1 for $r_m/s = 10$

λ	c/b	n=2	n=5

0.5	1/8	9.166	11.737
	1/4	8.706	8.297
1.0	1/8	10.100	13.116
	1/4	9.924	10.072
2.0	1/8	10.136	12.808
	1/4	10.004	9.896

Table B 2.2-10: Function values h_1 for $r_m/s = 20$

(4) Notations

A : cross-sectional area of uncracked cylinder

A_{NC} : area of uncracked ligament in a cracked cylinder

a_e : corrected effective crack depth (Irwin's small-scale yielding correction)

$2c_e$: corrected effective crack length (Irwin's small-scale yielding correction)

2b : pipe circumference (referred to mean diameter)

$2c_{Lig}$: uncracked ligament

E : modulus of elasticity

F : dimensionless function

I : inertia moment

M : bending moment

M_0 : limit load for un-cracked cylinder under bending

n : strain hardening exponent

N : tensile force

N_0 : limit load for un-cracked cylinder under pure tension

N_0' : limit load for un-cracked cylinder under combined tension and bending loading

P : internal pressure

P_0 : limit pressure for the geometry in the ideal-plastic case ($n = \infty$)

R_c : radial distance from center line to crack tip

R_i : inside radius

R_0 : outside radius

r_m : mean radius

s : wall thickness

α : Ramberg-Osgood model parameter

γ : half circumferential crack angle

ε_0 : strain at yield point (reference strain)

λ, λ_{Ax} : dimensionless parameter

ν : Poisson's ratio

σ_0 : yield point (reference stress with $E=\sigma_0/\varepsilon_0$)

ϕ : dimensionless function

B 2.2.3 Required input data

To calculate the J-integral the following input data are required in addition to the data of Section B 1:

a) stress-strain curve, e.g. to Ramberg-Osgood (see **Figure B 2.2-5**):

$$\frac{\varepsilon}{\varepsilon_0} = \frac{\sigma}{\sigma_0} + \alpha \cdot \left(\frac{\sigma}{\sigma_0}\right)^n \qquad \text{(B 2.2-51)}$$

where:

ε : true strain

σ : true stress

ε_0 : strain at yield point

σ_0 : yield point

α, n : Ramberg-Osgood material parameter

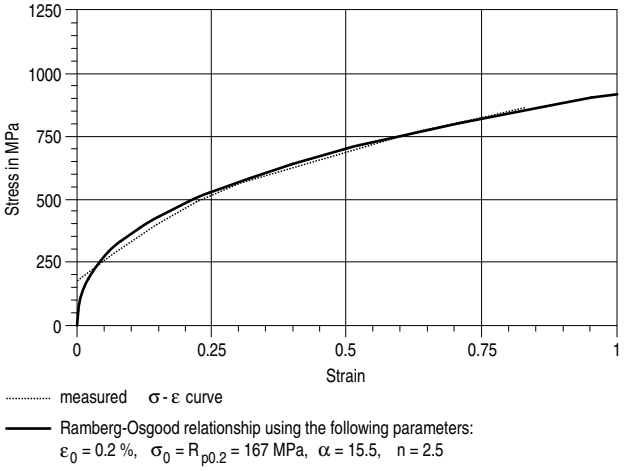

Figure B 2.2-5: True stress-strain curve (schematic)

b) J-T curve

$$T = \left(\frac{dJ}{da} \cdot \frac{E}{\sigma_0^2}\right) \qquad \text{(B 2.2-52)}$$

where:

T : tearing modulus

$\frac{dJ}{da}$: slope of the J-R curve

E : modulus of elasticity

σ_0 : yield point

c) J-R curve for the respective material written as:

$$J = C\,(\Delta a)^N \qquad \text{(B 2.2-53)}$$

J_{Ic} as characteristic value for the onset of stable crack growth

J_{max} as maximum J value in the J-R curve

B 2.2.4 Limits of application

(1) The J-integral may be calculated using numerical methods (finite element method) acc. to B 2.2.2 (1) a) principally without restriction for all metallic materials and geometries.

(2) For methods to B 2.2.2 (1) b) the limits of application of the solutions applied, especially with respect to the cylinder or crack geometry (s/r_m, a/s, a/c) as well as with respect to the Ramberg-Osgood coefficients, shall be adhered to. For the formula given in sub-clauses B 2.2.2 (2) to (4) the following limits of application are valid:

a) axial crack in a cylinder under internal pressure:

aa) Ramberg-Osgood coefficient : $1 \le n \le 10$

ab) relative crack depth: $0 < a/s \le 0.75$

ac) radius-to-wall thickness ratio: $5 \le r_m / s \le 20$

b) surface crack in circumferential direction of a cylinder under tension and bending:

ba) Ramberg-Osgood coefficient : $2 \le n \le 10$

bb) relative crack depth: $0{,}5 \le a/s \le 0.75$

bc) radius-to-wall thickness ratio: $r_m/s = 10$

c) through-thickness crack in circumferential direction of a cylinder under tension and bending (bending stress and axial stress from internal pressure are considered pure bending stress):

ca) Ramberg-Osgood coefficient : $1 \le n \le 7$

cb) crack length: $0 < c/b \le 0.5$

b : half the pipe circumference

cc) radius-to-wall thickness ratio: $5 \leq r_m / s \leq 20$

(3) For J-integral calculations as per B 2.2.2 (1) c) the limits of application given in [28] shall be adhered to.

B 2.3 Two-criteria method

B 2.3.1 Fundamentals

(1) The two-criteria method is used for assessing the failure behaviour of components between the limiting cases of linear-elastic and fully plastic material condition in a closed concept. The consideration of the fracture-mechanics characteristic values makes assessments possible with regard to crack initiation, stable crack propagation and crack instability. The two-criteria method was developed by CEGB (Central Electricity Board, Great Britain) and transposed into Routine R6 by British Energy [30]. The basic principles of the procedure were taken over in a series of fracture-mechanics evaluation procedures (e.g. flaw evaluation procedures SINTAP [31] and DNV/SAQ [32], into British Standard 7910 [33] and the Fitness-for-Service handbook API 579 [34] as well as into the FKM Guideline [35]. The individual calculation steps, the evaluation subject to different analysis levels, the approach for dissimilar welds and the consideration of further effects (e.g. weld residual stresses and secondary stresses) have been explained in R6 [30] as well as British Standard 7910 [33].

(2) The component shall be evaluated by means of a failure assessment diagram (FAD) which contains a limit curve $K_f = f(L_r)$ defined by the strength characteristics of the material as well as the loading parameters K_f and L_r. The limit curve enclosed the "safe" area where no failure of a cracked component is possible (see **Figure B 2.3-1**).

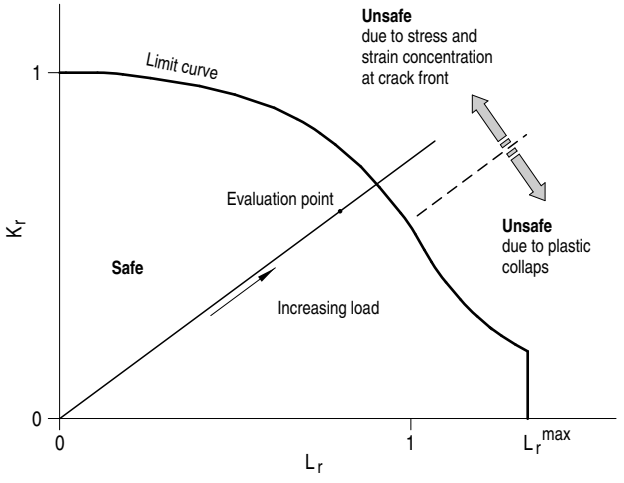

Figure B 2.3-1: Failure assessment diagram (FAD), principal sketch [35]

(3) K_r is the linear-elastic stress intensity factor K referred to the crack toughness K_{mat}

$$K_r = \frac{K}{K_{mat}} \qquad \text{(B 2.3-1)}$$

(4) L_r is the degree of plasticity, i.e. the loading F referred to the plastic instability load F_e of the cracked component.

$$L_r = \frac{F}{F_e} \qquad \text{(B 2.3-2)}$$

(5) According to the original formulation of the limit curve by Ainsworth [36] the loading parameters K_f and L_r can be converted to the elastic-plastic J-integral by means of the function $f(L_r)$. In this case, secondary stresses shall be accounted for additionally.

(6) For given geometry and loading conditions of the cracked component as well as for relevant material characteristic values the coordinates (L_f, K_r) of an evaluation point are calculated as limit state when considering crack initiation and be compared to the limit curve. Critical conditions at crack initiation are defined by point B on the limit curve (**Figure B 2.3-2**). The location of points beneath the limit curve (point A) means safe component conditions, and of points outside the limit curve (point C) unsafe component conditions.

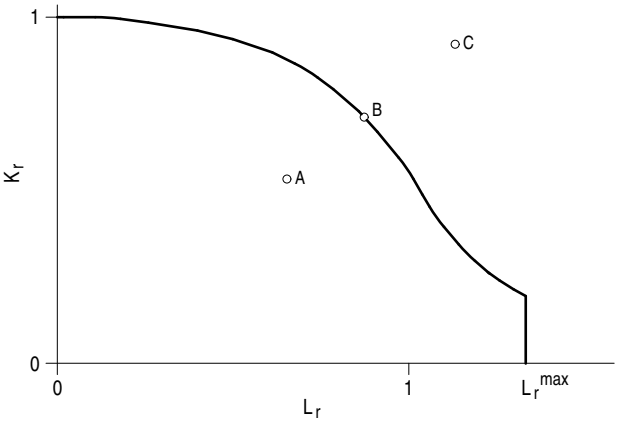

Figure B 2.3-2: Failure assessment diagram (FAD) for limit state crack initiation, principal sketch [35]

(7) As regards the failure upon stable ductile crack extension Δa, the coordinates (L_f, K_r) are determined for a number of evaluation points by step-by-step extension of crack size by Δa (typically: some tenth of mm only at each step) (**Figure B 2.3-3**). Critical conditions are defined by the number of evaluation points $B - B_1$. The points $A - A_1$ define safe component conditions and $C - C_1$ unsafe component conditions.

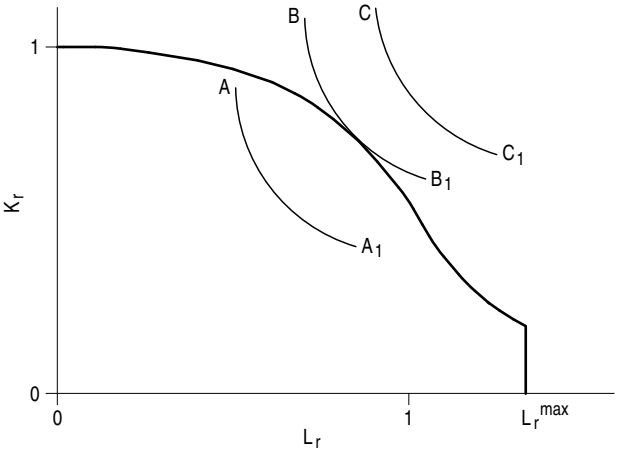

Figure B 2.3-3: Failure assessment diagram (FAD) for limit state crack instability, principal sketch [35]

B 2.3.2 Formulae to be applied

For fracture-mechanics analysis to the two-criteria method the following solutions can be applied:

a) analytical solutions described in handbook [32],

b) other analytical solutions for calculating the stress intensity factors and the plastic instability load as far as they have been confirmed for the respective application by comparison with numerical method or experimental investigations,

c) solutions based on numerical methods (e.g. with the finite element method).

B 2.3.3 Limits of application

When calculating the stress intensity factors and the plastic instability load the limits of application of the respective solutions applied (e.g. to [32]) shall be adhered to, especially with respect to the cylinder and crack geometries (s/R, a/s, a/c).

B 2.4 Damage mechanisms (local approach)

B 2.4.1 Fundamentals

(1) The local approach is based on the use of micro-mechanical material models. Among the various micro-mechanical methods to model the ductile material behaviour the GTN model of Needleman and Tvergaard to [38] based on the Gurson yield function to [39] is often applied. Other equivalent models may also be used, e.g. the Rousselier model [40]. The micro-mechanical model considers the formation and growth of voids as it is characteristic of the material behaviour of metallic materials. The void growth is here described by a modified yield function. In its essentials, the “damage” caused by the voids, thus expressed as damage mechanism, will cause a decrease of strength in which case the following mechanisms are effective, **Figure B 2.4-1** [40]:

a) nucleation of voids (pores)

b) growth (extension) of these voids

c) coalescence of voids (micro-cracks).

The damage is expressed by the share of voids in the total volume. At a void volume of 0 no damage exists and the yield function corresponds to that of the undamaged volume. If the voids fill the total volume, i.e. the void volume is 1, the considered volume has no remaining stability at all.

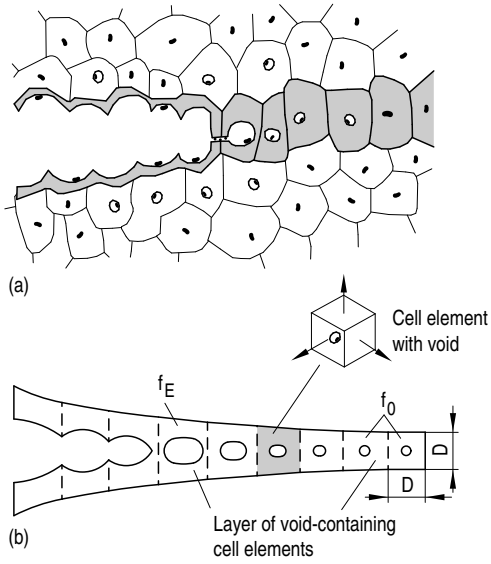

Figure B 2.4-1: a) Representation of the ductile fracture by nucleation, growth and coalescence of pores
b) Processing zone shown by cell elements, each cell with an initial volume f_0 contains one pore.

(2) Since the stress and strain field ahead of the crack must be determined exactly, as a rule numerical procedures, such as finite element techniques, are used for the application of the local approach, in which case the material models for the porous material behaviour have to be provided accordingly. Commercial finite element codes already offer the local approach option by implementing a material model for porous material plasticity, such as in [40].

In the following, the damage models to Gurson, Tvergaard & Needleman (GTN model) as well as to Rousselier are described.

B 2.4.2 GTN model (Gurson, Tvergaard & Needleman)

B 2.4.2.1 Formulae to be applied

(1) The damage is quantified through plastic yielding by extending the yield function, e.g. the von Mises theory. In this case, the influence of the voids is indicated by the specific void volume f, where for $f = 0$ the extended yield function is reduced to the known von Mises function. The formulae hereafter have been taken from [41]. Other criteria may also be used. The extended yield function is obtained as follows:

$$\Phi = \left(\frac{q}{\sigma_y}\right)^2 + 2\cdot q_1 \cdot f \cdot \cosh\left(-q_2 \cdot \frac{3\cdot p}{2\cdot \sigma_y}\right) - \left(1 + q_3 \cdot f^2\right) = 0 \qquad \text{(B 2.4-1)}$$

where

$$S = p \cdot I + \sigma \qquad \text{(B 2.4-2)}$$

as the deviating portion of the Cauchy stress tensor σ

and

$$q = \sqrt{\frac{3}{2}\cdot S : S} \qquad \text{(B 2.4-3)}$$

the effective von Mises stress;

$$p = -\frac{1}{3}\sigma : I \qquad \text{(B 2.4-4)}$$

is the hydrostatic pressure and

$$\sigma_y\left(\bar{\varepsilon}^{\,pl}_m\right)$$

the yield stress of the fully plastic matrix material as a function of $\bar{\varepsilon}^{\,pl}_m$, the plastic equivalent strain in the matrix. The material parameters are called q_1, q_2, q_3.

The Cauchy stress σ is defined to be the force per “unit square considered” in which case the unit square consists of the solid matrix material and the pores.

The function $f = 0$ ($r = 1$) implies that the material is fully plastic, but has no pores; therefore the Gurson yield function is reduced to the von Moses yield function.

$f = 1$ ($r = 0$) implies that the material is full of pores and is no more capable of resisting stress. In general, this model generally results in sensible physical values for $f < 0.1$ ($r > 0.9$).

(2) According to Tvergaard & Needleman [41] an effective damage $f^*(f)$ is defined and inserted into the yield function Φ. Referred to the pore volume portion, this function $f^*(f)$ is defined as follows:

$$f^* = \begin{cases} f & \text{if } f \le f_c \\ f_c + \dfrac{\bar{f}_F - f_c}{f_F - f_c}\cdot\left(f - f_c\right) & \text{if } f_c < f < f_F \\ \bar{f}_F & \text{if } f \ge f_F \end{cases} \qquad \text{(B 2.4-5)}$$

where

$$\bar{f}_F = \frac{q_1 + \sqrt{q_1^{\,2} - q_3}}{q_3} \qquad \text{(B 2.4-6)}$$

Up to a critical pore volume portion f_c f and f^* are identical. Complete failure occurs if f_F is attained.

The parameters f_c and f_F shall be available as input data which then predict material failure if $f_c < f < f_c$. These parameters are determined by the mechanisms of micro-fracture and coalescence of pores. Where $f \ge f_F$, total material failure will occur. In a finite element calculation failure is realized by removing the finite element having no more resistance to stress.

(3) Plastic yielding is assumed to be normal to the plasticized surface:

$$\dot{\varepsilon}^{pl} = \dot{\lambda} \cdot \frac{\partial \Phi}{\partial \sigma} \quad \text{(B 2.4-7)}$$

The hardening of completely dense material without pores is given by

$$\sigma_y = \sigma_y\left(\bar{\varepsilon}_m^{pl}\right) \quad \text{(B 2.4-8)}$$

The development of the plastic equivalent strain in the matrix is described by the following equation for plastic work:

$$(1-f)\cdot\sigma_y\dot{\bar{\varepsilon}}_m^{pl} = \sigma : \dot{\varepsilon}^{pl} \quad \text{(B 2.4-9)}$$

This model is shown in **Figure B 2.4-2** [40] in which case the plasticized surface is shown in the p-q plane for the various pore volume fractions.

In **Figure B 2.4-3** [40] the behavior of porous material under tension and bending loading is compared to the behavior of a perfectly plastic material. Under pressure the porous material will harden, under tension loading the material will soften due to pore nucleation and growth.

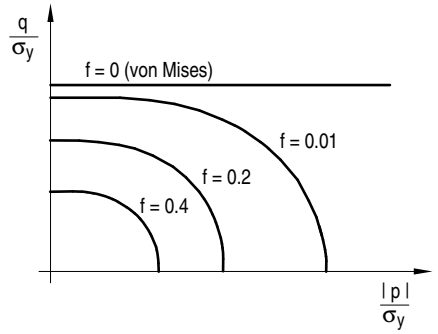

Figure B 2.4-2: Scheme of plasticized surface in the p-q plane

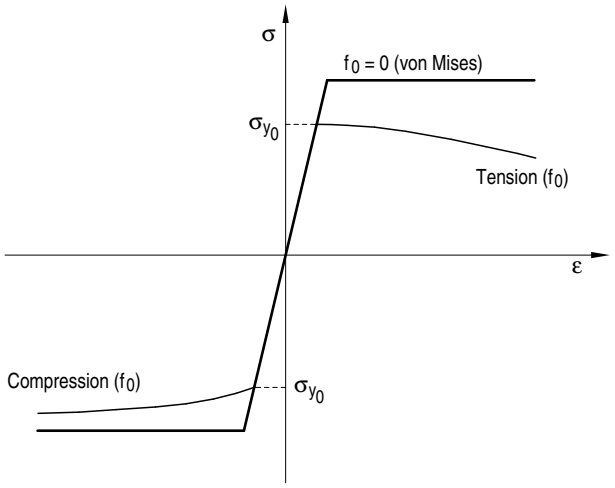

Figure B 2.4-3: Scheme of uni-axial behavior of porous material (perfectly plastic matrix material with an initial pore volume faction f_0)

(4) The total change in pore volume fraction is given by:

$$\dot{f} = \dot{f}_{gr} + \dot{f}_{nucl} \quad \text{(B 2.4-10)}$$

where $\dot{f}_{gr}$ represents the change due to growth of existing pores and $\dot{f}_{nucl}$ the change due to newly formed pores. The growth of existing pores is based on the mass conservation law and referred to the pore volume fraction is expressed as follows:

$$\dot{f}_{gr} = (1-f)\cdot\dot{\varepsilon}^{pl} : I \quad \text{(B 2.4-11)}$$

The pore nucleation is given by a strain-controlled relation:

$$\dot{f}_{nucl} = A\cdot\dot{\bar{\varepsilon}}_m^{pl} \quad \text{(B 2.4-12)}$$

where

$$A = \frac{f_N}{s_N\cdot\sqrt{2\cdot\pi}}\cdot\exp\left[-\frac{1}{2}\cdot\left(\frac{\bar{\varepsilon}_m^{pl}-\varepsilon_N}{s_N}\right)\right] \quad \text{(B 2.4-13)}$$

The normal strain distribution for pore nucleation has the mean value ε_N and the standard deviation s_N. f_N is the volume fraction of the existing pores in which case the pores can only be formed under tension.

The pore nucleation function A/f_N is assumed to be normally distributed for various values of the standard deviation s_N, as shown in **Figure B 2.4-4** [40].

Figure B 2.4-5 [40] shows the extent of softening for the uni-axial tensile test of a porous material for various values of f_N.

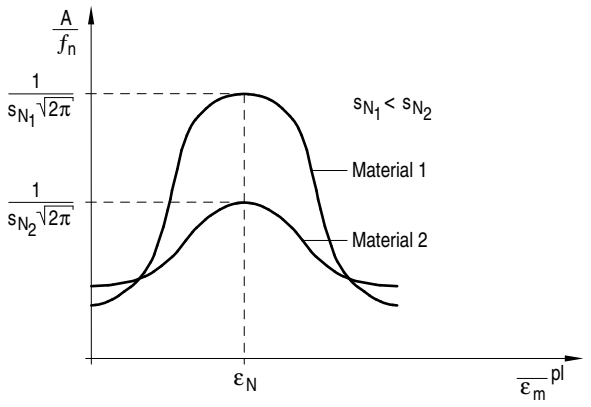

Figure B 2.4-4: Function of A/f_N for pore formation

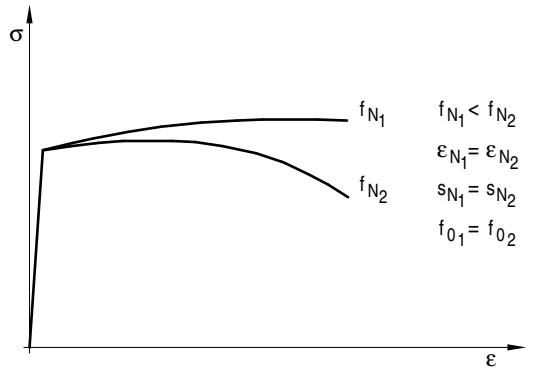

Figure B 2.4-5: Softening (under uni-axial tension) as a function of f_N

B 2.4.2.2 Required input data

a) Parameters q_1, q_2, and q_3

The parameters q_1, q_2 and q_3 are directly needed for the porous metal plasticity model. For typical metals the following values are given in literature: q_1 = 1.0 to 1.5; q_2 = 1.0 and $q_3 = q_1^2$ = 1.0 to 2. In the original Gurson model $q_1 = q_2 = q_3$ = 1.0. For greater accuracy, these values may be inserted in dependence of temperature.

b) r_0, for the relative initial density of the porous material,

c) ε_N, s_N and f_N; for a first approach the values taken from the literature ε_N = 0.1 to 0.3, s_N = 0.05 to 0.1 and f_N = 0.04 can be used.

d) f_c and f_F

B 2.4.3 Rousselier model

B 2.4.3.1 Formulae to be applied

(1) Rousselier [39] starts with a generally formulated thermo-mechanical approach for a material to be described with a continuum mechanics model. Here, the von Mises yield function is extended by a term which, in dependence of the actual damage, describes the influence of the hydrostatic stress portion on the yield behavior.

(2) The yield function to Rousselier is obtained as follows:

$$\Phi = \frac{q}{1-f} + \sigma_k \cdot D \cdot f \cdot \exp\left[\frac{-p}{(1-f)\cdot\sigma_k}\right] - \sigma_y = 0 \qquad \text{(B 2.4-14)}$$

where q describes the actual yield stress, p the hydrostatic pressure and σ_y the von Mises stress. The quantities σ_k and D are material constants. In addition, the yield function contains the damage variable f which represents the ratio of the volume of voids enclosed in the material to the total volume of the material, with:

$$f = \frac{V_{damaged}}{V_{total}} \qquad \text{(B 2.4-15)}$$

The damage variable f can assume values between 0 and 1. f = 1 would mean that no material volume is present. In the case where the material does not contain voids, f = 0 applies, and the yield function of Rousselier is reduced to the von Mises yield function. The dependence of the yield behaviour on the hydrostatic stress condition within the Rousselier model is demonstrated by comparing the von Mises yield function with the Rousselier function, **Figure B 2.4-6**.

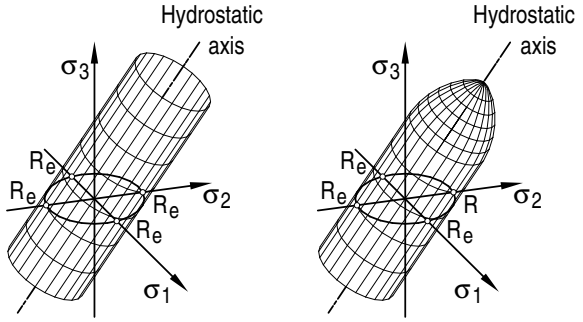

Source: MPA Universität Stuttgart

Figure B 2.4-6 Yield limit surface to von Mises (left) and to Rousselier (right)

(3) The formulae to be applied regarding hardening behaviour and yield law can be taken from clause B 2.4.2.1.

(4) Pore formation (nucleation of voids) takes place when the yield strength R_e is reached, i.e.:

$$q \geq R_e \qquad \text{(B 2.4-16)}$$

From the plastic distortion rate $\dot{\varepsilon}^{pl}$ the volume growth of the voids is obtained to read:

$$\dot{f} = (1-f)\cdot\dot{\varepsilon}^{pl} \qquad \text{(B 2.4-17)}$$

B 2.4.3.2 Required input parameters

a) Parameters σ_k and D

These parameters are material constants obtained from the derivation, but have no direct relation to the micro-structure. In [39] Rousselier proposes to select values between 1.5 and 2 for D presuming small initial void volumes. In literature, D = 2 is often used. σ_k describes the material resistance to void growth. Acc. to [39] the following can be taken

$$\sigma_k = (2/3)\cdot R_e \qquad \text{(B 2.4-18)}$$

b) Initial void volume f_0 and critical void volume f_c

These parameters can be determined either directly from the macro-structure or by numerical adaptation to the experimentally determined load-deformation behaviour.

B 2.4.4 Limits of application

(1) The models described in B 2.4.2 and B 2.4.3 can be applied to all geometries and crack types without restriction. The damage development exclusively depends on the local stress and strain condition. Due to this fact, these models are called local damage models. The disadvantage of local damage models is that due to materials softening the strains and the damage theoretically are localized in an infinitely thin area [39]. In this case, however, the damage mechanics solution depends on the size of the element. In practice, this problem can be circumvented by firmly linking the element size to the micro-structure of the material to be described. Often authors assume that the width of the experimentally observed localization zones directly depends on the distance of the primary voids leading to failure [39]. This approach will be problematic if due to high stress gradients or small component cross-sections very small elements are needed. So-called non-local damage models will provide approach solutions in this respect. In the past, various non-local approaches were presented to eliminate the dependence on element size [42], [43], [44], [45]. A non-local formulation of the damage model makes a description of the damage zone independently of the element size possible. The numerical expenditure, however, will be considerably increased.

(3) The GTN model requires a calibration of the parameters q_1, q_2 and q_3 as well as ε_N, s_N and f_N. Alternatively, the values given under B 2.4.2.2 can be used. In general, this model leads to sensible physical values for f < 0.1 (r > 0.9).

B 2.5 Procedure for calculating the fatigue crack growth

Note:
In this section only cracks are considered the dimensions of which exceed 0.5 mm (macro-cracks).

B 2.5.1 Fundamentals

(1) The sub-critical crack extension under cyclic loading is called fatigue crack growth and can principally be described with linear-elastic fracture mechanic (LEFM) methods. The crack propagation rate is defined as function da/dN = f(ΔK) with the crack depth a and the number of load cycles N. Where the experimentally determined crack growth rate da/dN is entered in a log-log system as function of the cyclic range of the stress intensity factor $\Delta K = K_{max} - K_{min}$, the so-called crack propagation curve is obtained with the characteristic course as shown in **Figure B 2.5-1**.

(2) The curve shown in **Figure B 2.5-1** may e.g. described by the crack growth equation acc. to Erdogan-Ratwani [46] for the areas I to III. As regards its practical application within the range of application of KTA 3206 only the stationary range II is relevant.

(3) The course of the crack growth curve depends on the material and is influenced by a number of factors (e.g. by the environment due to corrosion processes at the crack tip, by the temperature, by the ratio of $R = K_{min}/K_{max}$). As defined, cracks below the threshold value ΔK_{th} are not capable of propagating further. Instable crack propagation occurs at a value ΔK_c if the critical stress intensity factor $K_{max} \approx K_{Ic}$ is reached.

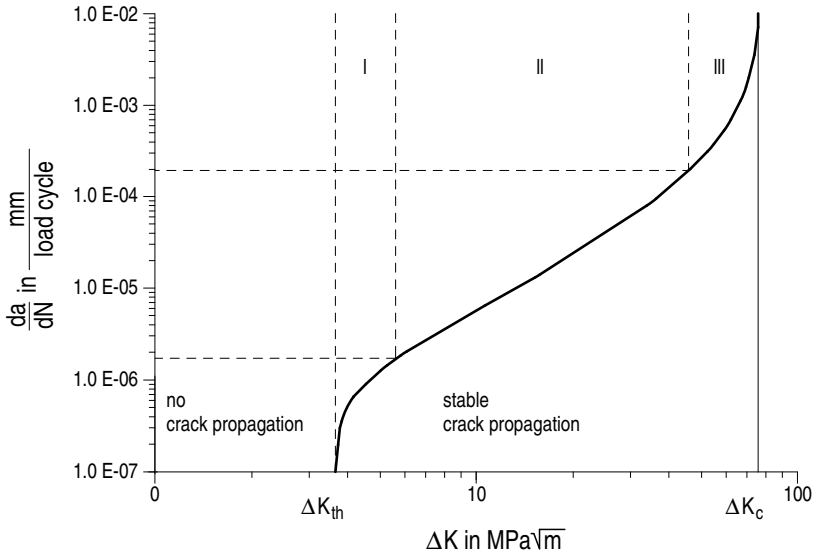

Figure B 2.5-1: Crack propagation at cyclic loading, principal sketch [35]

B 2.5.2 Procedures to be applied

(1) Crack propagation calculations may be made using the crack propagation equation to Paris-Erdogan [47]

$$\frac{da}{dN} = C \cdot (\Delta K)^m \qquad \text{(B 2.5-1)}$$

to follow the method described in ASME BPVC Section XI [48], by which the linear region (area II) of the crack propagation curve shown in **Figure B 2.5-1** has been approximated.

Note:
Further crack growth equations are e.g. given in [30], [35] and described with respect to their range of application.

(2) The factor C and the exponent m are material-dependent quantities. Covering values for air and defined water-chemical boundary conditions for PWR and BWR plants may be determined for ferritic materials [49] as well as for austenitic materials (without influence of the environment) [50] in dependence of the R value and the temperature in accordance with ASME BPVC Section XI.

Note:
Further values for C and m are e.g. shown in [31], [34].

(3) For austenitic materials the crack growth equation acc. to Paris-Erdogan shall be extended by the term da/dN_{Env} to calculate the crack growth under environmental conditions.

$$\left(\frac{da}{dN}\right)_{total} = \left(\frac{da}{dN}\right)_{Air} + \left(\frac{da}{dN}\right)_{Env} \qquad \text{(B 2.5-2)}$$

According to NUREG/CR-6176 [51] the following applies:

$$\left(\frac{da}{dN}\right)_{Env} = C_{Env} \cdot S(R)^{0.5} \cdot T_R{}^{0.5} \cdot (\Delta K)^{1.65} \qquad \text{(B 2.5-3)}$$

$$S(R) = 1 + 1.8 \cdot R \qquad \text{for } R \le 0.8 \qquad \text{(B 2.5-4)}$$

$$S(R) = -43.35 + 57.97 \cdot R \qquad \text{for } R > 0.8 \qquad \text{(B 2.5-4)}$$

T_R : rise time in seconds for one cycle

The values for C_{Env} given in [51] and [52] depend on the oxygen content of the environment of BWR and PWR plants and apply to 5 ppb, 0.2 ppm and 8 ppm O_2.

Note:
Depending on the rise time T_R further crack growth equations da/dN are given in [51] for austenitic materials and for Alloy 182 in [32].

(4) The crack growth shall be calculated by integration of the crack growth equation used.

(5) Crack growth is accelerated by existing residual tensile stresses. They have to be accounted for in the calculation of the stress intensity factors K_{max} and K_{min} and will change the ratio $R = K_{min}/K_{max}$. In addition crack growth may be influenced by the sequence of the load cycles within the load spectrums during the transition from low to high loadings. In the case of multistage spectrums the time sequence of the load cycles shall be considered appropriately (see e.g. the explanations in [35]).

B 2.5.3 Required input data

In addition to the data mentioned in section A 1 the following input data are required for fatigue crack growth calculation:

a) load spectrum
b) fluid conditions
c) residual stresses.

B 2.5.4 Limits of application

(1) Material property values shall be used which apply to the crack growth curve in area II.

(2) When calculating the stress intensity factors the limits of application of the solution, especially with respect to the cylinder and crack geometries (s/R, a/s, a/c) shall be observed.

B 3 Procedures for the determination of leak flow rates

B 3.1 Leakage area calculations

B 3.1.1 Fundamentals

(1) To verify the timely detection of through-thickness cracks the mass flow $\dot{m}$ escaping from a leak in dependence of the crack length 2c shall be determined. As the quantity of the fluid escaping depends on the size of the pertinent crack opening area, it is required to know the crack opening area as a function of the crack length.

(2) The analytical calculation models for leakage areas of through-thickness defects are primarily based on the approaches for flat plates the validity of which was extended by suitable modifications and theory of shell considerations to cover cylinders and spherical components. The models make calculations for simple pipe and vessel geometries with circumferential cracks and axial cracks under internal pressure and bending loading possible. In the case of ductile materials the leakage area will be enlarged by the formation of a plastic zone at the crack tip as well as by plastic deformations depending on

the ratio of membrane stress to flow stress. Besides the linear elastic models analytical calculation models for small plastic crack zones primarily to the Dugdale model as well as models considering the elastic-plastic material behaviour have been derived.

(3) The exactness of the various model approaches has been checked by experimental and numerical investigations. As the evaluation of these investigation shows, linear-elastic calculation models generally lead to lower bound values and thus conservative results with respect to the determination of detectable leakage crack lengths compared to models with plasticity correction [54].

B 3.1.2 Procedures to be applied

(1) Leakage areas shall be determined by means of

a) validated analytical methods or

b) finite element calculation or

c) experimental investigations.

(2) The procedure mentioned hereafter [55] shall normally be used for the analytical leakage area calculation of cracks in cylinders, spherical components and plates where primarily tensile loadings are effective normal to the crack:

a) for linear-elastic material behaviour

aa) leakage area for a plate of infinite dimensions

$$A_0 = 2 \cdot \pi \cdot \sigma \cdot c^2/E' \qquad \text{(B 3.1-1)}$$

where:

σ : membrane stress

c : half the crack length

E : modulus of elasticity

E‘ = E for plane stress condition

E‘ = E/(1-ν^2) for plane strain condition

ν : Poisson’s ratio

ab) leakage area for cylinders with longitudinal crack and circumferential cracks

$$A = \alpha(\lambda) \cdot A_o \qquad \text{(B 3.1-2)}$$

where

for longitudinal cracks:

$$\alpha(\lambda) = 1 + 0.1 \cdot \lambda + 0.16 \cdot \lambda^2;\ 0 \le \lambda \le 8 \qquad \text{(B 3.1-3)}$$

for circumferential cracks:

$$\alpha(\lambda) = (1 + 0.117 \cdot \lambda^2)^{0.5};\ 0 \le \lambda \le 5 \qquad \text{(B 3.1-4)}$$

$$\lambda = [12 \cdot (1 - \nu^2)]^{1/4} \cdot c \cdot (r_m \cdot s)^{-1/2} \qquad \text{(B 3.1-5)}$$

α : buckling factor

λ : shell parameter

ν : Poisson’s ratio

c : half the crack length

r_m : mean shell radius

s : wall thickness

ac) leakage area for cracked spherical shell

Equation B 3.1-2 with

$$\alpha(\lambda) = 1 + 0.02 \cdot \lambda + 0.22 \cdot \lambda^2;\ 0 \le \lambda \le 5 \qquad \text{(B 3.1-6)}$$

λ : shell parameter

b) For elastic-plastic material behaviour

To account for plastic deformation at the crack tip the leakage areas determined by means of equations B 3.1-1 or B 3.1-2 may be extended by the factor $\gamma(s)$.

$$\gamma(s) = \frac{1}{s} \cdot \left[(1-s)^2 \cdot \sec^2 \frac{\pi \cdot s}{2} + \frac{4}{\pi} \cdot (1-s) \cdot \tan \frac{\pi \cdot s}{2} - \frac{8}{\pi^2} \ln \cos \frac{\pi \cdot s}{2} \right] + \left(1 - \frac{1}{s}\right) \cdot \left[\frac{2}{\pi} \cdot \sqrt{\left(\sec^2 \frac{\pi \cdot s}{2} - 1 \right)} + (1-s) \cdot \sec^2 \frac{\pi \cdot s}{2} \right] \qquad \text{(B 3.1-7)}$$

where:

s = σ/σ_f , but not to exceed 0.9

σ : membrane stress

σ_f : flow stress

For the flow stress the following applies:

a) The following flow stresses may be used:

$\sigma_f = (R_p + R_m)/2$ for ferritic materials

$\sigma_f = 3 \cdot S_m$ for austenitic materials

with S_m : equivalent stress intensity to KTA 3201.2.

b) The use of $\sigma_f = R_m$ leads to the determination of minimum leakage areas.

(3) In case of more complex geometries and loadings where the analytical method to (2) cannot be applied, e.g. in the region of pipe bends, nozzles or abrupt wall thickness increase, the leakage areas shall be determined by means of other validated analytical procedures, finite element calculations or experimental investigations. The parameters and boundary conditions to be considered shall be selected on the basis of sensitivity considerations such that the leak opening area is not over-estimated.

B 3.1.3 Limits of application

When calculating leakage areas as a function of the through-thickness crack length, the limits of application of the calculation models e.g. referred to

a) the geometry of the component,

b) the R/s ratio,

c) the crack length 2c and

d) the type and extent of loading

shall be observed.

B 3.2 Determination of the leak flow rates

B 3.2.1 Fundamentals

Where a leak detection system is present, beak preclusion verifications for pressure-retaining components shall ensure that for the purpose of a conservative consideration, the leak rate calculation leads to the estimation of smaller values then would be obtained with the real leak flow. To ensure estimation with lower values, corresponding assumptions shall be made within the verification with approximation methods as regards both structure-mechanics and thermo-hydraulic aspects. In such case, the leakage area of the considered through-thickness crack shall be estimated to attain a reduced value by respective assumptions as regards its shape. In addition, the flow resistance of the flow through crack-type leaks shall be estimated to be higher (e.g. by a curve covering the connection between crack surface roughness and resistance value) and a flow model shall be used that generally delivers smaller leak rates compared to other model approaches. Comparative calculations show that leak flow calculations with simplified methods can contain great uncertainties [56].

Note:

(1) Where a compressible fluid flows from one vessel through a flow channel (leak, pipe, nozzle, etc.) to another vessel (or into the atmosphere), the mass flow, at constant pressure at the flow channel inlet region, will first increase to attain its maximum value, the critical mass flow, at the channel exit region with decreasing pressure.

Here, at the narrowest point or at the flow channel outlet, sound velocity is obtained. In the case of two-phase flow, critical mass flow is also observed and also when a nearly incompressible fluid (e.g. water) escapes if the pressure along the flow path is essentially less than the saturation pressure pertinent to the fluid temperature. The critical phenomena are influenced by thermodynamic and fluid-dynamic imbalance processes which depend on the flow channel geometry and the flow condition at the channel inlet [57].

(2) The critical mass flow density depends on external factors of influence such as the pressure and the enthalpy at the flow channel inlet region as well as on geometric factors such as the type of flow channel, the hydraulic diameter, the flow channel length and roughness of the surfaces. Internal factors of influence are possible differences between the velocities of the water and steam phase in the flow channel (fluid-dynamic imbalance) as well as conditions of thermal imbalance, e.g. superheated water [57].

B 3.2.2 Procedures to be applied

B 3.2.2.1 General

(1) Depending on the thermodynamic fluid condition prior to fluid entry into the flow channel and on the geometric boundary conditions different calculation formulae shall be used. For single-phase discharge of water with a temperature less than the saturation temperature of the ambient pressure (discharge of cold water) the Bernoulli equation should be used, and for the discharge of sub-cooled water with a temperature exceeding the saturation temperature of the ambient pressure as well as negligible steam portion the “modified” Bernoulli equation [64] should be used. With an increasing steam portion especially in the saturation region the use of two-phase models, e.g. the homogenous equilibrium model (HEM) [57] is recommended. For the superheated steam region the use of equations for escaping gas flow with friction is recommended. For simplified leak rate calculations the methods to Pana [58), Moody [59], Fauske [60], Henry [61], and Estorf [62] are basically suited for the purpose of one-dimensional flow modelling assuming critical (i.e. maximum) mass flow densities especially for the two-phase region, in which cases the respective limits of application shall be observed. These methods have been sufficiently confirmed by recalculations within leak flow experiments (see e.g. [65].

(2) It shall be noted that especially in case of small crack-type leaks in relatively thick-walled structures sub-critical discharge flows have to be expected. For sub-critical discharge flows a conservative assumption of the flow resistance factor is subject to other uncertainties than for critical discharge. For the calculation of sub-critical discharge flows thermo-hydraulic solution algorithms (e.g. [63]) or experimentally validated simplified procedures should be used that differ from the procedures mentioned. In addition, it is recommended in individual cases to perform even complex fluid-dynamic calculations, e.g. CFD – computational fluid dynamics methods.

B 3.2.2.2 Single-phase discharge of a sub-cooled liquid

(1) According to the modified Bernoulli equation, the mass flow density G (leak rate divided by leakage area) for the frictional single-phase discharge of sub-cooled water with a temperature above the saturation temperature of the ambient pressure and negligible steam portion through a crack-type leak depends on the difference between the stagnation pressure p_0 at the flow channel inlet and the saturation pressure p_S for the stagnation temperature as assumption for the pressure in the leak discharge region. In addition, G depends on the fluid density ρ_S for the stagnation temperature and the flow resistance ζ. According to [64] the functional correlation can be written as follows:

$$G = \sqrt{\frac{2 \cdot [p_0 - p_S(T_0)] \cdot \rho_S(T_0)}{1 + \zeta}} \qquad \text{(B3.2-1)}$$

where

G : mass flow density

p_0 : stagnation pressure (static pressure of the fluid upstream of inlet into the crack)

$p_S(T_0)$: saturation pressure at stagnation temperature T_0

T_0 : stagnation temperature (fluid temperature fluid upstream of inlet into the crack)

$\rho_S(T_0)$: saturation value of fluid density at stagnation temperature

ζ : flow resistance

The validity of this equation is given if the thermodynamic condition of the fluid at the mouth of the crack exit is even nearing saturation conditions.

(2) The flow resistance values is composed as follows:

$$\zeta = \zeta_{Ein} + \lambda \cdot \frac{s}{D_h} + \zeta_{Aus} \qquad \text{(B 3.2-2)}$$

where

D_h : hydraulic diameter

s : wall thickness (flow path length)

ζ_{Ein} : flow inlet loss

ζ_{Aus} : flow outlet loss

λ : flow resistance factor

For break preclusion verifications the inlet loss ζ_{Ein} = 0.5 and and outlet loss ζ_{Aus}= 0 shall be taken.

For the hydraulic diameter D_h the relation

$$D_h = 4 \cdot A/U \qquad \text{(B 3.2-3)}$$

should be taken, where

A : leakage area

U : leak circumference.

B 3.2.2.3 Two-phase discharge flow

(1) A simple model for assessing two-phase flow discharge through cracks is the homogenous equilibrium model which is based on the following assumptions:

a) the flow is isentropic,

b) the flow is homogenous (same velocities of the two phases) and

c) there is thermodynamic equilibrium (pressure and temperature of the two phases are the same).

Figure B 3.2-1 schematically shows the two-phase discharge flow through a crack.

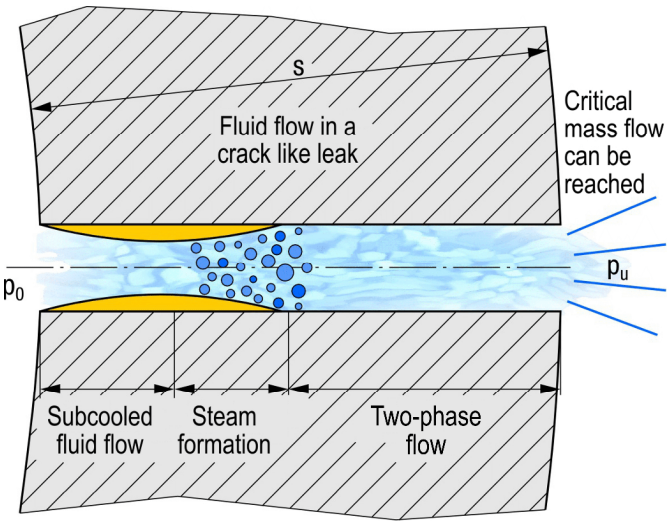

Figure B 3.2-1: Schematic illustration of two-phase discharge flow through a crack

(2) The starting point for the derivation of the mass flow density G is the following relation for single-phase flow (at first without friction):

$$G = \frac{1}{v_2} \cdot \sqrt{2 \cdot (h_0 - h_2)} \qquad \text{(B 3.2-4)}$$

Here h_0 is the total enthalpy ahead of the crack inlet, h_2 the enthalpy at the mouth of the crack exit and v_2 the specific volume at the crack exit. For two-phase flow now the enthalpy and specific volume are described by the following summations:

$$h = x \cdot h_g + (1 - x) \cdot h_l \qquad \text{(B 3.2-5)}$$

$$v = x \cdot v_g + (1 - x) \cdot v_l \qquad \text{(B 3.2-6)}$$

where x is the steam content and the indices “g” and “l” represent steam and water, respectively.

It follows that:

$$G = \sqrt{\frac{2 \cdot \left[h_0 - (1-x) \cdot h_l - x \cdot h_g\right]}{\left[x \cdot v_g + (1-x) \cdot v_l\right]^2}} \qquad \text{(B 3.2-7)}$$

The steam content x can be determined from the respective entropies “s” under the condition of isentropic flow:

$$x = \frac{s_0 - s_l}{s_g - s_l} \qquad \text{(B 3.2-8)}$$

Here, the flow resistance ζ as per equation B 3.2-2 is accounted for by using the pressure drop momentum:

$$\zeta = -2 \cdot \int_{p_1}^{p_2} \frac{1 + G^2 \cdot \frac{dv}{dp}}{G^2 \cdot v} dp \qquad \text{(B 3.2-9)}$$

where

p_1 : pressure at flow channel inlet

p_2 : pressure at flow channel outlet

(3) Now the following condition must be satisfied to determine the critical mass flow density:

$$\frac{dG}{dp} = 0 \qquad \text{(B 3.2-10)}$$

Usually this is solved by iteration by decreasing the pressure p to ambient pressure. If the mass flow then takes a maximum value, critical mass flow density is determined. Where no maximum is reached, the flow can be assumed to remain sub-critical.

B 3.2.2.4 Single-phase discharge of superheated steam

If single-phase steam is discharged, the steam can be treated as ideal gas and according to [64] under frictionless isotropic consideration the critical discharge rate is obtained to read:

$$G = \sqrt{\kappa \cdot p_0 \cdot \rho_0 \cdot \left(\frac{2}{\kappa + 1}\right)^{\frac{\kappa+1}{\kappa-1}}} \qquad \text{(B 3.2-11)}$$

where

κ : isentropic exponent ($p \cdot v^\kappa$ = const.)

For frictional flow this discharge rate is multiplied with the factor η which according to equation B 3.2-12 depends on the flow resistance ζ .

$$\eta = a_i \cdot e^{-b_i \cdot \zeta} \qquad \text{(B 3.2-12)}$$

where

ζ : flow resistance to equation B 3.2-2

a_i und b_i : parameters

The parameters a_i and b_i are given for κ = 1.0 and κ = 1.3 in **Table B 3.2-1**.

Lfd. Nr.	ζ	κ = 1.0		κ = 1.3	
		a_i	b_i	a_i	b_i
1	0 to 1	1.00	0.24	1.00	0.28
2	1 to 5	0.85	0.09	0.82	0.09
3	5 to 20	0.63	0.03	0.59	0.03

Table B 3.2-1: Parameters for equation B 3.2-12

B 3.2.2.5 Resistance factor

According to the calculations and experiments documented in [65] the relation hereafter at $1 \le D_h/(2 \cdot R_Z)$ results in a curve covering the resistance factor λ as a function of the hydraulic diameter D_h and the crack surface roughness R_Z:

$$\lambda = \min \left\{ 2 ; \frac{1}{2\left[\log\left(1{,}5 \cdot \frac{D_h}{2 \cdot R_z}\right)\right]^2} \right\} \qquad \text{(B 3.2-13)}$$

Typical values for the crack surface roughness of fatigue cracks are

a) for austenitic steels $R_Z \approx 10$ µm to 30 µm [66], [67],

b) for ferritic steels $R_Z \approx 10$ µm [67].

B 3.2.3 Required input data

(1) The input data required for the leak rate determination using simplified procedures are limited to data on the crack geometry and thermo-hydraulic values. To describe the crack geometry the following data are required:

a) leakage area,

b) circumference of leakage area,

c) wall thickness (flow path length),

d) crack surface roughness.

(2) The following is required to characterize the thermos-hydraulic boundary conditions in the flow channel inlet and outlet regions:

a) pressure at inlet,

b) temperature at inlet,

c) pressure at outlet,

d) steam content at inlet.

B 3.2.4 Limits of application

When determining the mass flow density the applicable discharge flow models and the pertinent equations shall be used. In each case, the boundary conditions and limits of application pertinent to the respective models and equations shall be observed.

Annex C (normative)

Material data for fracture-mechanics analysis

C 1 Stress-strain curves

(1) Technical stress-strain curves shall be determined at the pertinent temperatures in accordance with DIN EN ISO 6892-1 and DIN EN ISO 6892-2.

(2) The true stress-strain curves shall be determined for the pertinent temperatures

a) from the technical stress-strain curves to obtain strain before reduction in area to the following equations:

$$\varepsilon_w = \ln(1+\varepsilon) \quad \text{(C 1-1)}$$

$$\sigma_w = \sigma \cdot (1+\varepsilon) \quad \text{(C 1-2)}$$

where

ε : nominal strain

σ : nominal stress

ε_w : true strain

σ_w : true stress

or

b) by measuring the cross-section reduction with correction to Bridegeman [68].

C 2 Characteristic crack initiation values

C 2.1 Characteristic physical crack initiation values (J_i)

(1) The characteristic physical crack initiation values J_i shall be determined to ISO 12135.

Note:
The characteristic values thus determined are transferrable to the component independently of the multi-axial stress state.

(2) For the materials 20MnMoNi5-5 (1.6310), 22NiMoCr3-7 (1.6751), X6CrNiNb18-10 (1.4550), X6CrNiTi18-10 (1.4541), 15NiCuMoNb5 (1.6368), 15MnNi6-3 (1.6210) the characteristic crack initiation values given in **Tables C 2-1 to C 2-2** may be used if the impact energy assigned to the crack initiation values are verified by notched-bar impact testing. In the case of dissimilar welds the characteristic values given in **Table C 2-3** may be used for the weld metal consisting of nickel alloy NiCr70Nb.

Note:
The crack initiation values given in the tables are representative for the materials used for piping and pressure vessels in German nuclear power plants. A statistical evaluation was not possible due to the small random specimen selection for each set of parameters.

(3) In lieu of the physical crack initiation values to (1) or (2), the correlation between J_i and the impact energy obtained by notched-bar impact testing as per equation C 2-1 to [69] may be used for the fracture mechanics analysis of ferritic and austenitic materials (base metal and weld metal). **Figure C 2-1** shows this relation in the range between KV = 100 J and KV = 300 J.

$$J_i = -21.55 + \exp\left(\frac{KV + 373.5}{119}\right) \quad \text{(C 2-1)}$$

Where

J_i : characteristic physical crack initiation value in N/mm

KV : impact energy from notched-bar impact testing in J

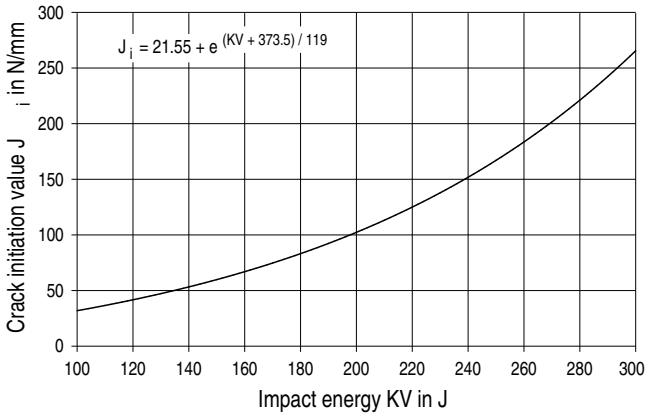

Figure C 2-1: Correlation between J_i and the impact energy KV obtained by notched-bar impact testing

Note:
*The curve shown in **Figure C 2-1** is based on a statistical evaluation of test data and corresponds to the curve of average values minus two-times the standard deviation (-2s curve). This curve is not applicable to dissimilar welds with weld metal of nickel alloys, such as NiCr70Nb.*

C 2.2 Characteristic technical crack initiation values ($J_{0.2}$, $J_{0.2BL}$, J_{Ic})

(1) The characteristic technical crack initiation values shall be determined in accordance with ESIS P1-92 ($J_{0.2}$) or ASTM E1820 (J_{Ic}) or ISO 12135 ($J_{0.2BL}$).

(2) For the material mentioned in C 2.1 (2) the J_{Ic} values shown by **Table C 2-4** may be used if the impact energy assigned to the J_{Ic} values has been proved by notched-bar impact testing.

Note:
The J_{Ic} values given in the table are representative for the materials used for piping and pressure vessels in German nuclear power plants. A statistical evaluation was not possible due to the small random specimen selection for each set of parameters.

(3) When transferring the characteristic technical crack initiation values on the component the multi-axiality of stress state in the component shall be considered.

Note:
Possible procedures for evaluating the transferability are e.g. described in [70] and [71].

C 3 Crack-resistance curves (J-R curves)

(1) J-R curves shall be determined either to ASTM E 1820 or ISO 12135.

(2) For the material mentioned in C 2.1 (2) the J-R curves shown by **Tables C 2-1 to C 2-4** as well as **Figures C 2-2 to C 2-17** may be used if the impact energy assigned to the J-R curves has been proved by notched-bar impact testing.

Note:
The J-R curves given in the tables are representative for the materials used for piping and pressure vessels in German nuclear power plants. A statistical evaluation was not possible due to the small random specimen selection for each set of parameters.

(3) J-R curves may be determined for the materials mentioned in C 2.1 (2) (base material and weld metal) by correlation with the upper-shelf energy obtained from impact testing as follows:

$$J_R(\Delta a) = C_1 \cdot \Delta a^{C_2} \quad \text{for } \Delta a \geq 1.0 \text{ mm} \qquad \text{(C 3-1)}$$

$$C_1 = 0.53 \cdot KV^{1.28} \cdot \exp\left(\frac{20 - T}{400}\right) \qquad \text{(C 3-2)}$$

$$C_2 = 0.133 \cdot KV^{0.254} \cdot \exp\left(\frac{20 - T}{2000}\right) - \frac{\sigma_y}{4664} + 0.03 \qquad \text{(C 3-3)}$$

where

J_R : crack resistance in N/mm

Δa : crack extension in mm

T : Temperature in °C

KV : impact energy from notched-bar impact testing in J

σ_y : yield strength R_e or $R_{p0.2}$ in N/mm^2

In the range Δa = 0.0 mm up to 1.0 mm the J-R curve is conservatively described to show a bi-linear course as follows:

Δa in mm	J_R in N/mm
0.0	0.0
Δa_i	J_i
1.0	J_R (Δa = 1.0 mm)

where

J_i as per equation C 2-1,

J_R as per equation C 3-1 and

Δa_i as per equation C 3-4.

$$\Delta a_i = 7.28 \cdot 10^{-4} \cdot KV - 5.06 \cdot 10^{-4} \qquad \text{(C 3-4)}$$

where

Δa_i : as per equation in mm at J_i as per equation C 2-1

KV : impact energy from notched-bar impact testing in J

Note:

*The J_R curves thus determined will cover the curves listed under **Tables C 2-1** to **C 2-4**. The KV-J_R curves correlation cannot be applied to dissimilar welds with weld metal of nickel alloys, such as NiCr70Nb.*

(4) When transferring the J-R curves on the component the multi-axiality of stress state in the component shall be considered.

Note:

Possible procedures for evaluating the transferability are e.g. described in [70] and [71].

Material	Compo-nent	Type	Temperature	Flaw		Specimens		KV_T	J_i	Δa_i	Δa_{max}	$J = K01 x \Delta a^{EX1} + K02 x \Delta a^{EX2} + K03 x \Delta a^{EX3}$						Figure and curve no.
				Orienta-tion	Type	Orien-tation	Num-ber	J	N/mm	mm	mm	K01	K02	K03	EX1	EX2	EX3	
15MnNi6-3	pressure vessel	base material	RT	axial	through-thickness crack	T-L	3	228	269	0.1574	2.6709	80.56	-1029.06	1997.88	0.1	0.3	0.5	C 2-2/1
			up to 200 °C	axial	through-thickness crack	T-L	3	231	257	0.1874	2.7527	130.91	-532.82	1082.52	0.1	0.3	0.5	C 2-2/2
20MnMoNi5-5	pressure vessel	base material	RT	axial	surface crack	T-S	2	158	292.9	0.105	1.2033	0	0	904.64	0	0	0.5	C 2-3/1
			up to 300 °C	axial	surface crack	T-S	1	209	186.9	0.167	1.4125	0	0	457.82	0	0	0.5	C 2-3/2
	pipe	base material	RT	axial	surface crack	T-S	5	200	129.7	0.131	2.1634	-109.54	37.12	549.6	0.1	0.3	0.5	C 2-4/1
					through-thickness crack	T-L	8	204	110.9	0.128	2.1511	-66.49	-9.28	475.35	0.1	0.3	0.5	C 2-4/2
				circum-ferential	surface crack	L-S	5	215	197	0.133	2.5403	-36.74	-202.82	926.23	0.1	0.3	0.5	C 2-4/3
					through-thickness crack	L-T	1	208	201.5	0.14	2.4544	10.23	-343.09	1024.45	0.1	0.3	0.5	C 2-4/4
			up to 300 °C	axial	surface crack	T-S	1	181	195.3	0.135	2.4753	-380.12	926.68	-4.89	0.1	0.3	0.5	C 2-4/5
					through-thickness crack	T-L	1	202	207.7	0.113	2.2984	302.67	-443.56	580.01	0.1	0.3	0.5	C 2-4/6
			up to 240 °C	circum-ferential	surface crack	L-S	3	247	164.8	0.1347	2.827	-173.53	472.43	130.52	0.1	0.3	0.5	C 2-4/7
					through-thickness crack	L-T	1	245	200.9	0.1456	3.201	258.24	-397.15	552.34	0.1	0.3	0.5	C 2-4/8
15NiCuMoNb5	pressure vessel	base material	RT	axial	through-thickness crack	T-L	1	79	69.9	0.065	2.0957	-20.99	81.89	195.42	0.1	0.3	0.5	C 2-5/1
			up to 250 °C	axial	through-thickness crack	T-L	2	85	54.7	0.061	2.504	-39.24	224.46	-51.17	0.1	0.3	0.5	C 2-5/2
	pipe	base material	RT	axial	surface crack	T-S	2	54	44.5	0.044	2.5602	-132.01	322.06	71.11	0.1	0.3	0.5	C 2-6/1
					through-thickness crack	T-L	2	54	55.7	0.074	0.6004	190.62	51.84	0	0.5	1	0	C 2-6/2
				circum-ferential	surface crack	L-S	1	147	149.3	0.0459	1.7099	-31.5	232.03	375.27	0.1	0.3	0.5	C 2-6/3
					through-thickness crack	L-T	6	137	73	0.061	1.9604	-19.2	89.09	198.4	0.1	0.3	0.5	C 2-6/4
			up to 250 °C	axial	surface crack	T-S	1	92	48.9	0.0333	1.5094	70.58	-59.9	110.78	0.1	0.3	0.5	C 2-6/5
					through-thickness crack	T-L	1	99	71.4	0.036	1.9873	123.96	-125.57	151.78	0.1	0.3	0.5	C 2-6/6
				circum-ferential	surface crack	L-S	2	185	90.2	0.078	1.933	55.71	-234.29	558.95	0.1	0.3	0.5	C 2-6/7
		weld metal	RT	circum-ferential	through-thickness crack	L-T	2	75	52.2	0.0488	1.6156	-47.53	195.1	38.33	0.1	0.3	0.5	C 2-7/1
			up to 210 °C	circum-ferential	through-thickness crack	L-T	1	114	57.9	0.0586	2.0882	12.85	42.84	123.83	0.1	0.3	0.5	C 2-7/2
22NiMoCr3-7	pressure vessel	base material	RT	axial	through-thickness crack	T-L	4	44	79	0.063	2.1106	-17.75	189.76	38.01	0.1	0.3	0.5	C 2-8/1 [1]
			up to 300 °C	axial	surface crack	T-S	4	86	51.8	0.064	3.6032	1756.07	-2587	977.31	0.7	0.8	0.9	C 2-8/2 [1]
					through-thickness crack	T-L	2	86	77.1	0.062	2.777	81.63	13.96	36.99	0.1	0.3	0.5	C 2-8/3 [1]
			RT	axial	surface crack	T-S	6	109	65	0.087	2.5738	26.94	-242.24	542.99	0.1	0.3	0.5	C 2-9/1 [2]
			up to 300 °C	axial	surface crack	T-S	2	131	81	0.073	2.984	-30.34	111.96	195.97	0.1	0.3	0.5	C 2-9/2 [2]
			RT	axial	surface crack	T-S	15	151	127	0.183	3.0561	386.29	-1561.86	1727.73	0.1	0.3	0.5	C 2-10/1 [3]

[1] Approx. 90 J at upper shelf (lower bound for the toughness requirements to KTA 3201.1 und KTA 3211.1)

[2] Bent plates (150 mm thick), longitudinally welded

[3] Forged rings with great wall thicknesses (250 mm to 500 mm)

Table C 2-1: Characteristic physical crack initiation values and J-R curves for ferritic steels

Material	Component	Type	Temperature	Flaw		Specimens		KV_T	J_i	Δa_i	Δa_{max}	$J = K01 x \Delta a^{EX1} + K02 x \Delta a^{EX2} + K03 x \Delta a^{EX3}$						Figure and curve no.
				Orientation	Type	Orientation	Number	J	N/mm	mm	mm	K01	K02	K03	EX1	EX2	EX3	
X6CrNiNb18-10	pipe	base material	RT	circumferential	surface crack	L-S	7	190	350.9	0.203	1.9436	-1546.85	4825.85	-2237.75	0.5	0.7	0.9	C 2-11/1
					through-thickness crack	L-T	12	190	213.6	0.1686	4.0379	-1348.7	3680.21	-1445.03	0.5	0.7	0.9	C 2-11/2
			up to 350 °C	circumferential	surface crack	L-S	1	275	409	0.258	0.3518	0	0	805.3	0	0	0.5	C 2-11/3
					through-thickness crack	L-T	2	275	347.1	0.158	2.33	-62.76	471.01	323.34	0.1	0.3	0.5	C 2-11/4
		weld metal	RT	circumferential	surface crack	L-S	2	106	79.7	0.0798	2.5145	-152.19	827.96	-178.74	0.5	0.7	0.9	C 2-12/1
					through-thickness crack	L-T	1	100	117.2	0.081	2.1537	180.43	393.76	-18.92	0.5	0.7	0.9	C 2-12/2
			up to 350 °C	circumferential	surface crack	L-S	1	138	145.3	0.128	2.6057	114.11	-241.66	511.1	0.1	0.3	0.5	C 2-12/3
					through-thickness crack	L-T	1	133	176	0.11	2.5082	107.21	-152.07	507.81	0.1	0.3	0.5	C 2-12/4
X6CrNiTi18-10	pipe	base material	RT	circumferential	surface crack	L-S	3	247	306.4	0.196	2.2004	243.73	-1234.06	1933.81	0.1	0.3	0.5	C 2-13/1
					through-thickness crack	L-T	5	237	331.2	0.203	1.1296	599.45	-2818.02	3477.33	0.1	0.3	0.5	C 2-13/2
			up to 300 °C	circumferential	surface crack	L-S	2	270	315.3	0.187	2.9816	-375.48	626.63	587.18	0.1	0.3	0.5	C 2-13/3
					through-thickness crack	L-T	2	263	293.4	0.201	2.161	-70.81	-219.47	1091.47	0.1	0.3	0.5	C 2-13/4
		weld metal	RT	circumferential	surface crack	L-S	2	100	78.4	0.078	2.9957	33.63	118.76	190.81	0.1	0.5	0.9	C 2-14/1
					through-thickness crack	L-T	4	100	94.9	0.086	4.3191	83.66	-1.46	272.03	0.1	0.5	0.9	C 2-14/2
			up to 300 °C	circumferential	surface crack	L-S	2	141	108.5	0.092	3.0103	27.86	-132.59	499	0.1	0.3	0.5	C 2-14/3
					through-thickness crack	L-T	2	152	122.7	0.102	2.4162	30.91	-160.78	561.08	0.1	0.3	0.5	C 2-14/4

Table C 2-2: Characteristic physical crack initiation values and J-R curves for austenitic steels

Material	Bauteil	Type	Temperature	Flaw		Specimens		KV_T	J_i	Δa_i	Δa_{max}	$J = K01 x \Delta a^{EX1} + K02 x \Delta a^{EX2} + K03 x \Delta a^{EX3}$						Figure and curve no.
				Orientation	Type	Orientation	Number	J	N/mm	mm	mm	K01	K02	K03	EX1	EX2	EX3	
Dissimilar weld NiCr70Nb	pipe	weld metal	RT	circumferential	surface crack	L-S	15	104	35.6	0.023	2.8101	25.03	33.75	49.57	0.1	0.3	0.5	C 2-15/1
					through-thickness crack	L-T	1	116	31.1	0.0354	2.94	-38.05	101.94	111.05	0.1	0.3	0.5	C 2-15/2
			up to 350 °C	circumferential	through-thickness crack	L-T	1	131	114.2	0.051	3.15	86.51	195.79	111.86	0.1	0.5	1	C 2-15/3

Table C 2-3: Characteristic physical crack initiation values and J-R curves for weld metal NiCr70Nb in dissimilar welds

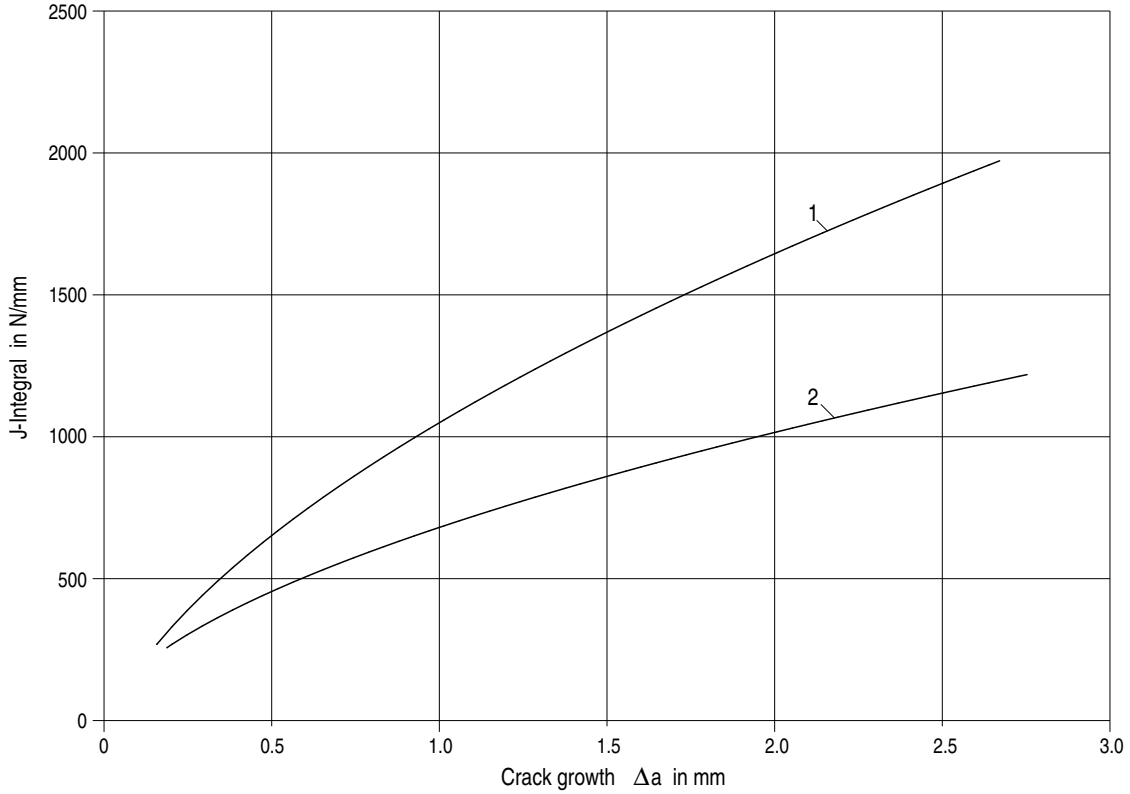

Figure C 2-2: J-R curves of the steel 15MnNi6-3 for pressure vessels

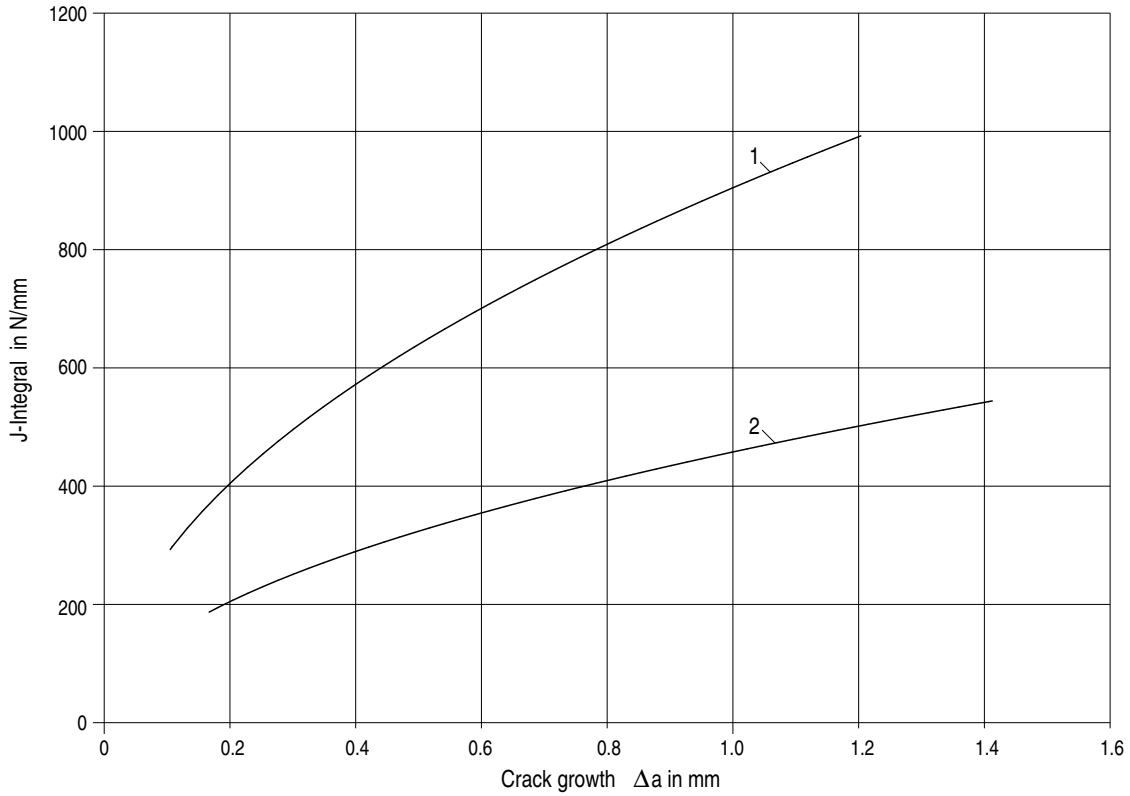

Figure C 2-3: J-R curves of the steel 20MnMoNi5-5 for pressure vessels

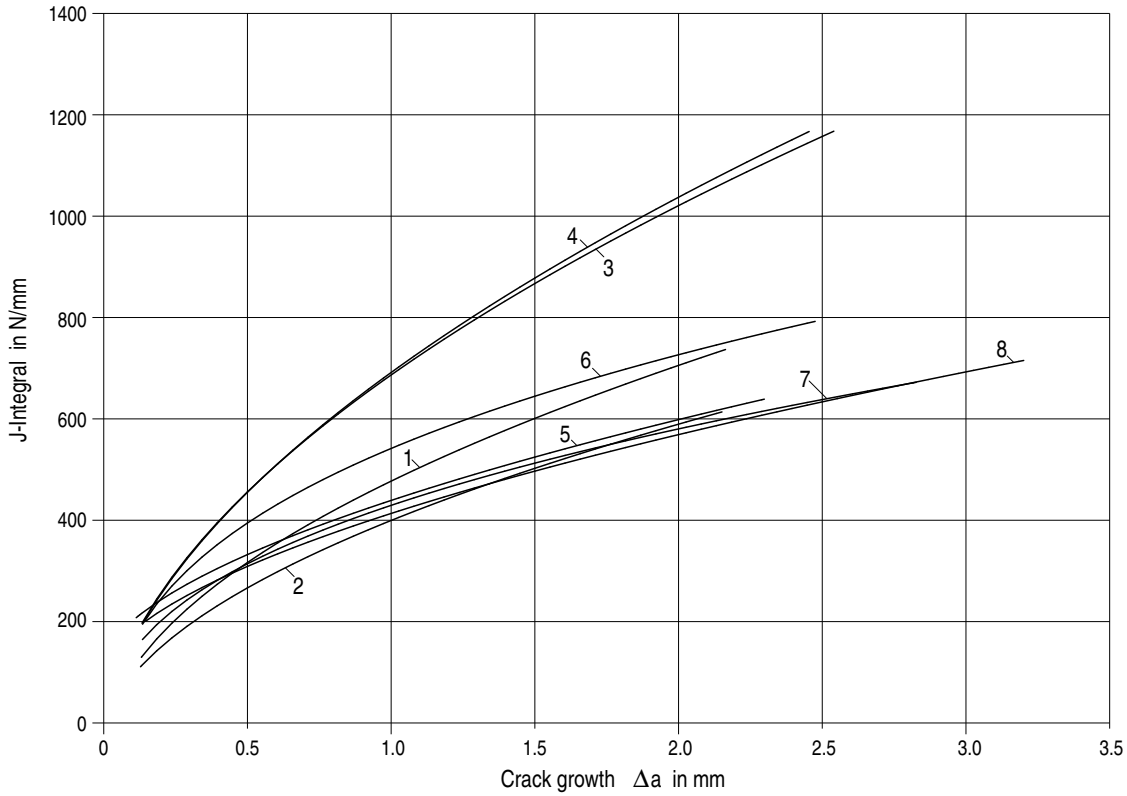

Figure C 2-4: J-R curves of the steel 20MnMoNi5-5 for pipe

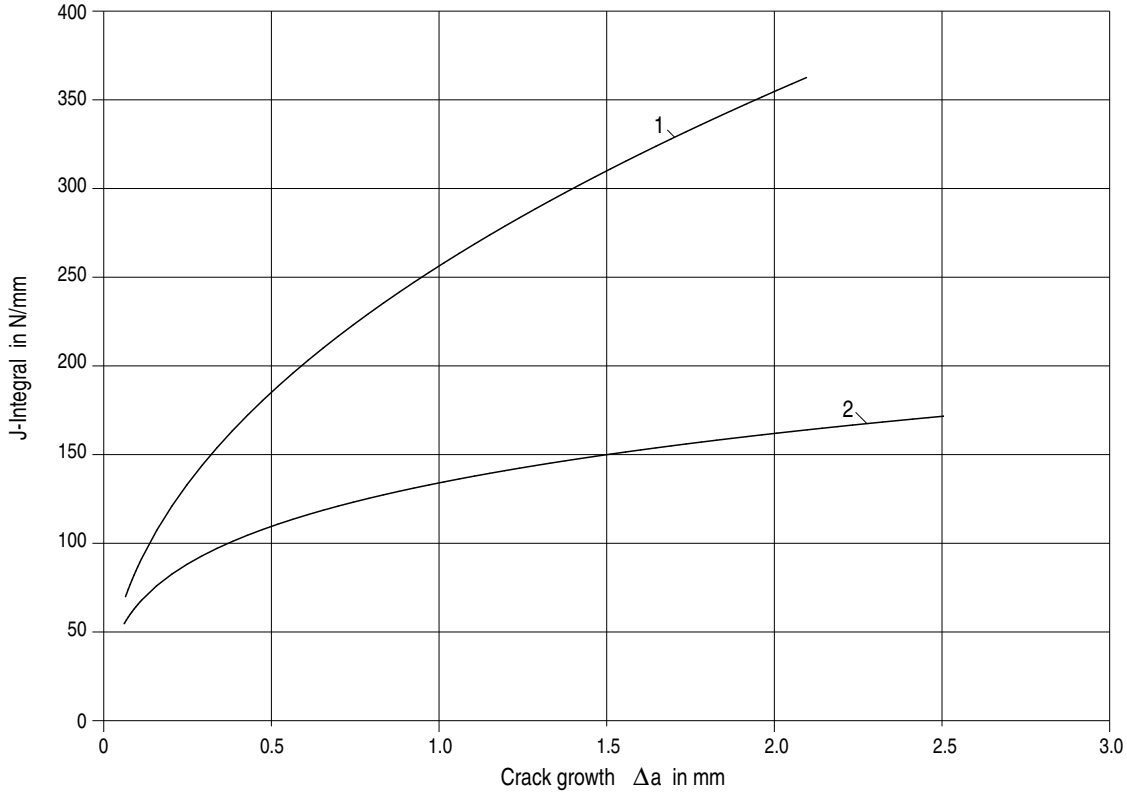

Figure C 2-5: J-R curves of the steel 15NiCuMoNb5 for pressure vessels

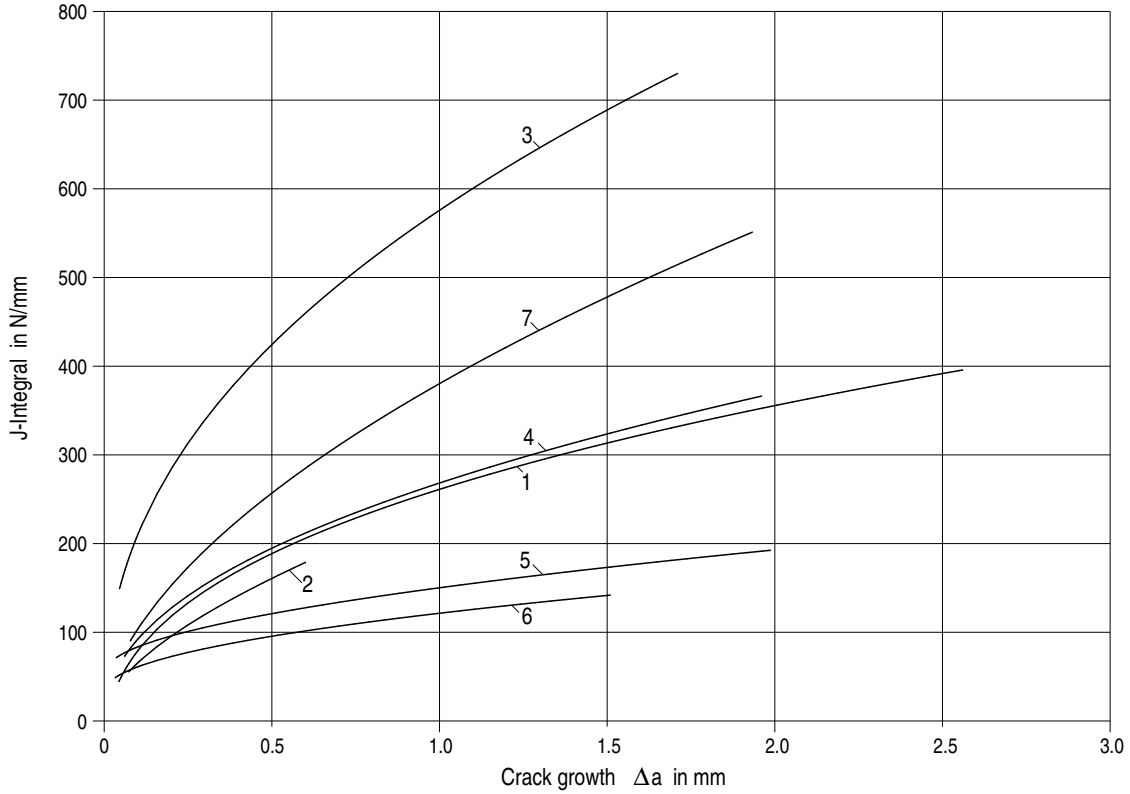

Figure C 2-6: J-R curves of the steel 15NiCuMoNb5 for pipe

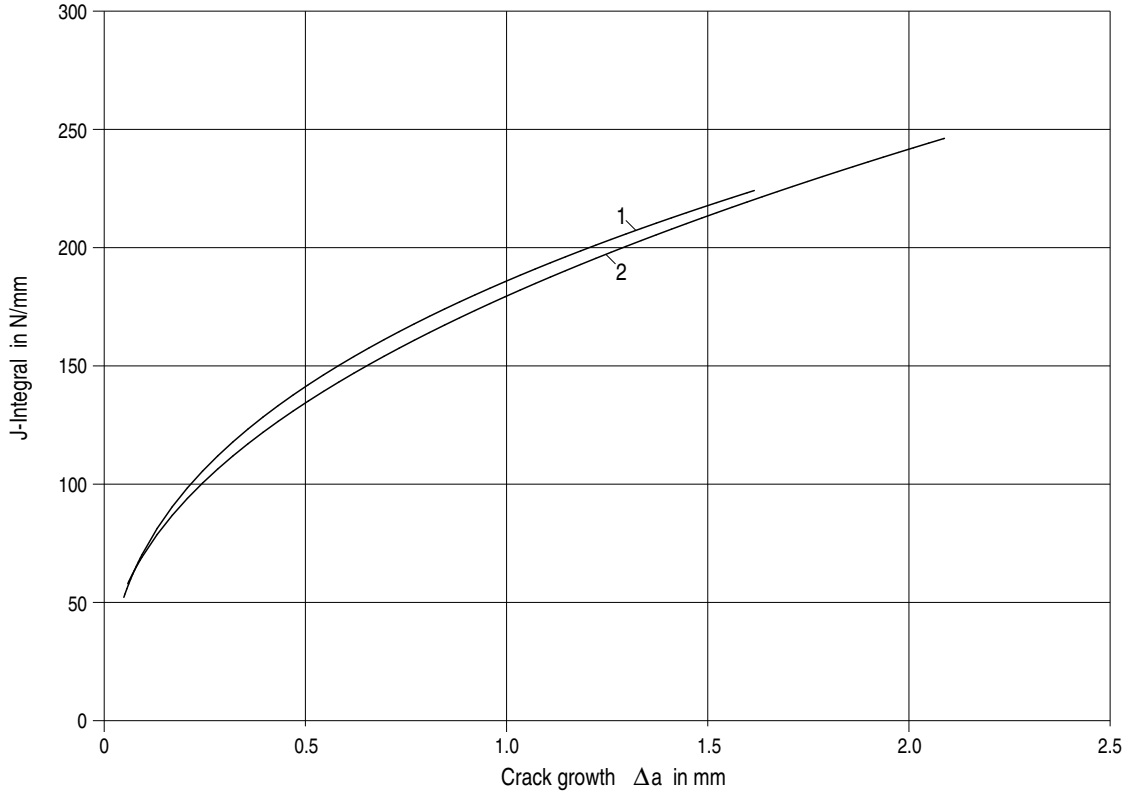

Figure C 2-7: J-R curves for the weld metal S3 NiMo 1 in welded joints of the steel 15NiCuMoNb5

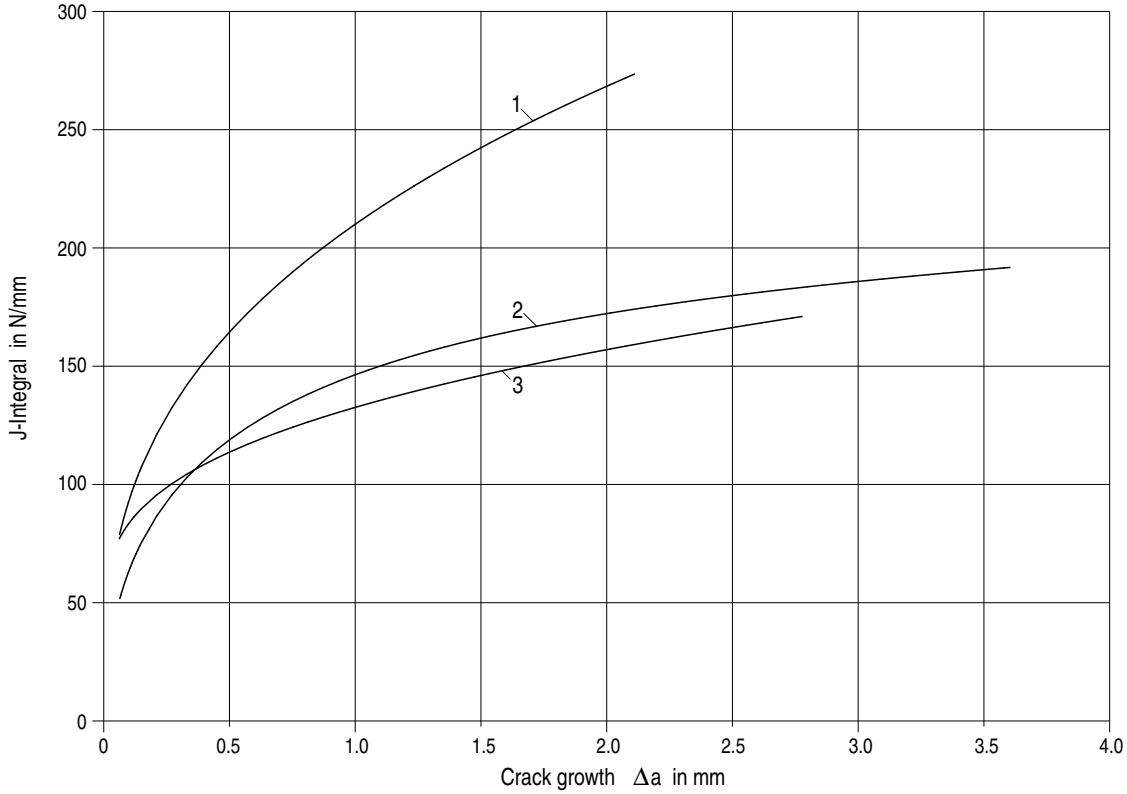

Figure C 2-8: J-R curves of the steel 22NiMoCr3-7 for pressure vessels (lower bound for the toughness requirements to KTA 3201.1 and KTA 3211.1)

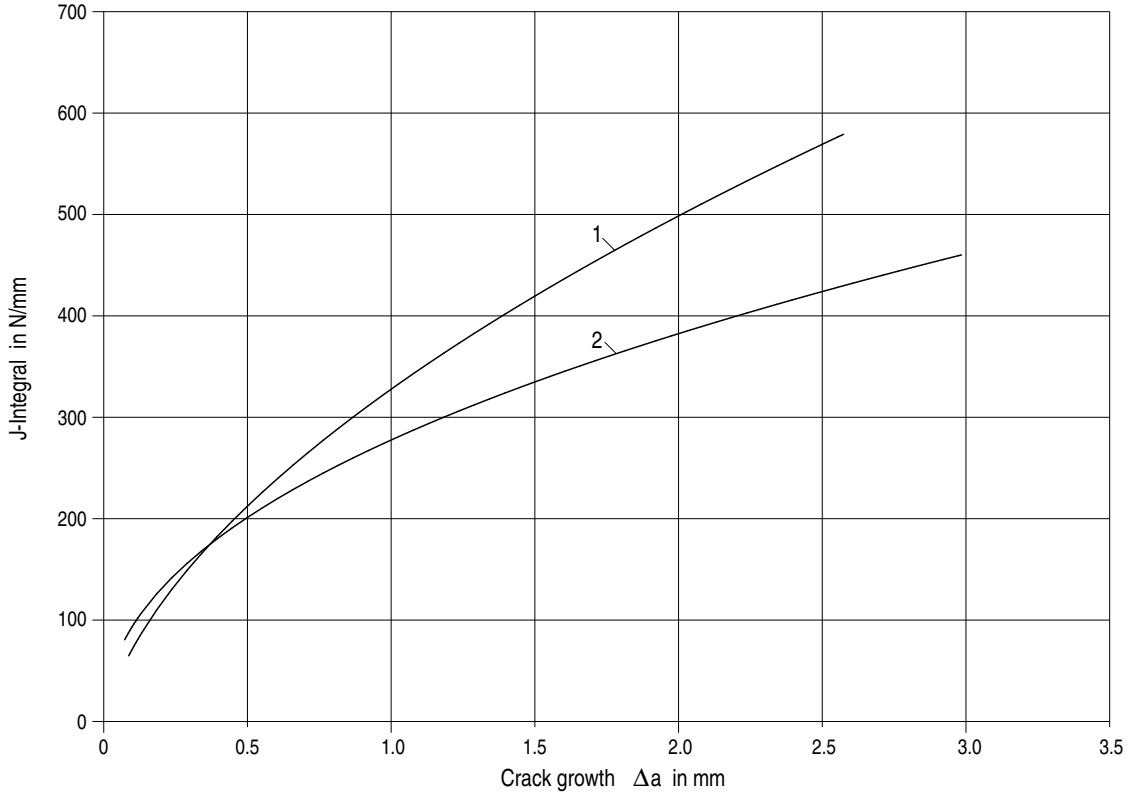

Figure C 2-9: J-R curves of the steel 22NiMoCr3-7 for pressure vessels (bent plate 150 mm thick, longitudinally welded)

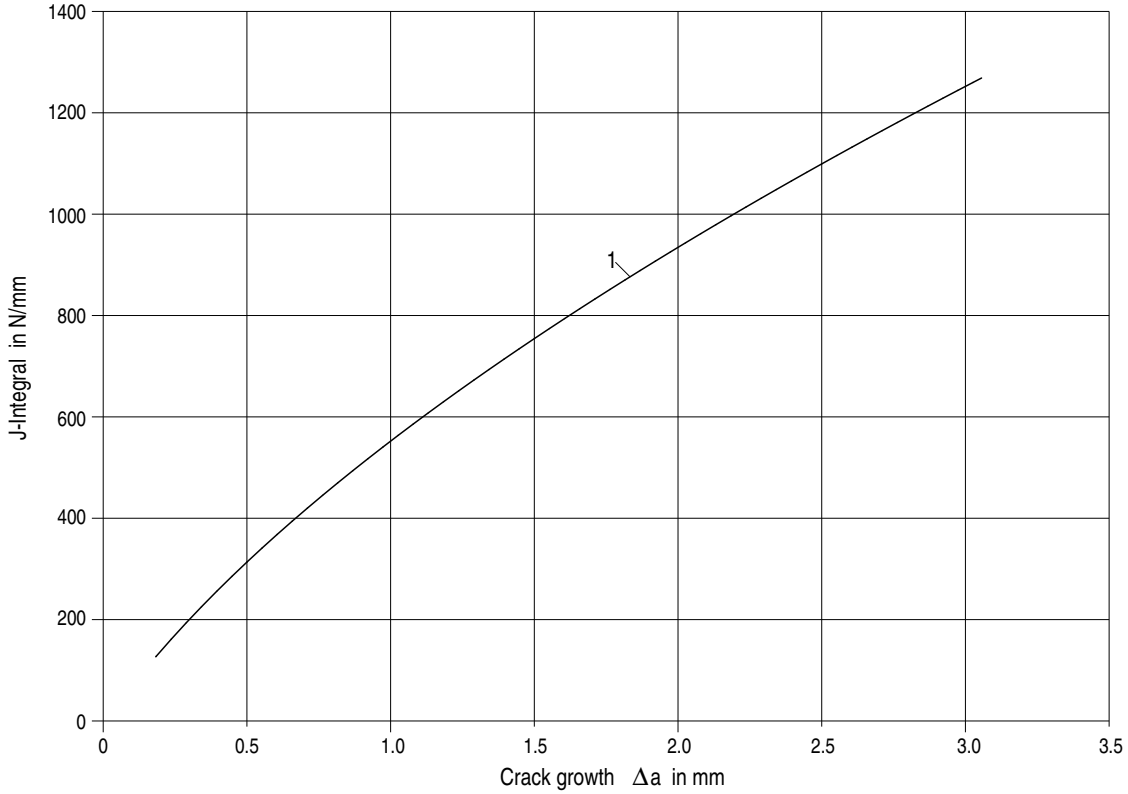

Figure C 2-10: J-R curves of the steel 22NiMoCr3-7 for pressure vessels (forged rings with wall thicknesses of 250 mm up to 500 mm)

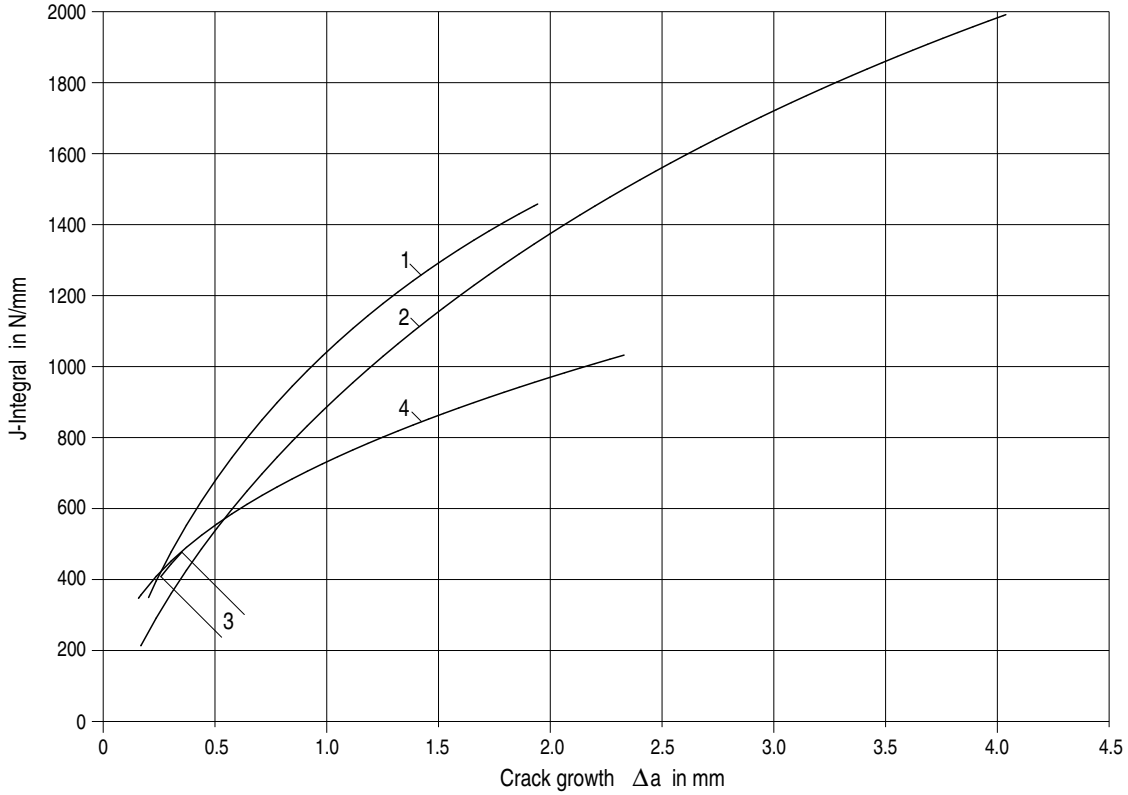

Figure C 2-11: J-R curves of the steel X6CrNiNb18-10, base material

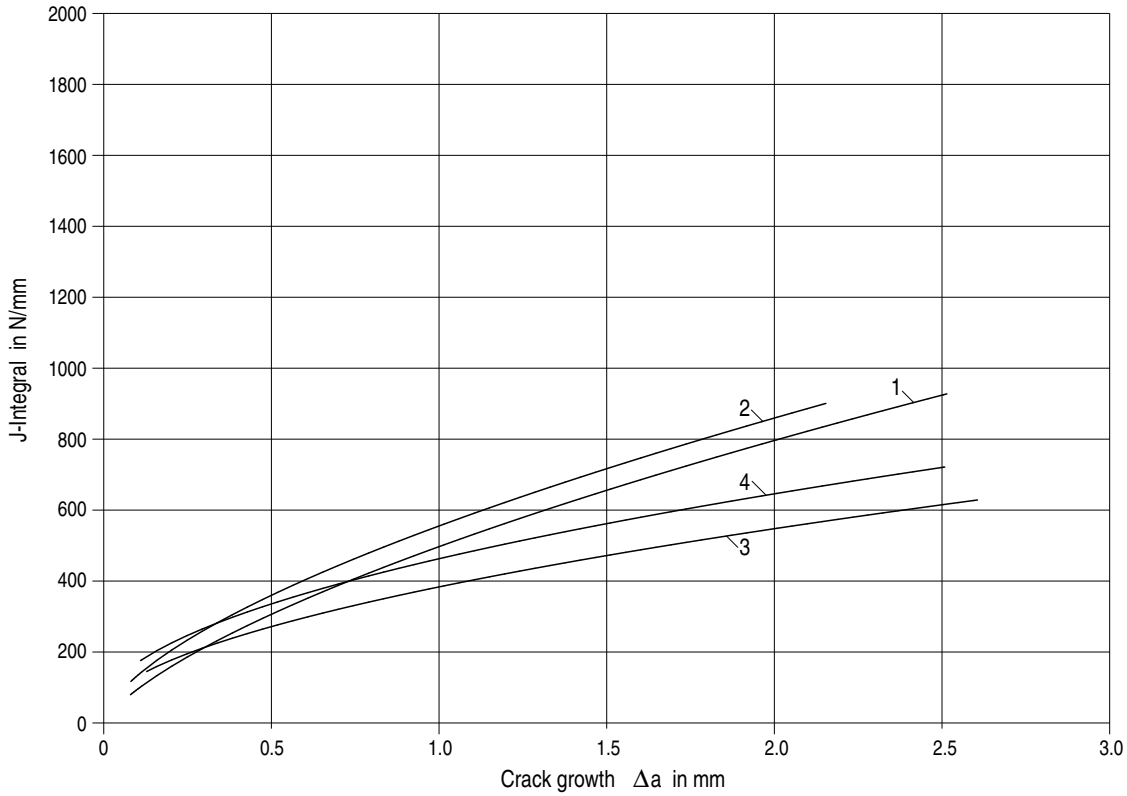

Figure C 2-12: J-R curves for the weld metal E 19.9 Nb B 20 in welded joints of the steel X6CrNiNb18-10

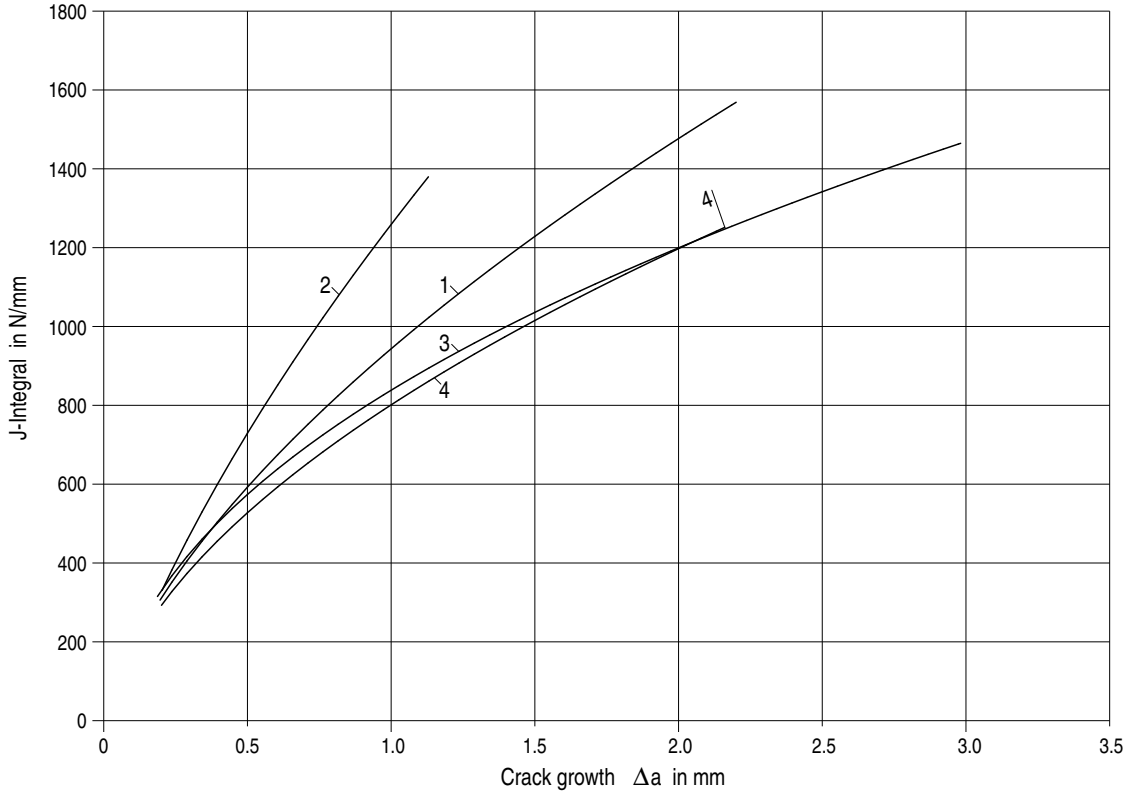

Figure C 2-13: J-R curves of the steel X6CrNiTi18-10, base material

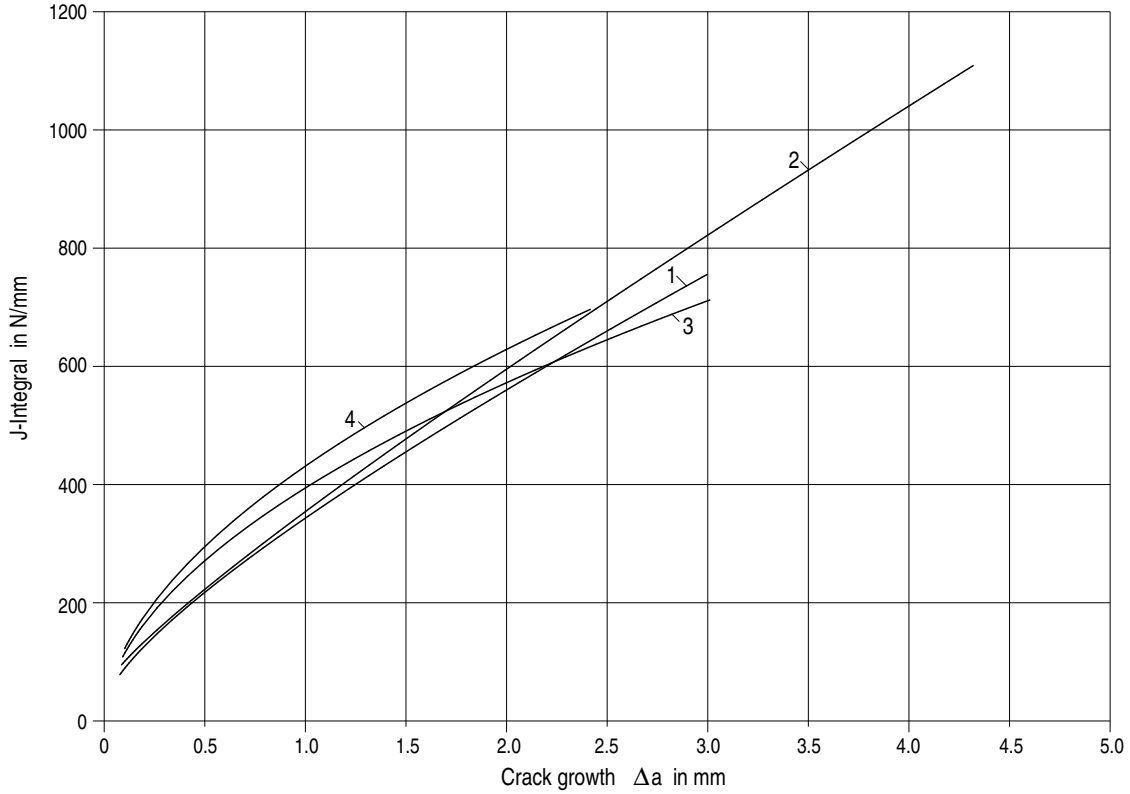

Figure C 2-14: J-R curves for the weld metal 19 9 Nb in welded joints of the steel X6CrNiTi18-10

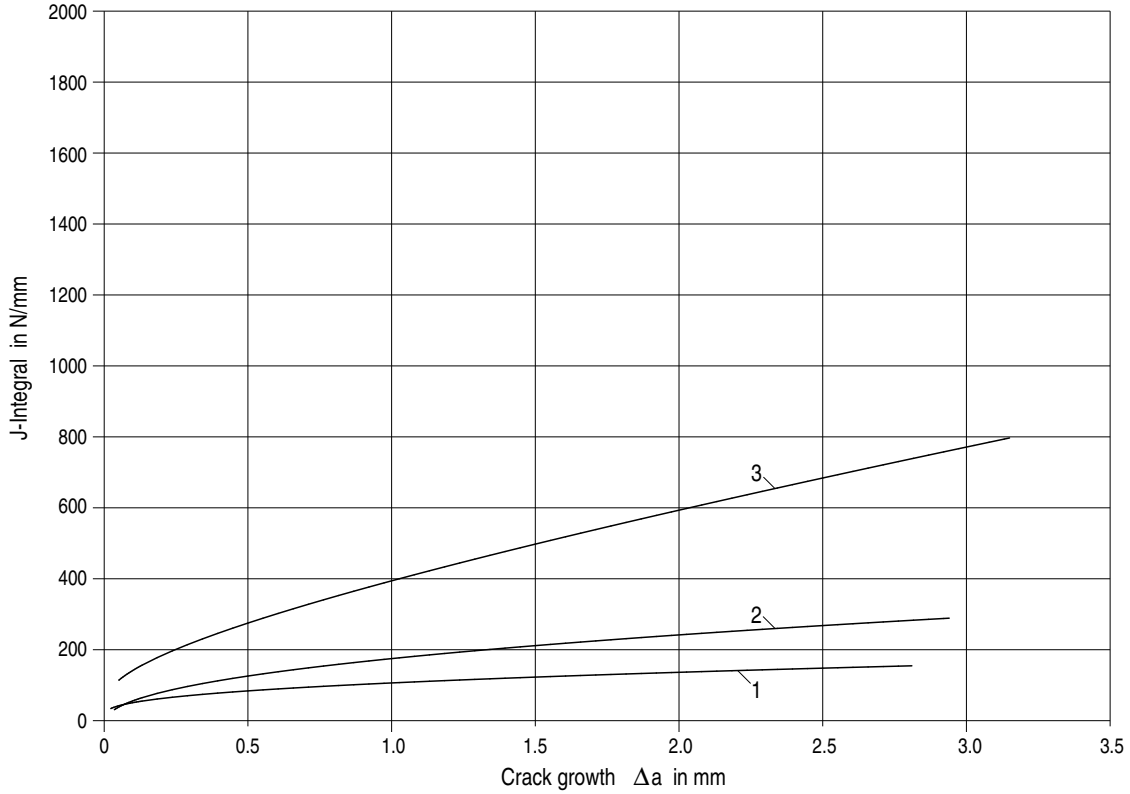

Figure C 2-15: J-R curves for the weld metal NiCr70Nb in dissimilar welds

Material	Component	Type	Temperature	Flaw		Specimens		KV_T	J_{Ic}	Δa_i	Δa_{max}	$J = Kx\Delta a^{EX}$		Figure and curve no.
				Orienta-tion	Type	Orientation	Number	J	N/mm	mm	mm	K	EX	
15 MnNi6-3	pressure vessel	base material	RT	axial	through-thickness crack	T-L	3	228	1450.0					
			up to 200 °C		through-thickness crack	T-L	3	231	623.4					
20MnMoNi5-5	pressure vessel	base material	up to 300 °C	axial	surface crack	T-S	1	209	245.8					
15NiCuMoNb5	pressure vessel	base material	RT	axial	through-thickness crack	T-L	1	79	162.6	0.34319	2.0957	256.73	0.42706	C 2-16/1
			up to 250 °C		through-thickness crack	T-L	2	85	105.0	0.30811	2.504	135.15	0.21441	C 2-16/2
	pipe	base material	RT	axial	surface crack	T-S	2	54	164.8	0.33697	2.5602	265.11	0.43706	C 2-16/3
				circum-ferential	surface crack	L-S	1	147	411.0					
					through-thickness crack	L-T	6	137	147.2					
			up to 250 °C	axial	surface crack	T-S	1	92	76.2					
					through-thickness crack	T-L	1	99	92.9					
				circum-ferential	surface crack	L-S	2	185	176					
		weld metal	RT	circum-ferential	through-thickness crack	L-T	2	75	107.9					
			up to 210 °C		through-thickness crack	L-T	1	114	92.3					
22NiMoCr3-7	pressure vessel	base material [1)]	RT	axial	through-thickness crack	T-L	4	44	151.7					
			240 °C up to 300 °C [1)]		surface crack	T-S	4	86	97.8					
			RT [2)]	axial	surface crack	T-S	6	109	178.5	0.36975	2.5738	327.50	0.61	C 2-17/1
			240 °C up to 300 °C [2)]		surface crack	T-S	2	131	169.1	0.36642	2.984	273.80	0.48	C 2-17/2
			RT [3)]	axial	surface crack	T-S	15	151	337.0	0.52517	3.0561	549.80	0.76	C 2-17/3

1) Approx. 90 J at upper shelf (lower bound for the toughness requirements to KTA 3201.1 and KTA 3211.1)

2) Bent plates (150 mm thick), longitudinally welded

3) Forged rings with great wall thicknesses (250 mm to 500 mm)

Table C 2-4: Characteristic technical crack initiation values and J-R curves for ferritic steels

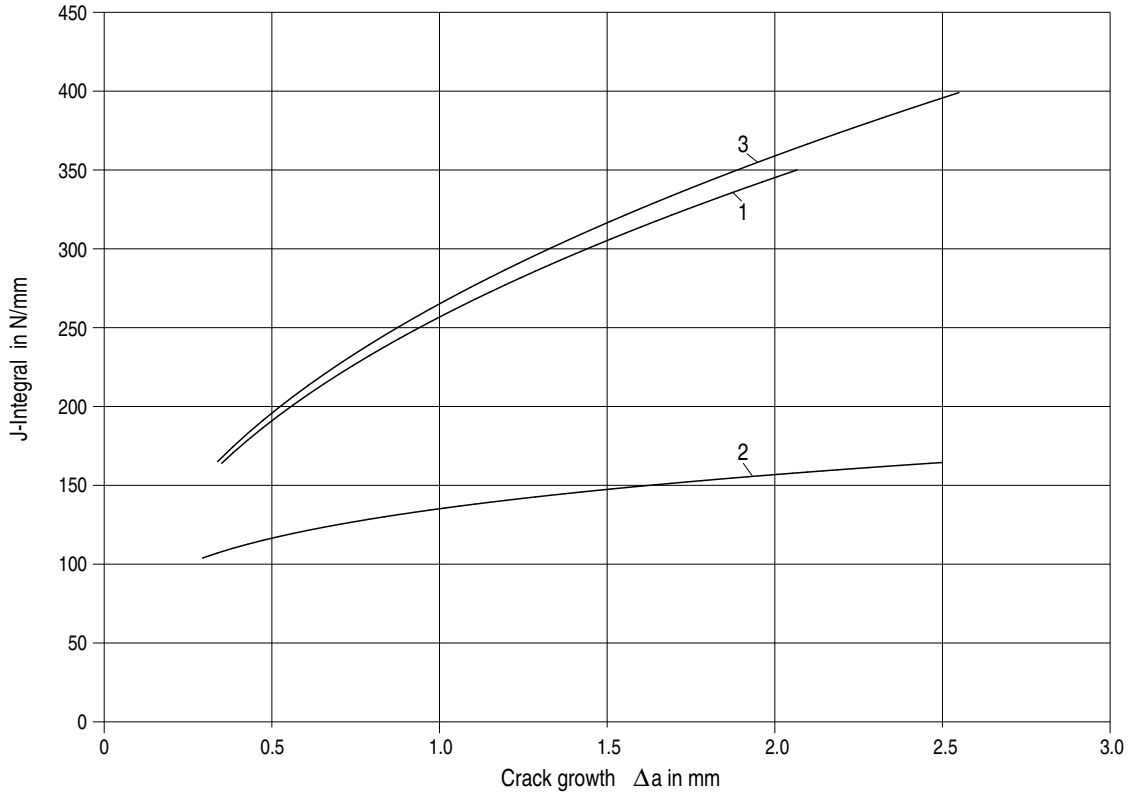

Figure C 2-16: Technical J-R curves for the steel 15NiCuMoNb5

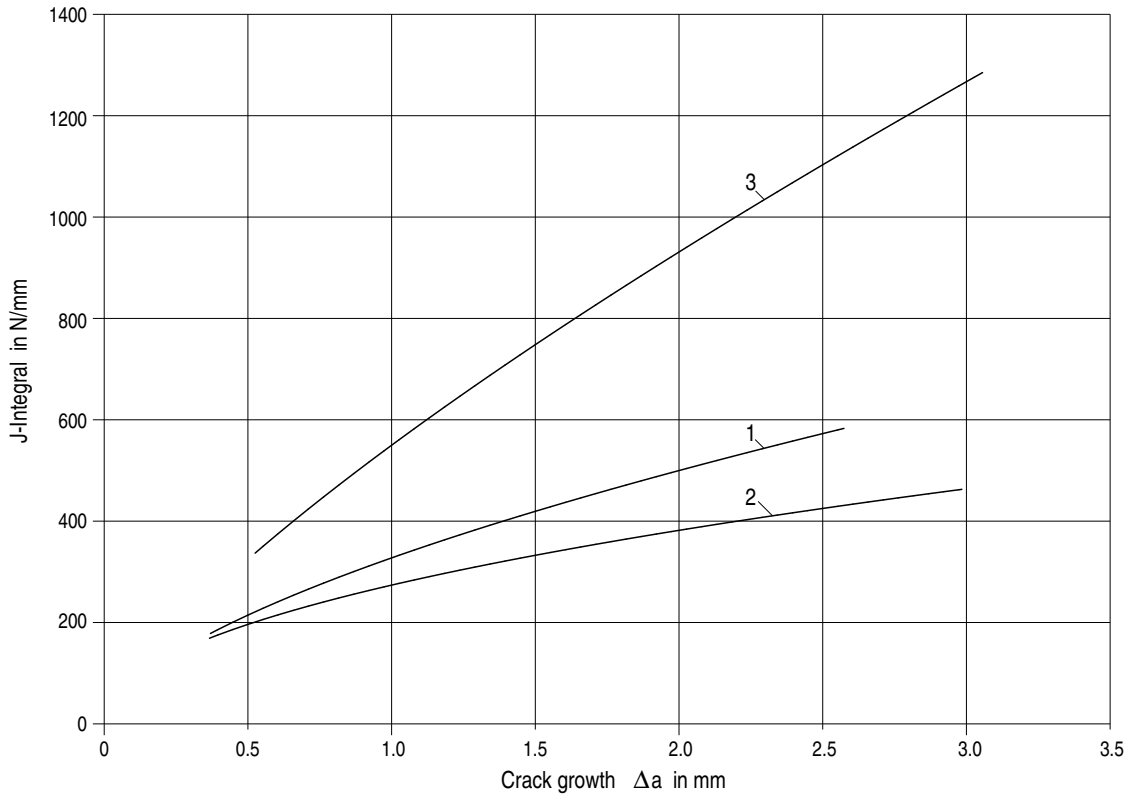

Figure C 2-17: Technical J-R curves for the steel 22NiMoCr3-7

Annex D (informative)
Examples for fracture-mechanics analysis

D 1 Austenitic piping with circumferential crack

D 1.1 Input data

(1) Loading data

a) from the governing load case level D (for fracture mechanics calculation)

Pressure:	$p = 7.4$ MPa
Temperature:	$T = 150.0$ °C
Bending moment due to dead weight and load in case of damage:	$M_{EG+Last} = 39.7$ kNm
Bending moment due to thermal expansion in case of damage:	$M_{Wd} = 32.6$ kNm
Total bending moment in case of damage:	$M_{ges} = 72.3$ kNm

b) From load case combination shutdown (for crack growth calculation)

Max. pressure:	$p_{max} = 7.4$ MPa
Min. pressure:	$p_{min} = 0.0$ MPa
Max. temperature:	$T_{max} = 150.0$ °C
Min. temperature:	$T_{min} = 20.0$ °C
Bending moment due to dead weight:	$M_{EG} = 4.2$ kNm
Bending moment due to thermal expansion:	$M_{WD} = 32.6$ kNm
Max. bending moment ($= M_{EG} + M_{WD}$):	$M_{max} = 36.8$ kNm
Min. bending moment ($= M_{EG}$):	$M_{min} = 4.2$ kNm

(2) Geometry

Inside diameter:	$D_i = 243.0$ mm
Wall thickness:	$s = 15.0$ mm

(3) Material

Material designation:	X6CrNiNb18-10 (1.4550)
Modulus of elasticity:	$E = 186$ kN/mm^2
Poisson's ratio:	$\nu = 0.3$
0.2% proof stress (at 150 °C as per KTA 3201.1):	$R_{p0.2T} = 167.0$ N/mm^2
1 % proof stress (at 150 °C as per KTA 3201.1):	$R_{p1,0T} = 196.0$ N/mm^2
Tensile strength (at 150 °C as per KTA 3201.1 by interpolation):	$R_{mT} = 409.0$ N/mm^2
Equivalent stress intensity as per KTA 3201.2:	$S_m = 131.0$ N/mm^2
J-R curve	as per **Figure D 1-1**

Note:
The transferability of the J-R curve to pipes with circumferential cracks under internal pressure and bending moment loading was proved in [72] for comparable pipes made of austenitic material.

D 1.2 Step 1 to Figure A-3: determination of initial crack

(1) Determination to equation A 2-1 and equation A 2-5:

$$a_a = 0.3 \cdot s = 4.5 \text{ mm} \qquad \text{(D 1.2-1)}$$

$$2 \cdot c_a \geq 6 \cdot a_a = 27 \text{ mm} \qquad \text{(D 1.2-2)}$$

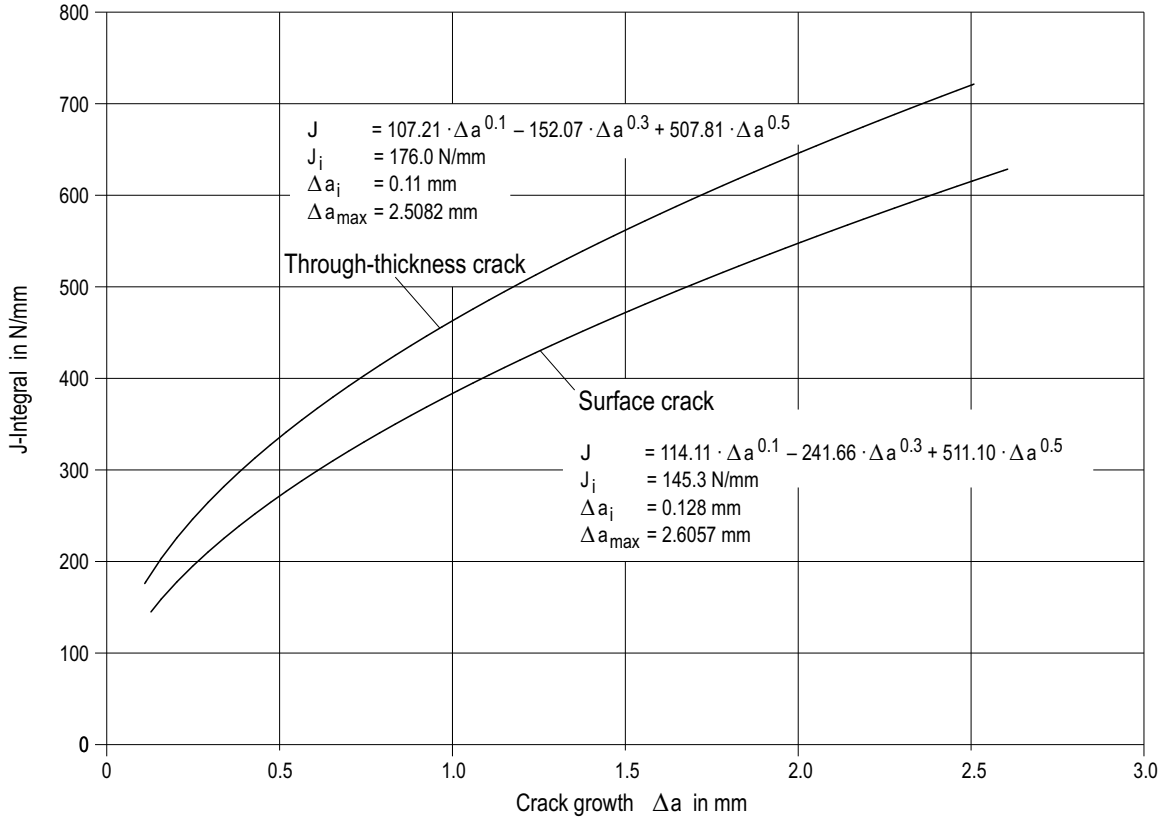

Figure D 1-1: J-R curve for the considered austenitic piping with circumferential crack

D 1.3 Step 2 to Figure A-3: determination of crack development Δa and 2Δc

(1) Determination of stress intensity factors K [73]

$$K = \left[(A_0 + A_P)\cdot G_0 + A_1 \cdot G_1\right]\cdot\sqrt{\pi \cdot a/Q} \qquad \text{(D 1.3-1)}$$

with $Q = 1 + 4.593 \cdot (a/2c)^{1.65} - q_y$ (D 1.3-2)

where

a : calculated crack depth

2c : calculated crack length

G_0, G_1 : correction factors to ASME BPVC Section XI, App. A, Table A-3320-1 and Table A-3320-2, which differ depending on the calculation of the stress intensity factor at point 1 (crack depth) or point 2 (crack length); G_1 is not relevant if constant stress through the wall is assumed

A_0, A_1 : polynomial coefficients to describe the stress distribution through the wall to ASME BPVC Section XI, App. A, Article A-3200 (b); not relevant if constant stress through the wall is assumed

A_p : internal pressure (for surface cracks at pipe inner wall, otherwise equal to zero)

q_y : plastic zone correction factor; = 0 acc. to ASME BPVC Section XI, Article A-5200

(2) Determination of minimum (K_{min}) and maximum (K_{max}) stress intensity factor (determination for minimum and maximum loading)

$K_{min,j}$ = K ($A_{0,min}$, $A_{p,min}$, $G_{0,j}$, $A_{1,min}$, $G_{1,j}$, a, 2c) (D 1.3-3)

$K_{max,j}$ = K ($A_{0,max}$, $A_{p,max}$, $G_{0,j}$, $A_{1,max}$, $G_{1,j}$, a, 2c) (D 1.3-4)

j = point 1 (crack depth) or at point 2 (crack length)

$$A_{0,min/max} = \left(\frac{p_{min/max}}{10}\cdot\frac{D_i + s}{4\cdot s}\right) + \left(\frac{M_{EG}\cdot 10^6}{\frac{\pi}{32}\cdot\left(\frac{(D_i+2\cdot s)^4 - D_i^4}{(D_i+2\cdot s)}\right)}\right) + \left(\frac{M_{WD}\cdot 10^6}{\frac{\pi}{32}\cdot\left(\frac{(D_i+2\cdot s)^4 - D_i^4}{(D_i+2\cdot s)}\right)}\right) \qquad \text{(D 1.3-5)}$$

Assuming constant stress through the wall the following is obtained for the initial crack in the example:

$K_{min,P1}$ = 22.8 N/mm$^{3/2}$,

$K_{max,P1}$ = 366.2 N/mm$^{3/2}$,

$K_{min,P2}$ = 14.6 N/mm$^{3/2}$ and

$K_{max,P2}$ = 234.3 N/mm$^{3/2}$

Residual stresses have not been considered in the determination of stress intensity factors.

(3) Calculation of stress intensity range

$$\Delta K_j = K_{max,j} - K_{min,j} \qquad \text{(D 1.3-6)}$$

At constant stress through the wall the following is obtained for the initial crack in the example:

ΔK_{P1} = 343.2 N/mm$^{3/2}$ and ΔK_{P2} = 219.7 N/mm$^{3/2}$

(4) Determination of the ratio R:

$$R = \frac{K_{min}}{K_{max}} \qquad \text{(D 1.3-7)}$$

At constant stress through the wall the following is obtained for the initial crack in the example: R = 0.062

(5) Crack growth calculation to equation B 2.5-2 with equation B 2.5-3

$$\frac{da}{dN} = C\cdot(\Delta K)^m + C_{Env}\cdot S(R)^{0.5}\cdot T_R^{0.5}\cdot(\Delta K)^{1.65} \qquad \text{(D 1.3-8)}$$

(6) Calculation of Δa and Δc per cycle for the example (equations to Annex B 2.5):

$C = 10^F \cdot S(R) = 2.84 \cdot 10^{-8}$ for P1 and P2

$C_{Env} = 8.33 \cdot 10^{-11}$ to [51] for 0.2 ppm DO

m = 3.3

T_R = 3600 s

S(R) = 1+1,8 R = 1,1115 (D 1.3-9)

$F_j = -8.714 + 1.34 \cdot 10^{-3}\cdot T_j - 3.34 \cdot 10^{-6}\, T_j^2 + 5.95 \cdot 10^{-9}\cdot T_j^3$ = - 8.57 for P1 and P2 (D 1.3-10)

$\Delta a = C \cdot \Delta K_{P1}^m + C_{Env}\cdot T_R^{0.5}\cdot S(R)^{0.5}\cdot \Delta K_{P1}^{1.65}$

$= 0.28 \cdot 10^{-3}$ mm (D 1.3-11)

$\Delta c = C \cdot \Delta K_{P2}^m + C_{Env}\cdot T_R^{0.5}\cdot S(R)^{0.5}\cdot \Delta K_{P2}^{1.65}$

$= 0.12 \cdot 10^{-3}$ mm (D 1.3-12)

and from this the following is derived for the point in time after the first cycle

new flaw depth:

$a_{1Z} = a_a + \Delta a$ = 4.50028 mm (D 1.3-13)

new flaw length:

$2c_{1Z} = 2c_a + 2\cdot\Delta c$ = 27.00024 mm (D 1.3-14)

(7) For the period of operating time to follow, the flaw dimension calculated before is used as new initial value and the calculation is restarted at point (1).

Until the end of life (EOL = 40 years; 240 start-up/shutdown cycles) the following values are obtained:

flaw depth: a_e = 4.57 mm

flaw length: $2c_e$ = 27.06 mm

D 1.4 Step 3 to Figure A-3: calculation of critical through-thickness crack length $2c_{krit}$

D 1.4.1 Determination of the necessary input values to be calculated

(1) Axial stress due to internal pressure (primary stress) to equation B 2.1-14 with p = 7.4 MPa:

$\sigma_{ax,p}$ = 28.3 N/mm^2 (D 1.4-1)

(2) Elastic resistance moment of pipe to equation B 2.1-16:

W_{pipe} = 743606.4 mm^3 (D 1.4-2)

(3) Axial stress due to moment (bending stress) to equation B 2.1-15 with M = 72.3 kNm:

$\sigma_{ax,M}$ = 97.2 N/mm^2 (D 1.4-3)

D 1.4.2 Plastic limit load approach (PLL)

(1) Flow stress to Table B 2.1-1 for the austenitic steel 1.4550:

$$\sigma_f = \frac{(R_{p0.2T} + R_{mT})}{2.4} = 240 \text{ N/mm}^2 \qquad \text{(D 1.4-4)}$$

(2) The crack angle 2α of the though-wall crack at which failure of the cracked pipe under the loadings mentioned before (equation D 1.4-1 and D 1.4-3) cannot be excluded, are calculated using equation B 2.1-13 in consideration of a through-thickness crack with a/s = 1.

A critical crack angle of 2α = 121.6° is obtained. Based on the mean diameter D_m this corresponds to a critical through-thickness crack length $2c_{krit,PLL}$ = 273.9 mm.

(3) The pertinent leak-before-break diagram for the plastic limit load approach is shown in **Figure D 1-2**. The critical crack depth a_{krit} ($2c_e$) for step 4 (acc. to **Figure A-3**) is given by a_{krit} ($2c_e$) = s = 15 mm.

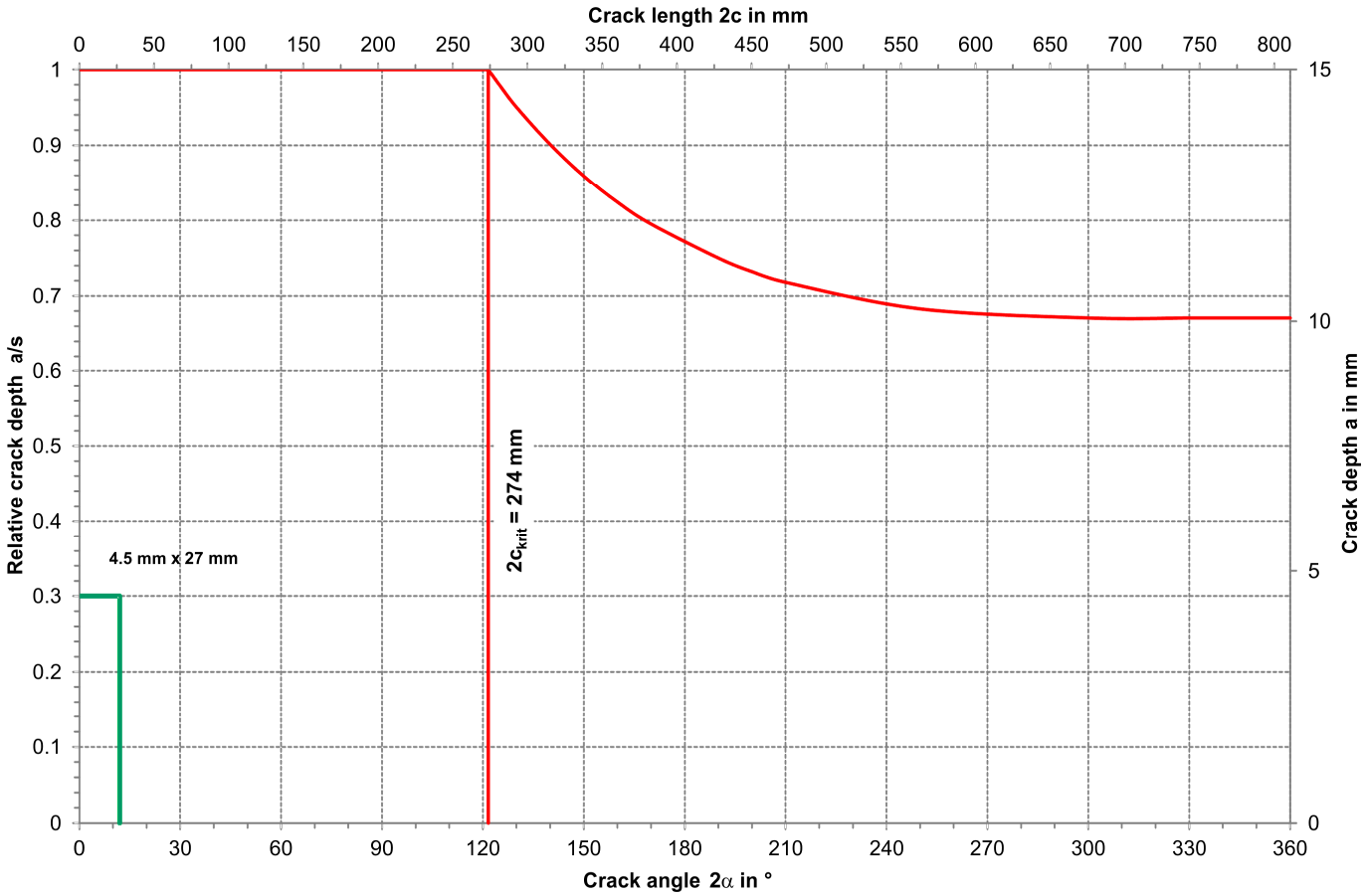

Figure D 1-2: Leak-before-break diagram – plastic limit load approach (PLL)

D 1.4.3 Flow stress concept (FSC)

D 1.4.3.1 Calculation according to MPA (FSC/MPA)

(1) For base material areas the flow stress is obtained from Table B 2.1-1 for the austenitic steel 1.4550:

$$\sigma_{F,FSC/MPA} = \frac{(R_{p0.2T} + R_{mT})}{2} = 288 \text{ N/mm}^2 \qquad \text{(D 1.4-5)}$$

(2) The crack angle 2α of the through-thickness crack at which failure of the cracked pipe under the loadings mentioned before (internal pressure 7.4 MPa and bending moment M = 72.3 kNm) cannot be excluded, is given by solving equation B 2.1-17. A critical crack angle of 2α = 90.03° is obtained. Based on the mean diameter D_m this corresponds to a critical through-thickness crack length $2c_{krit\ FSC/MPA}$ = 202.7 mm.

(3) The pertinent leak-before-break diagram for the FSC/MPA method is shown in **Figure D 1-3.** The critical crack depth a_{krit} ($2c_e$) for step 4 (acc. to Figure A-3) is given by a_{krit} ($2c_e$) = s = 15 mm.

D 1.4.3.2 Calculation according to Siemens-KWU (now AREVA) (FSC/KWU)

(1) Flow stress to Table B 2.1-1 for the austenitic steel 1.4550:

$$\sigma_{F,FSC/KWU} = 0.6 \cdot (R_{p0.2} + R_m) = 345.6 \text{ N/mm}^2 \qquad \text{(D 1.4-6)}$$

(2) The crack angle 2α of the through-thickness crack at which failure of the cracked pipe under the loadings mentioned before (equations D 1.4-1 and D 1.4-3) cannot be excluded, is given by solving equations B 2.1-19 and B 2.1-21. For a through-thickness crack the stress intensification factors for point B (a/s = 1) given by equations B 2.1-22 and B 2.1-23 are considered. A critical crack angle of 2α = 105.9° is obtained. Based on the mean diameter D_m this corresponds to a critical through-thickness crack length $2c_{krit,FSC/KWU}$ = 238.3 mm.

(3) The pertinent leak-before-break diagram for the FSC/KWU method is shown in **Figure D 1-4.** The critical crack depth a_{krit} ($2c_e$) for step 4 (acc. to Figure A-3) is given by a_{krit} ($2c_e$) = s = 15 mm.

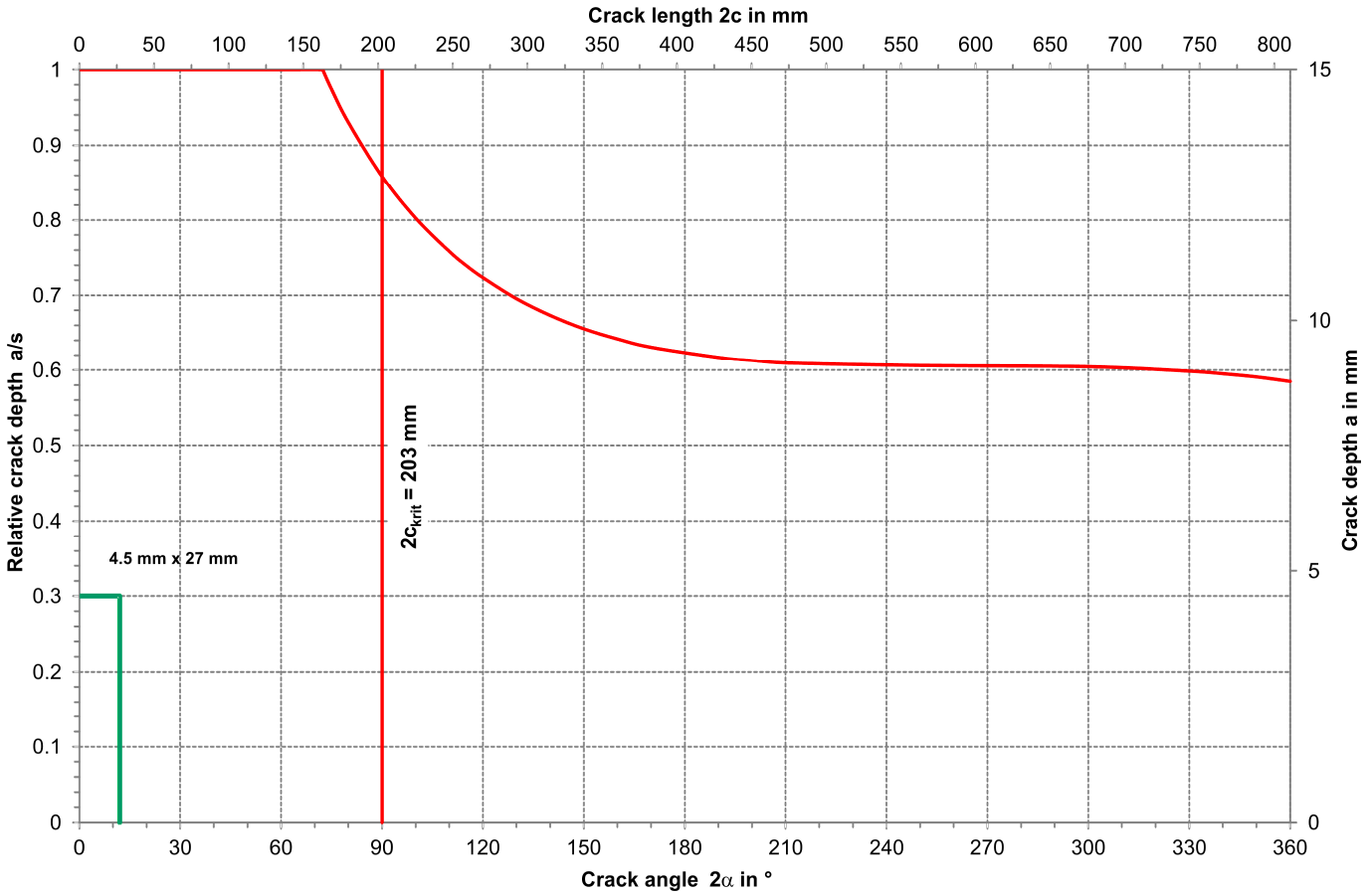

Figure D 1-3: Leak-before-break diagram – FSC / MPA

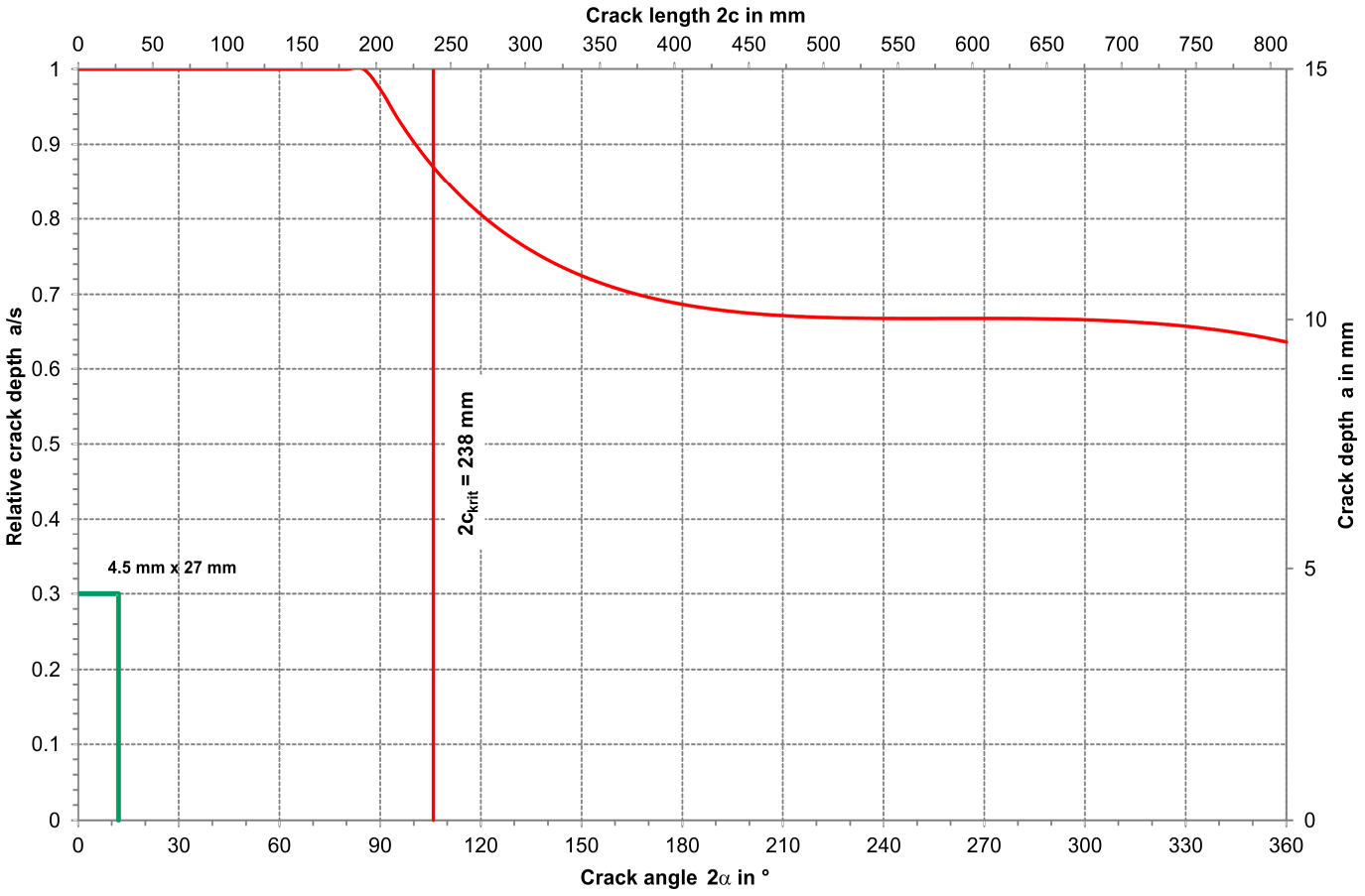

Figure D 1-4: Leak-before-break diagram – FSC / KWU

D 1.4.4 J-Integral/Tearing modulus procedure

D 1.4.4.1 Stress-strain curve

For the example the stress-strain curve to Annex B, **Figure B 2.2-5** was taken with the following Ramberg-Osgood parameters:

E	186000	MPa
α	15.5	
$R_{p0.2}$	167	MPa
n	2.5	

D 1.4.4.2 Analytical procedure

(1) Bending only

a) Stable crack growth in the structure in crack length orientation of Δc_{max} = 2.5 mm occurs for a through-thickness crack with a length between 2 · 125 mm and 2 · 130 mm ($2c_{2.5mm}$ between 250 mm and 260 mm, based on external diameter). At a stable crack growth of Δc_{max} = 2.5 mm no instability will occur in crack length orientation.

b) The total angle lies between 104.9° (for 250 mm) and 109.1° (for 260 mm), based on external diameter.

See **Figures D 1-5** and **D 1-6**.

(2) Internal pressure only

a) Under internal pressure no stable crack growth in crack length orientation to exceed Δc_{max} = 2.5 mm will occur at an angle up to 180°.

b) With bending stresses = bending stress due to moment and axial stresses due to internal pressure stable crack growth will occur in the structure in crack length orientation of Δc_{max} = 2.5 mm between 2 · 90 mm und 2 · 95 mm ($2c_{2.5mm}$ between 180 mm and 190 mm, based on external diameter).

c) The total angle lies between 75.6° (for 180 mm) and 79.7° (for 190 mm), based on external diameter.

See **Figures D 1-7** and **D 1-8**.

(3) For the calculation of the critical crack size a maximum stable crack growth of Δc_{max} = 2.5 mm in crack length orientation is considered.

This leads to the following critical through-thickness crack length:

$2c_{krit}$ = 170 mm (based on mean radius)

Angle = 75.6°.

Note:

Due to the limitation of the J-R curve to Δc_{max} in the structure in crack length orientation no instability is yet obtained at $2c_{krit}$.

D 1.4.4.3 Finite element analysis

(1) The analysis is made using the FE model (ABAQUS) shown in **Figure D 1-9**. Square elements and wedge elements are used for the crack tip.

(2) The distribution of axial stresses is shown in **Figure D 1-10**.

(3) The J-integral has been evaluated under the same loading for several crack angles along the crack front (average values over the wall thickness) (see **Figure D 1-11**). The results are shown in **Table D 1-1**.

(4) For the calculation of the critical crack size a maximum stable crack growth of Δc_{max} = 2.5 mm in crack length orientation is considered.

This leads to the following critical through-thickness crack length:

$2c_{krit}$ = 273.5 mm (based on mean radius)

Angle = 121.4°.

Note:

Due to the limitation of the J-R curve to Δc_{max} in the structure in crack length orientation no instability is yet obtained at $2c_{krit}$.

Crack angle in Grad	Flaw length [1] in mm	J-integral in N/mm
100	225.15	134.89
120	270.18	585.74
140	315.21	2313.79
160	360.24	7055.50

[1] Flaw length based on : mean radius

Table D 1-1: J-Integral depending on crack angle

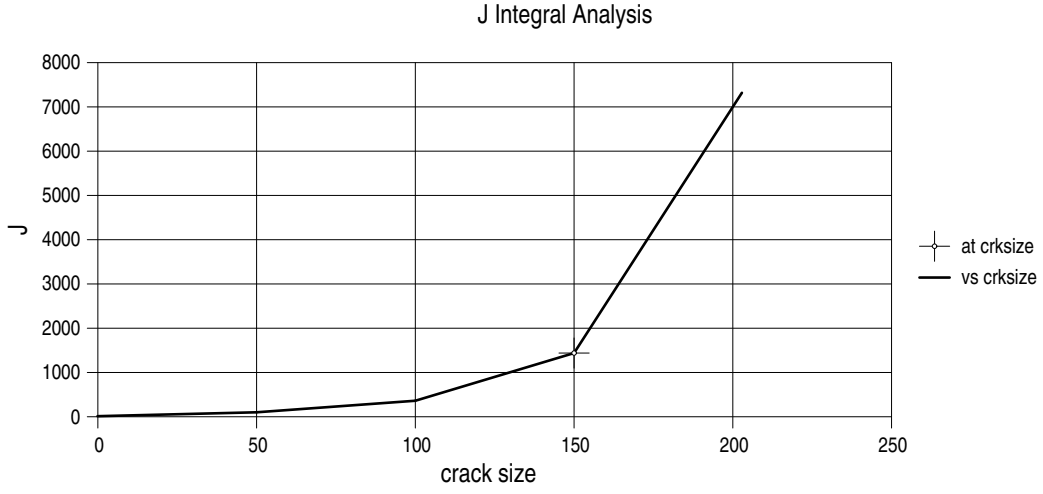

crack size : one half the crack length

Figure D 1-5: J-integral analysis for bending

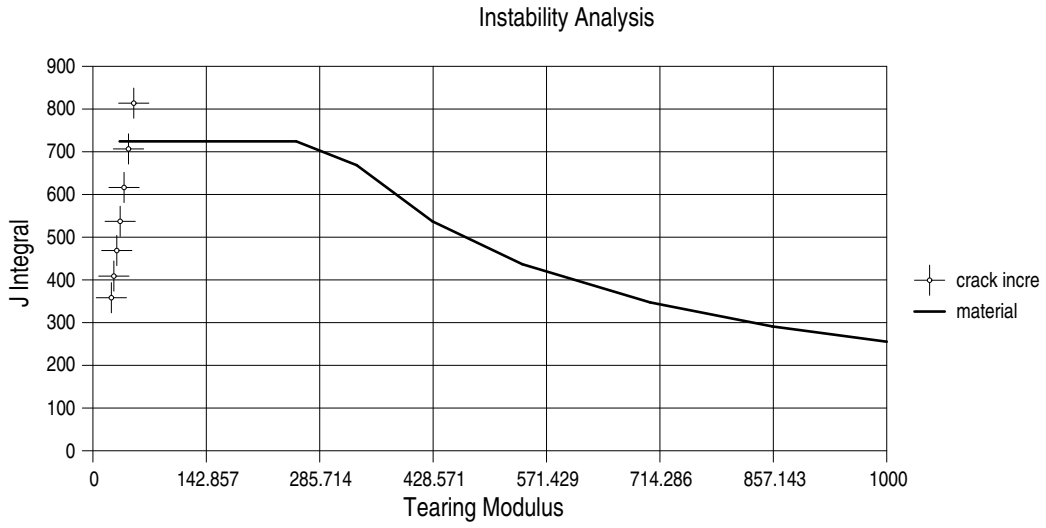

Figure D 1-6: Instability analysis for bending

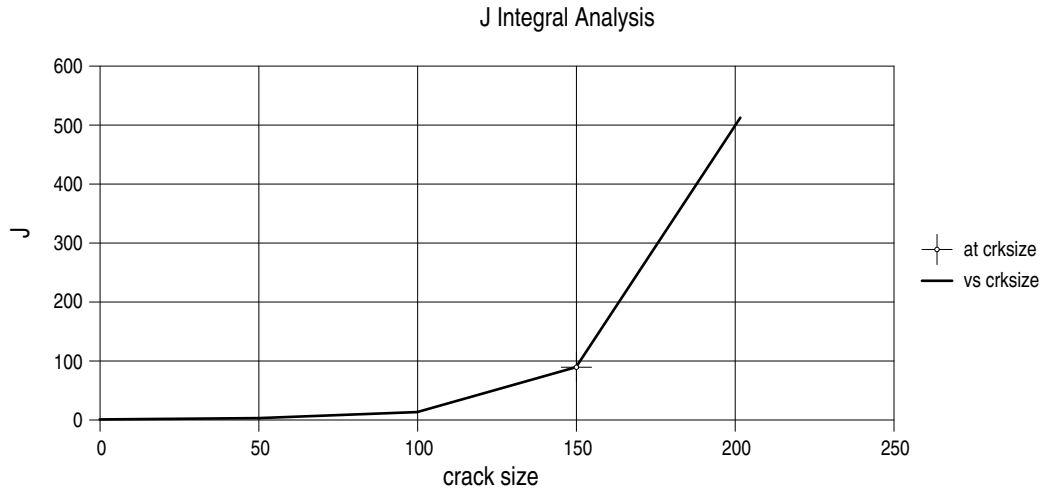

Figure D 1-7: J-integral analysis for internal pressure

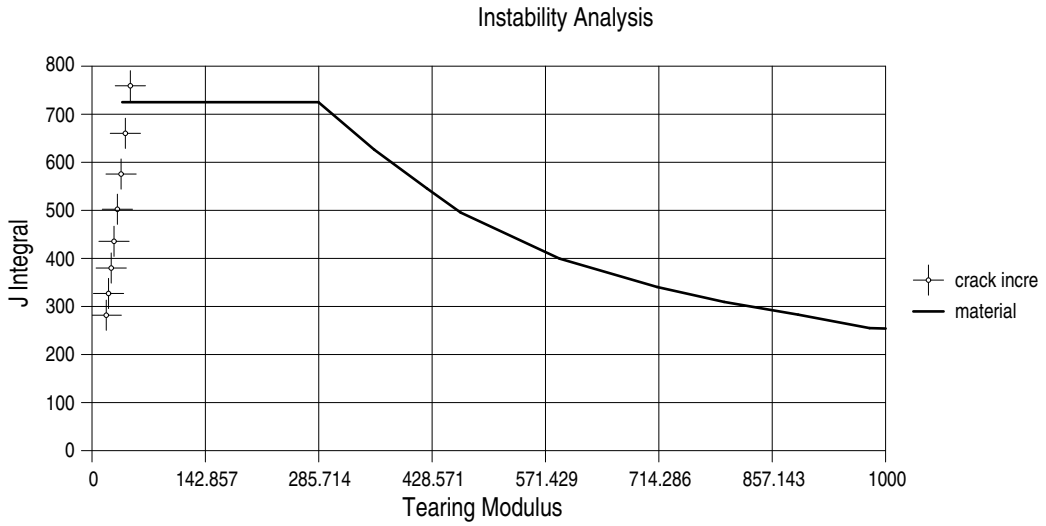

Figure D 1-8: Instability analysis for internal pressure

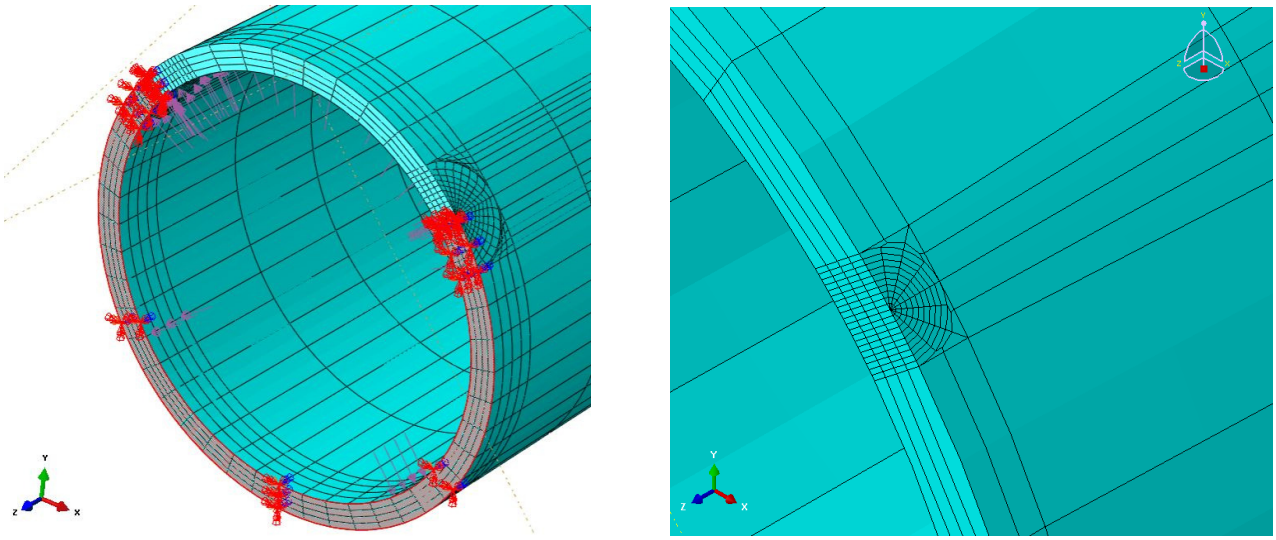

Figure D 1-9: Finite element model and boundary conditions
(Through-thickness crack at the connection of pipe to a component; all degrees of freedom fixed in the ligament thus minimizing the leakage area compared to other restraints)

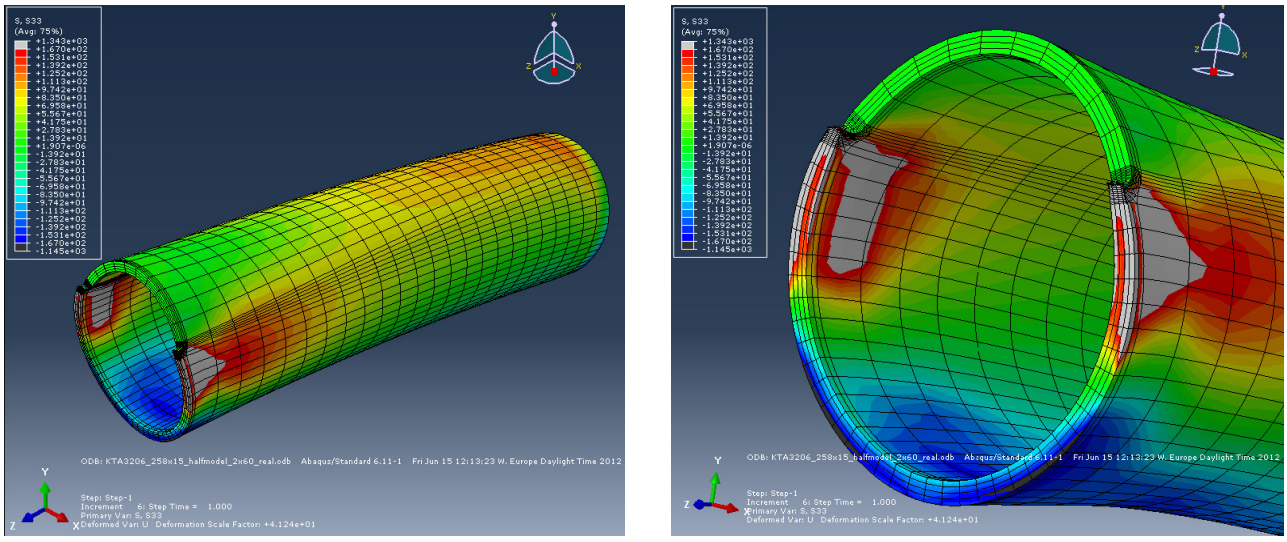

Figure D 1-10: Distribution of axial stresses

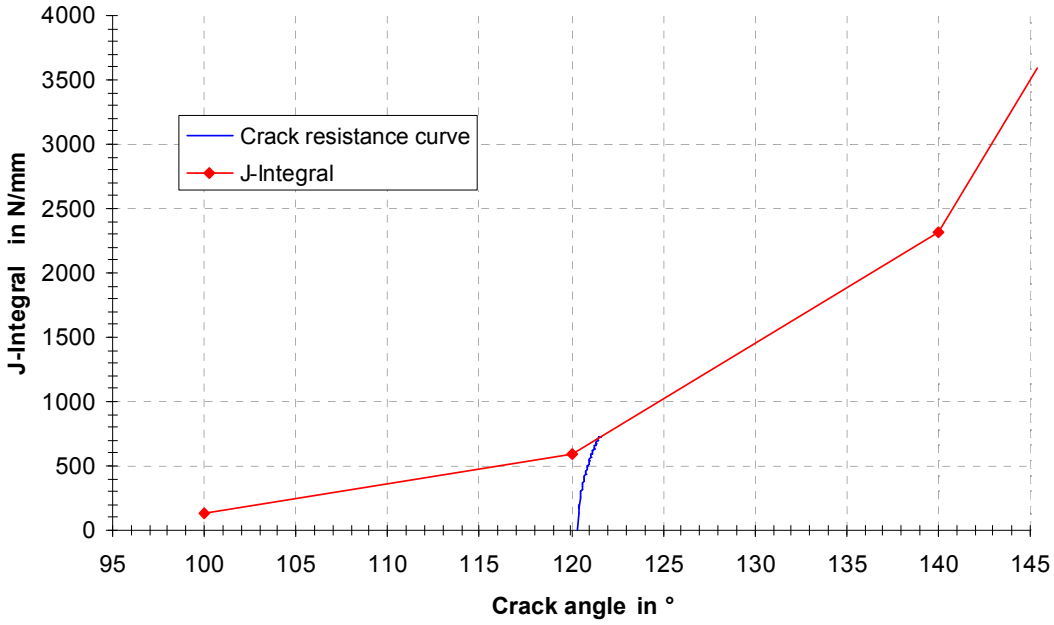

Figure D 1-11: Progression of J-integral and J-R curve

D 1.4.5 Two-criteria method

(1) The calculation in this example are made to [32] for point A acc. to **Figure D 1-12** with and without consideration of welding residual stresses.

Note:
The calculation for point A leads to higher crack loadings compared to point B and thus is conservative for this example.

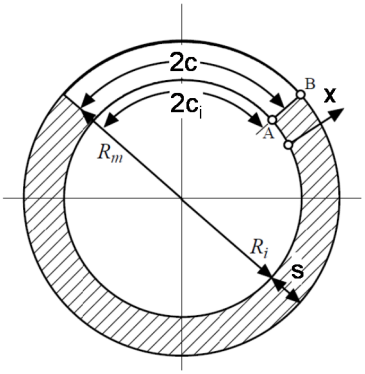

Figure D 1-12: Crack configuration

(2) The determination of secondary stresses to Table R5 in connection with Table R1 in [32] results in a linear course across the wall thickness:

$$\sigma^S = (1.5884 - 0.05284 \cdot s) \cdot R_{p1.0T} [1 - 2 \cdot (x \cdot s^{-1})] \quad \text{(D 1.4-7)}$$

$$\sigma^S = (1.5884 - 0.05284 \cdot s) \cdot (196\ \text{MPa}) \cdot [1 - 2 \cdot (x \cdot s^{-1})] \quad \text{(D 1.4-8)}$$

$\sigma_i^S{}_{(x=0.0)} = 156$ MPa

$\sigma_a^S{}_{(x=1.0)} = -156$ MPa

(3) The critical through-thickness crack length $2c_{krit}$ and the critical crack depth a_{krit} of the surface crack shall be determined using the J-R curves of **Figure D 1-1**.

(4) The "Failure Assessment Curve" (FAC) is calculated acc. to the following relationship:

$$K_r \le f_{R6} = (1 - 0.14 \cdot L_r^2) \cdot [0.3 + 0.7\exp(-0.65 \cdot L_r^6)] \quad \text{(D 1.4-9)}$$

$$L_r \le L_r^{max} = \frac{\sigma_f}{R_{p0.2}} \quad \text{for materials without Lüders plateau} \quad \text{(D 1.4-10)}$$

$$\sigma_f = 3 \cdot S_m \quad \text{(D 1.4-11)}$$

(5) K_r is calculated for point A using the tabulated shape functions for K_I to Appendix K3.5.

(6) The calculation of L_r does not depend on the considered evaluation point and is performed according to Appendix L3.5.

(7) Determination of the critical crack depth a_{krit}

$a_{krit} > 0.75 \cdot s = 11.25$ mm, see **Figure D 1-13**.

$a_{zul} = 0.75 \cdot s = 11.25$ mm.

(8) Determination of the critical through-thickness crack length $2c_{krit}$

Note:
Due to the limitation of the J-R curve to Δa_{max} no instability is yet obtained at $2c_{krit}$.

a) The critical through-thickness crack length without consideration of residual stresses results in $2c_{krit} = 231$ mm, see **Figure D 1-14**.

b) The critical through-thickness crack length with consideration of residual stresses results in $2c_{krit} = 223$ mm, see **Figure D 1-15.**

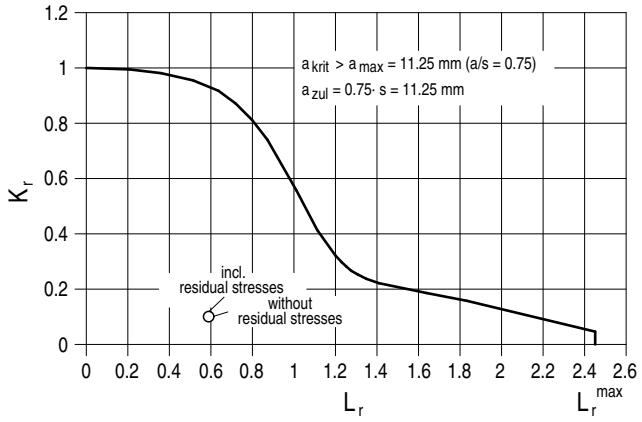

Figure D 1-13: Determination of allowable crack depth

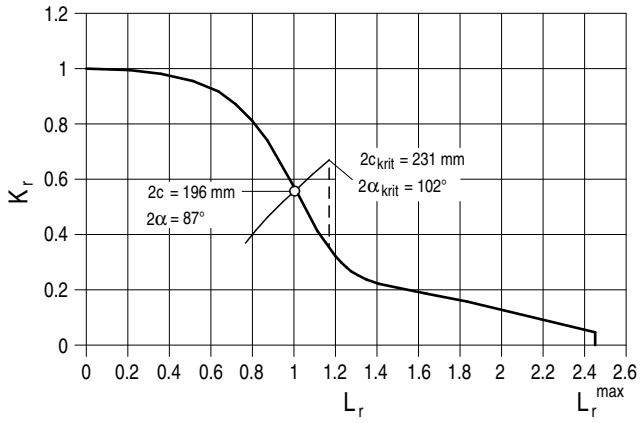

Figure D 1-14: Determination of critical crack length without consideration of residual stresses

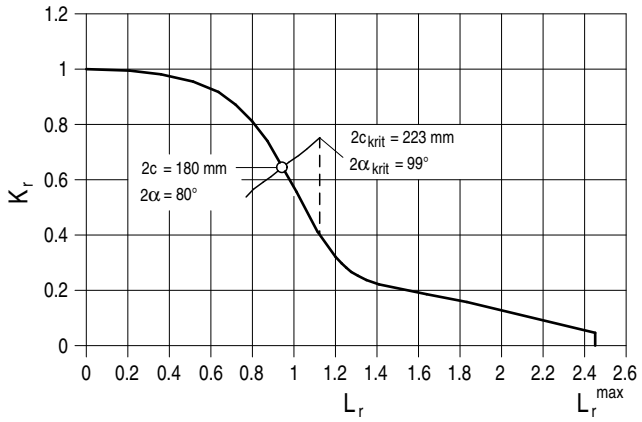

Figure D 1-15: Determination of critical crack length with consideration of residual stresses

D 1.5 Step 5 to Figure A-3: calculation of the detectable through-thickness crack length $2c_{LÜS}$

(1) Input values from D 1.1 and the following additional data:

a) crack surface roughness: $R_Z = 20.0$ µm

b) flow inlet loss: $\zeta_{Ein} = 0.5$

c) flow outlet loss: $\zeta_{Aus} = 0.0$

d) flow channel length: s = 15 mm (= wall thickness)

e) fluid density: ρ_S = 917.0 kg/m^3
(saturation value to [74])

f) saturation pressure: p_0 = 0.48 MPa
(at T_0 = 150 °C to [74])

g) detectable leak rate: $\dot{m}_{LÜS}$ = 200 kg/h

(2) Leakage area calculation depending on crack length 2c

The leakage area depending on the crack length 2c is shown in **Figure D 1-16**.

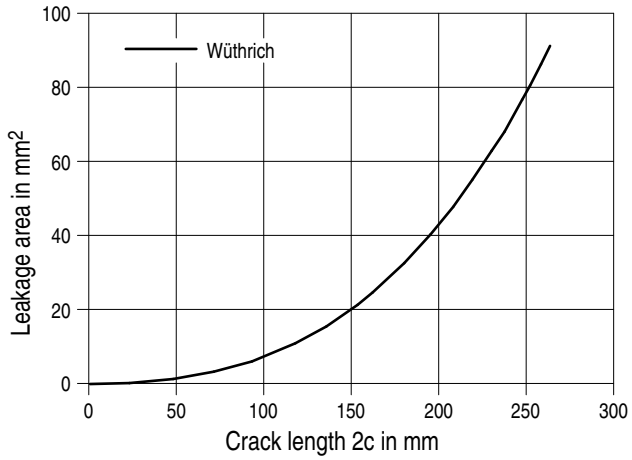

Figure D 1-16: Leakage area depending on crack length 2c for the considered austenitic piping with circumferential crack

For the purpose of clarity only the individual results for the critical through-thickness crack length $2c_{krit}$ = 202.7 mm determined by the FSC/MPA method are given hereafter by means of formulas as example.

a) $\sigma = \sigma_p + \sigma_{Mb}$ = 78 N/mm^2

Note:
The consideration of the bending stress as membrane stress in the present example within the calculation procedure as per [55] is justified (see [65]).

b) $E' = E/(1-\nu^2)$ = 204.4 kN/mm^2

c) Leakage area for infinitely large plate:
A_0 = 24.54 mm^2 as per equation B 3.1-1

d) shell parameter:
λ = 4.2 as per equation B 3.1-5

e) buckling factor for circumferential crack:
$\alpha(\lambda)$ = 1.75 as per equation B 3.1-4

f) stress ratio:
$s = \sigma/\sigma_f = 78/(3 \cdot 131) = 0.20$

g) plasticity correction factor:
$\gamma(s)$ = 1.03 as per equation B 3.1-7

h) leakage area for circumferential crack:
$A = \alpha(\lambda) \cdot \gamma(s) \cdot A_0$ = 44.16 mm^2 as per equation B 3.1-2

(3) Leak rate calculation depending on crack length 2c

a) It is assumed that the leakage area can be modelled by a rhombus, therefore, the leakage area circumference is:
$U = \{4 \cdot A^2/c^2 + 16 \cdot c^2\}^{0.5}$ = 405 mm

b) Hydraulic diameter:
$D_h = 4 \cdot A/U$ = 0.436 mm as per equation B 3.2-3

c) Acc. to clause B 3.2.2.5 the following applies:
$D_h/(2 \cdot R_z)$ = 10.89,
thus the resistance factor results in
λ = 0.340 as per equation B 3.2-13

d) Flow resistance:
$\zeta = \zeta_{Ein} + \lambda \cdot s/D_h + \zeta_{Aus}$ = 12.19 as per equation B 3.2-2

e) Mass flow density:

$$G = \sqrt{\frac{2 \cdot [p_0 - p_S(T_0)] \cdot \rho_S(T_0)}{1+\zeta}} = 0.031 \text{ kg} \cdot \text{s}^{-1} \cdot \text{mm}^{-2}$$

as per equation B 3.2-1

f) Leak rate:
$\dot{m}_{LÜS} = G \cdot A$ = 1.39 kg/s $\geq$ 200 kg/h

At a crack length $2c_{LÜS}$ = 87 mm the leak rate of 200 kg/h detectable by the leakage monitoring system is already attained, see **Figure D 1-17**:

D 1.6 Step 6 to Figure A-3: Evaluation whether integrity is proved

In D 1.3 the possible crack growth as well as possible crack lengths and crack depths have been determined. In D 1.4 the critical crack length has been determined. The following evaluation shows that integrity has been proved:

a) flaw length: $2c_e$ = 27.06 mm < $2c_{krit}$ = 202.7 mm

b) flaw depth: a_e = 4.57 mm < a_{zul} = 11.25 mm

Note:
a_{krit} has not been calculated here and will be greater than 0.75 · s acc. to the calculation in sub-clause D 1.4.5 (7).

D 1.7 Step 7 to Figure A-3: Evaluation whether leak-before-break is proved

In D 1.4 the critical crack length $2c_{krit}$ has been calculated. In D 1.5 the detectable crack length $2c_{LÜS}$ has been determined. The evaluation hereafter shows that leak-before-break behaviour has been proved:

$$2c_{LÜS} = 87 \text{ mm} < 2c_{krit} = 202.7 \text{ mm}$$

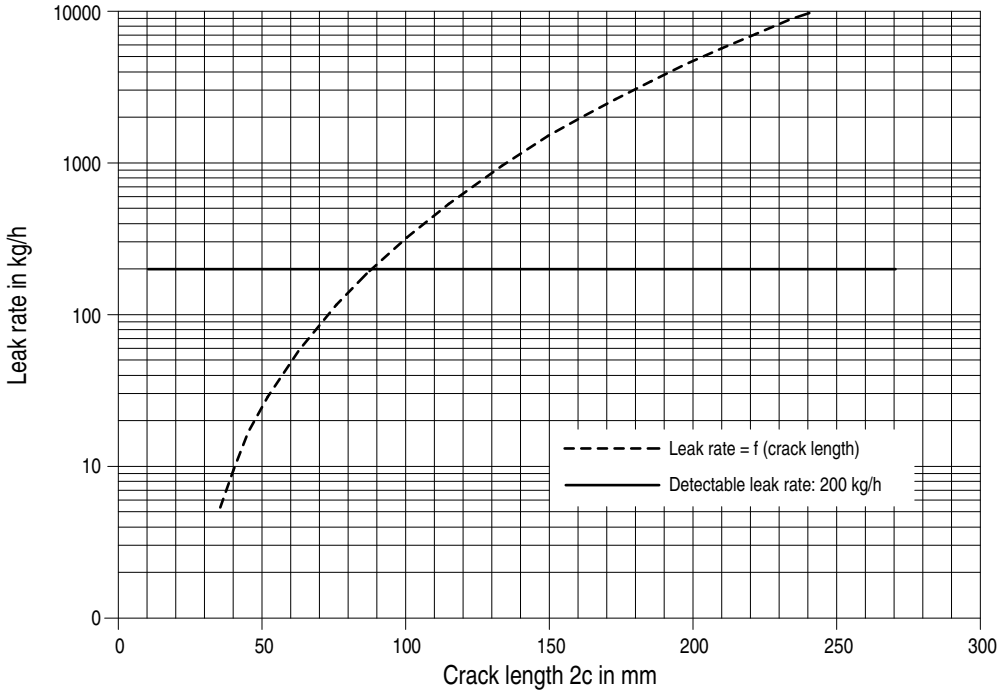

Figure D 1-17: Leak rate for the considered austenitic piping with circumferential crack in dependence of the crack length 2c

D 2 Ferritic piping with circumferential crack

D 2.1 Input data

(1) Input data

a) from the governing load case level D (for fracture mechanics calculation)

Pressure:	p = 15.8 MPa
Temperature:	T = 319 °C
Bending moment during operation:	M_{EG+WD} = 2400 kNm
Bending moment in case of damage:	$M_{EG+WD+SEB}$ = 3737 kNm

b) from load case combination start-up/shutdown (for crack growth calculation)

Max. pressure:	p_{max} = 15.8 MPa
Min. pressure:	p_{min} = 0.0 MPa
Max. temperature:	T_{max} = 319 °C
Min. temperature:	T_{min} = 20.0 °C
Max. bending moment (= M_{EG} + M_{WD}):	M_{max} = 2400 kNm
Min. bending moment:	M_{min} = 0 kNm

(2) Geometry

External diameter:	D_a = 864.0 mm
Wall thickness:	s = 52.0 mm (without cladding)

(3) Material

Material designation:	20MnMoNi5-5 (1.6310)
Modulus of elasticity:	E = 192 kN/mm^2 (bei 300 °C)
Poisson's ratio:	ν = 0.3
0.2% proof stress (at 350 °C as per KTA 3201.1):	$R_{p0.2T}$ = 363.0 N/mm^2
Tensile strength (at 350 °C as per KTA 3201.1 by interpolation):	R_{mT} = 513.0 N/mm^2
Equivalent stress intensity as per KTA 3201.2:	S_m = 190.0 N/mm^2
J-R curve	as per **Figure D 2-1**

Note:
The transferability of the J-R curve to pipes with circumferential cracks under internal pressure and bending moment loading was proved in [72] for comparable pipes made of austenitic material. These results also apply to the highly ductile material 20MnMoNi5-5 considered here.

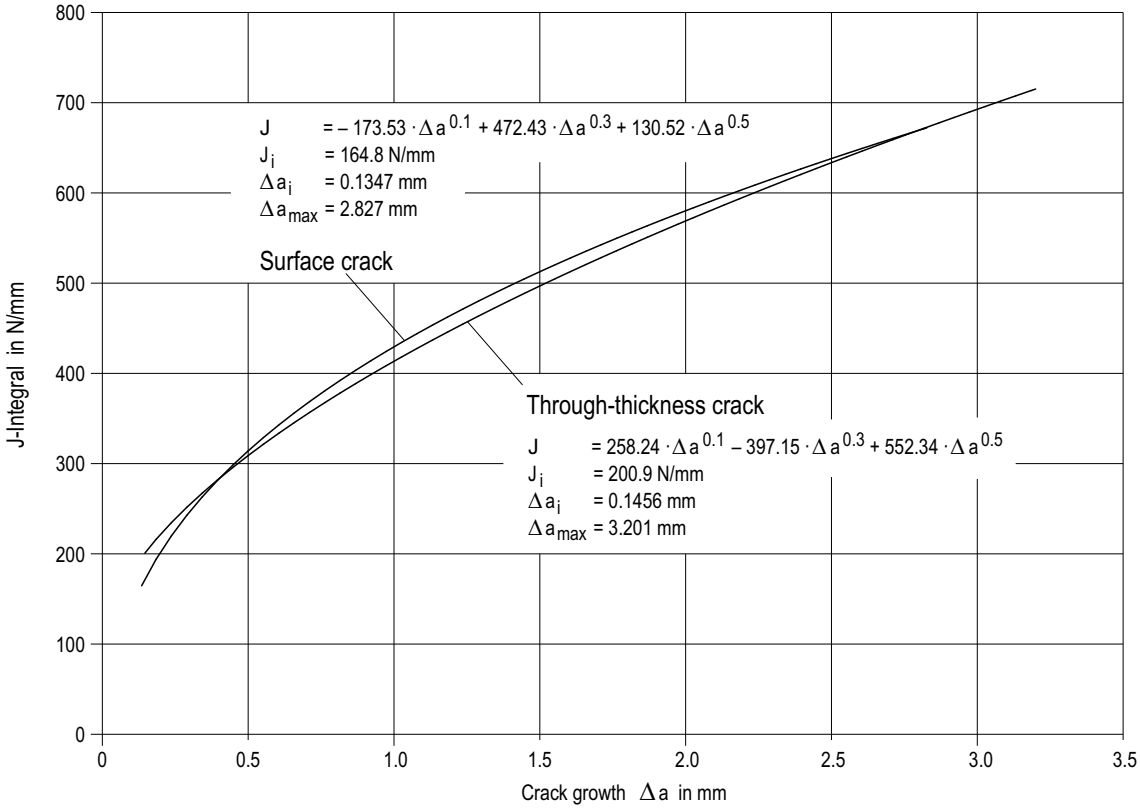

Figure D 2-1: J-R curve for the considered ferritic piping with circumferential crack

D 2.2 Step 1 to Figure A-3: determination of initial crack

(1) Determination to equation A 2-1 and equation A 2-5:

$a_a = 0.1 \cdot s = 5.2$ mm (D 2.2-1)

$2 \cdot c_a \geq 6 \cdot a_a = 31.2$ mm (D 2.2-2)

D 2.3 Step 2 to Figure A-3: determination of crack development Δa and 2Δc

(1) Determination of stress intensity factors K [73]

$$K = \left[(A_0 + A_P) \cdot G_0 + A_1 \cdot G_1\right] \cdot \sqrt{\pi \cdot a/Q} \quad \text{(D 2.3-1)}$$

with $$Q = 1 + 4.593 \cdot (a/2c)^{1.65} - q_y \quad \text{(D 2.3-2)}$$

where

a : calculated crack depth

$2c$: calculated crack length

G_0, G_1 : correction factors to ASME BPVC Section XI, App. A, Table A-3320-1 and Table A-3320-2, which differ depending on the calculation of the stress intensity factor at point 1 (crack depth) or point 2 (crack length); G_1 is not relevant if constant stress through the wall is assumed

A_0, A_1 : polynomial coefficients to describe the stress distribution through the wall to ASME BPVC Section XI, App. A, Article A-3200 (b); not relevant if constant stress through the wall is assumed

A_p : internal pressure (for surface cracks at pipe inner wall, otherwise equal to zero)

q_y : plastic zone correction factor; = 0 acc. to ASME BPVC Section XI, Article A-5200

(2) Determination of minimum (K_{min}) and maximum (K_{max}) stress intensity factor (determination for minimum and maximum loading)

$K_{min,j} = 0$ (D 2.3-3)

$K_{max,j} = K\ (A_{0,max}, A_{p,max}, G_{0,j}, A_{1,max}, G_{1,j}, a, 2c)$ (D 2.3-4)

j = point 1 (crack depth) or at point 2 (crack length)

$$A_{0,min/max} = \left(\frac{p_{min/max}}{10} \cdot \frac{D_i + s}{4 \cdot s}\right) + \left(\frac{M_{EG} \cdot 10^6}{\frac{\pi}{32} \cdot \left(\frac{(D_i + 2 \cdot s)^4 - D_i^4}{(D_i + 2 \cdot s)}\right)}\right) + \left(\frac{M_{WD} \cdot 10^6}{\frac{\pi}{32} \cdot \left(\frac{(D_i + 2 \cdot s)^4 - D_i^4}{(D_i + 2 \cdot s)}\right)}\right) \quad \text{(D 2.3-5)}$$

Assuming constant stress through the wall the following is obtained for the initial crack in the example:

$K_{min,P1} = 0$ N/mm$^{3/2}$,

$K_{max,P1} = 703.5$ N/mm$^{3/2}$,

$K_{min,P2} = 0$ N/mm$^{3/2}$ und

$K_{max,P2} = 444.3$ N/mm$^{3/2}$

Residual stresses have not been considered in the determination of stress intensity factors.

(3) Calculation of stress intensity range

$$\Delta K_j = K_{max,j} - K_{min,j} \quad \text{(D 2.3-6)}$$

At constant stress through the wall the following is obtained for the initial crack in the example:

$\Delta K_{P1} = 703.5$ N/mm$^{3/2}$ und $\Delta K_{P2} = 444.3$ N/mm$^{3/2}$

(4) Determination of the ratio R:

$$R = \frac{K_{min}}{K_{max}} \quad \text{(D 2.3-7)}$$

At constant stress through the wall the following is obtained for the initial crack in the example: R = 0

(5) Crack growth calculation to equation B 2.5-1

$$\frac{da}{dN} = C \cdot (\Delta K)^m \quad \text{(D 2.3-8)}$$

(6) Calculation of Δa and Δc per cycle for the example using the values for crack growth in water given in [49]):

$S = 1$ for P1 and P2

$C_1 = 2.13 \cdot 10^{-6}$ for P1

$m_1 = 1.95$ for P1

$C_2 = 1.48 \cdot 10^{-11}$ for P2

$m_2 = 5.95$ for P2

$\Delta a = 0.9025 \cdot 10^{-3}$ mm (D 2.3-9)

$\Delta c = 0.1 \cdot 10^{-3}$ mm (D 2.3-10)

and from this the following is derived for the point in time after the first cycle

new flaw depth:

$$a_{1Z} = a_a + \Delta a = 5.2009 \text{ mm} \quad \text{(D 2.3-11)}$$

new flaw length:

$$2c_{1Z} = 2c_a + \Delta 2c = 31.2002 \text{ mm} \quad \text{(D 2.3-12)}$$

(7) For the period of operating time to follow, the flaw dimension calculated before is used as new initial value and the calculation is restarted at point (1).

This is repeated until reaching a given point in time or exceeding a given crack growth (e.g. through-thickness crack, allowable crack depth of 75% of the wall thickness).

Until the end of life (EOL = 40 years; 240 start-up/shutdown cycles) the following values are obtained:

flaw depth: $a_e = 5.42$ mm

flaw length: $2c_e = 31.25$ mm

D 2.4 Step 3 to Figure A-3: calculation of critical through-thickness crack length $2c_{krit}$

D 2.4.1 Determination of the necessary input values to be calculated

For the determination of stresses in the piping the load bearing capacity of the cladding will not be considered in the calculation of the critical through-thickness crack length (conservative).

Axial stress due to internal pressure (primary stress) to equation B 2.1-14 with p =15.8 MPa:

$$\sigma_{ax,p} = 54.03 \text{ N/mm}^2 \quad \text{(D 2.4-1)}$$

Elastic resistance moment of pipe to equation B 2.1-16:

$$W_{pipe} = 25411189.2 \text{ mm}^3 \quad \text{(D 2.4-2)}$$

Axial stress due to moment (bending stress) to equation B 2.1-15 with M = 3737 kNm:

$$\sigma_{ax,M} = 147.06 \text{ N/mm}^2 \quad \text{(D 2.4-3)}$$

D 2.4.2 Plastic limit load approach (PLL)

(1) Flow stress to Table B 2.1-1 for the ferritic steel 1.6310:

$$\sigma_{F,PLL} = R_{p0.2} = 363 \text{ N/mm}^2 \quad \text{(D 2.4-4)}$$

(2) The crack angle 2α of the though-thickness crack at which failure of the cracked pipe under the loadings mentioned before (equations D 2.4-1 and D 2.4-3) cannot be excluded, are calculated using equation B 2.1-13 in consideration of a through-thickness crack with a/s = 1.

A critical crack angle of $2\alpha = 115.29°$ is obtained. Based on the mean diameter D_m this corresponds to a critical through-thickness crack length $2c_{krit,PLL} = 816.9$ mm.

(3) The pertinent leak-before-break diagram for the plastic limit load approach is shown in **Figure D 2-2**. The critical crack depth a_{krit} $(2c_e)$ for step 4 (acc. to **Figure A-3**) is given by a_{krit} $(2c_e) = s$ (52 mm).

D 2.4.3 Flow stress concept (FSC)

D 2.4.3.1 Calculation according to MPA (FSC/MPA)

(1) For base material areas the flow stress is obtained from Table B 2.1-1 for the ferritic steel 1.6310:

$$\sigma_{F,FSC/MPA} = R_m = 513 \text{ N/mm}^2 \quad \text{(D 2.4-5)}$$

(2) The crack angle 2α of the through-thickness crack at which failure of the cracked pipe under the loadings mentioned before (internal pressure 15.8 MPa and bending moment M = 3737 kNm) cannot be excluded, is given by solving equation B 2.1-17. A critical crack angle of $2\alpha = 98.81°$ is obtained. Based on the mean diameter D_m this corresponds to a critical through-thickness crack length $2c_{krit\ FSC/MPA} = 700.2$ mm.

(3) The pertinent leak-before-break diagram for the FSC/MPA method is shown in **Figure D 2-3.** The critical crack depth a_{krit} $(2c_e)$ for step 4 (acc. to Figure A-3) is given by a_{krit} $(2c_e) = s = 52$ mm.

D 2.4.3.2 Calculation according to Siemens-KWU (now AREVA) (FSC/KWU)

(1) Flow stress to Table B 2.1-1 for the ferritic steel 1.6310:

$$\sigma_{F,FSC/KWU} = R_m = 513 \text{ N/mm}^2 \quad \text{(D 2.4-6)}$$

(2) The crack angle 2α of the through-thickness crack at which failure of the cracked pipe under the loadings mentioned before (equations D 2.4-1 and D 2.4-3) cannot be excluded, is given by solving equations B 2.1-19 and B 2.1-21. For a through-thickness crack the stress intensification factors for point B (a/s = 1) given by equations B 2.1-22 and B 2.1-23 are considered. A critical crack angle of $2\alpha = 98.16°$ is obtained. Based on the mean diameter D_m this corresponds to a critical through-thickness crack length $2c_{krit,FSC/KWU} = 695.6$ mm.

(3) The pertinent leak-before-break diagram for the FSC/KWU method is shown in **Figure D 2-4.** The critical crack depth a_{krit} $(2c_e)$ for step 4 (acc. to Figure A-3) is given by a_{krit} $(2c_e) = s$ (52 mm).

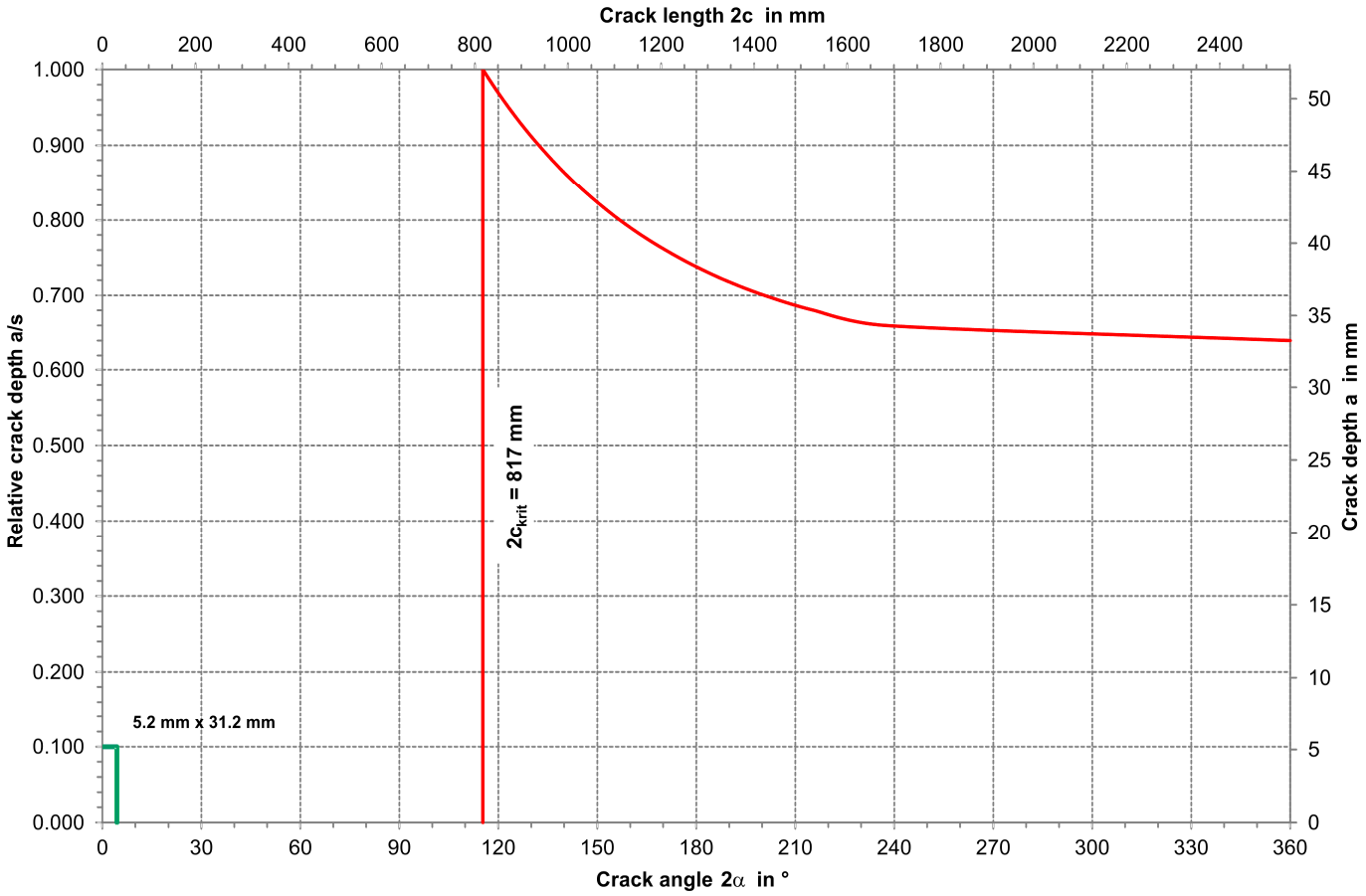

Bild D 2-2: Leak-before-break diagram – plastic limit load approach (PLL)

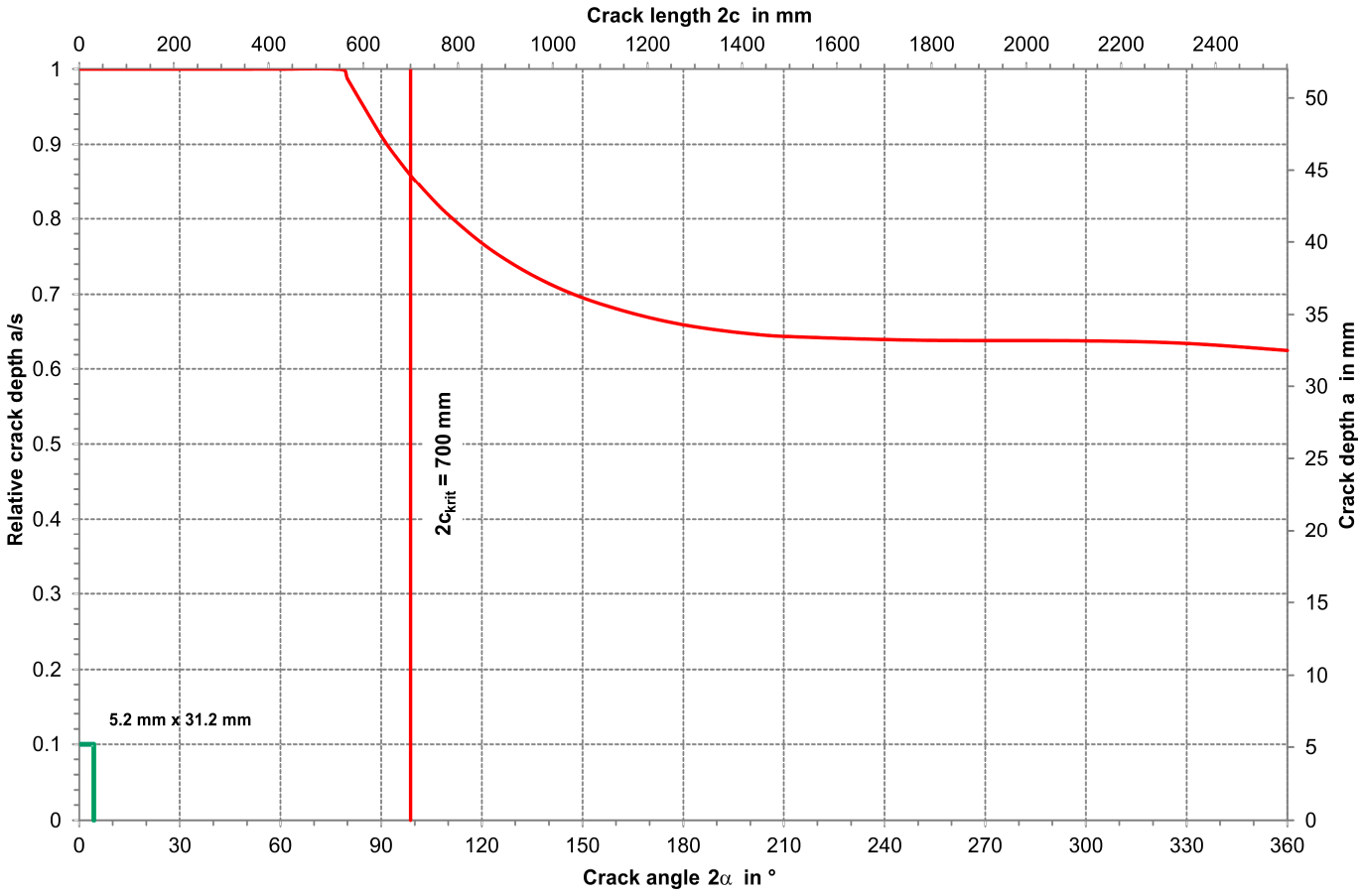

Bild D 2-3: Leak-before-break diagram – FSC / MPA

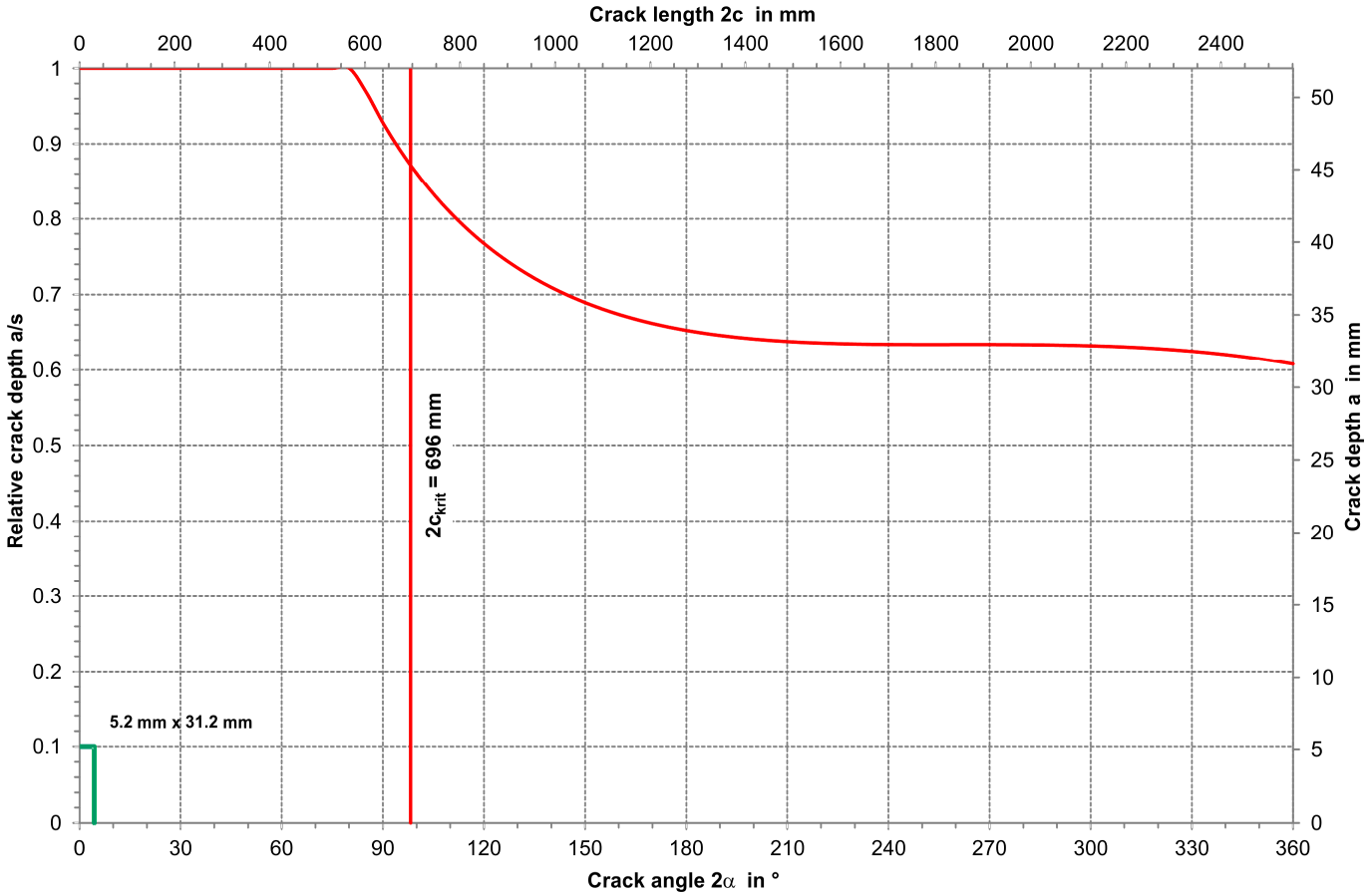

Bild D 2-4: Leak-before-break diagram – FSC / KWU

D 2.4.4 J-Integral/Tearing modulus procedure

D 2.4.4.1 Stress-strain curve

For the example the stress-strain curve was taken with the following Ramberg-Osgood parameters:

E	192000	MPa
α	10	
$R_{p0.2}$	363	MPa
n	4.5	

D 2.4.4.2 Analytical procedure

(1) Bending only

a) Stable crack growth in the structure in crack length orientation of Δc_{max} = 3.2 mm occurs for a through-thickness crack with a length between 2 · 360 mm and 2 · 370 mm ($2c_{3.2mm}$ between 720 mm and 740 mm, based on external diameter). At a stable crack growth in the structure of Δc_{max} = 3.2 mm no instability will occur in crack length orientation.

b) The total angle lies between 95.4° (for 720 mm) and 98° (for 740 mm).

See **Figures D 2-5** and **D 2-6**.

(2) Internal pressure only:

a) Stable crack growth in the structure in crack length orientation of Δc_{max} = 3.2 mm occurs for a through-thickness crack with a length between 2 · 560 mm and 2 · 570 mm ($2c_{3.2mm}$ between 1120 mm and 1140 mm, based on external diameter). At a stable crack growth in the structure of Δc_{max} = 3.2 mm no instability will occur in crack length orientation.

b) The total angle lies between 148° (for 1120 mm) and 151° (for 1140 mm).

See **Figures D 2-7** and **D 2-8**.

c) with bending stresses = bending stress due to moment + axial stresses due to internal pressure stable crack growth will occur in the structure in crack length orientation of Δc_{max} = 3.2 between 2 · 230 mm and 2 · 240 mm (based on external diameter).

d) The total angle lies between 61° (460 mm) and 63.6° (480 mm), see **Figure D 2-9**.

(3) Critical through-thickness crack length

For the calculation of the critical crack size a maximum stable crack growth in the structure of Δc_{max} = 3.2 mm in crack length orientation is considered.

Upon interpolation, the following critical through-thickness crack length is obtained:

$2c_{krit}$ = 432 mm (based on mean radius)

Angle = 61°.

Note:
Due to the limitation of the J-R curve to Δc_{max} in the structure in crack length orientation no instability is yet obtained at $2c_{krit}$.

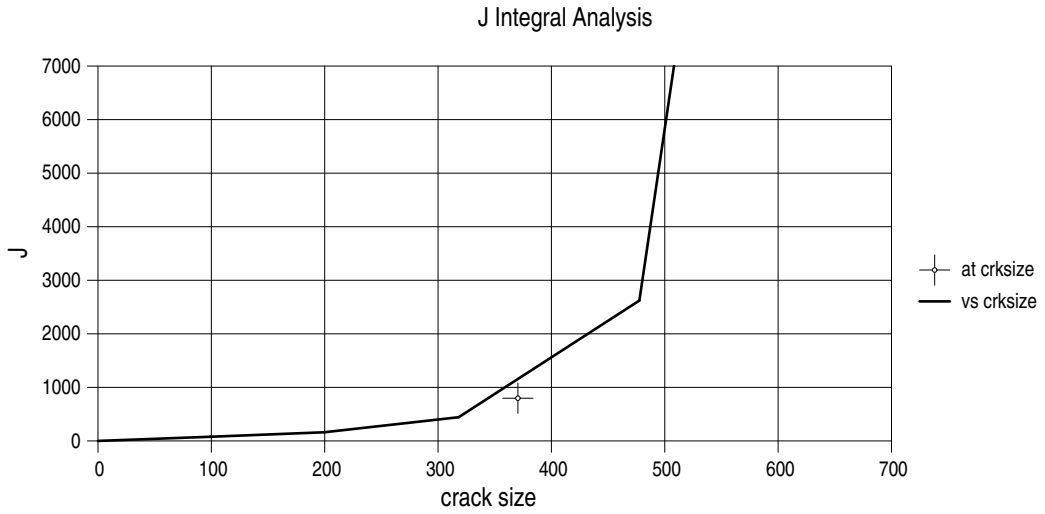

crack size : one half the crack length

Figure D 2-5: J-integral analysis for bending

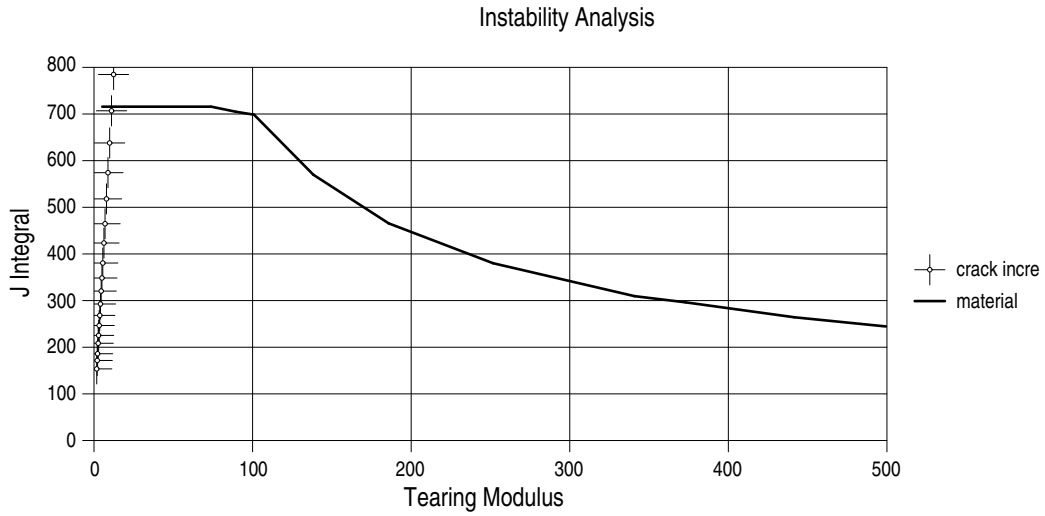

Figure D 2-6: Instability analysis for bending

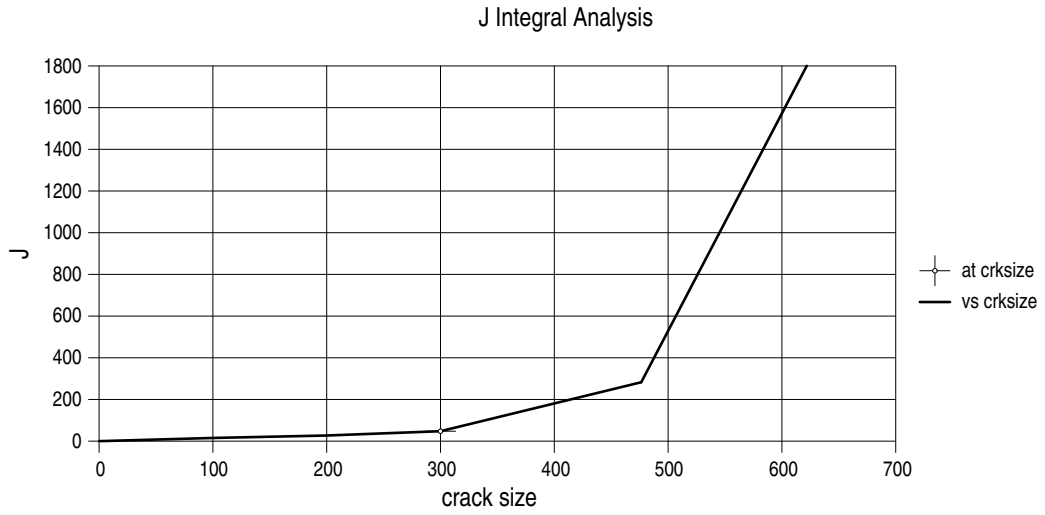

Figure D 2-7: J-integral analysis for internal pressure

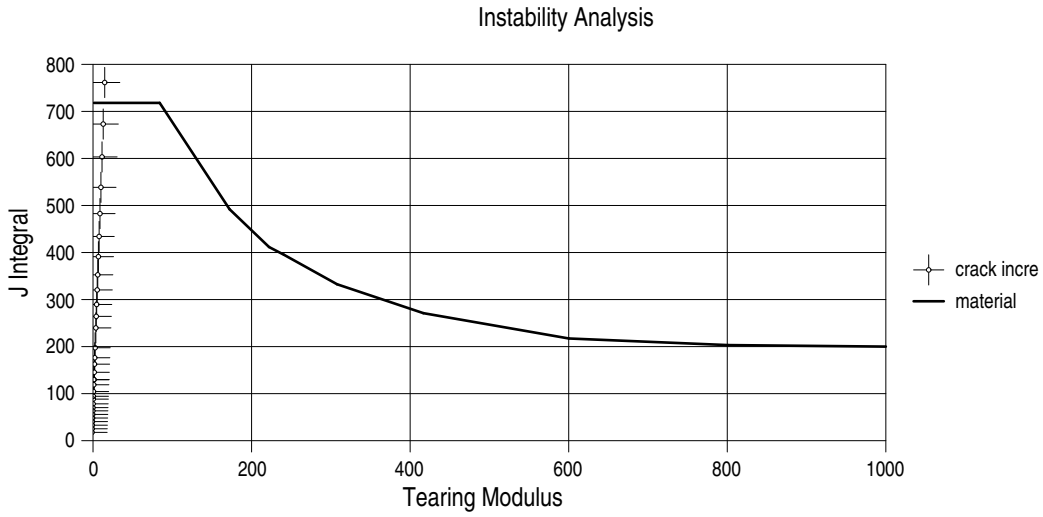

Figure D 2-8: Instability analysis for internal pressure

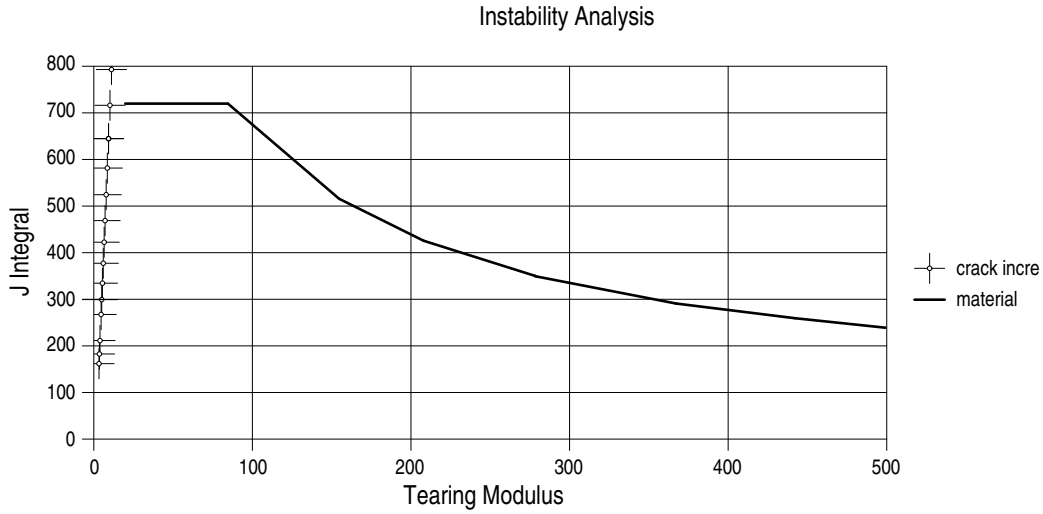

Figure D 2-9: Instability analysis for bending + internal pressure

D 2.4.4.3 Finite element analysis

(1) The analysis is made using an FE model analogously to clause D 1.4.4.3.

(2) The stresses occurring (acc. to von Mises) are shown in **Figure D 2-10**.

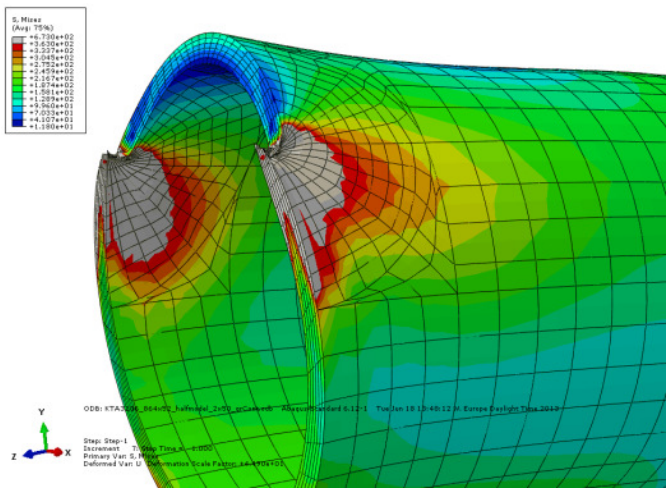

Figure D 2-10: Distribution of stresses

(3) The J-integral has been evaluated under the same loading for several crack angles along the crack front (average values over the wall thickness) (see **Figure D 2-11**). The results are shown in **Table D 2-1**.

Crack angle in degrees	Flaw length [1] in mm	J-Integral in N/mm
80	566.9	364
90	637.7	480
100	708.6	652
120	850.3	1309
[1] Flaw length based on : mean radius		

Table D 2-1: J-Integral depending on crack angle

(4) For the calculation of the critical crack size a maximum stable crack growth in the structure of Δc_{max} = 3.2 mm in crack length orientation is considered.

This leads to the following critical through-thickness crack length:

$2c_{krit}$ = 713 mm (based on mean radius)

Angle = 100.6°.

Note:

Due to the limitation of the J-R curve to Δc_{max} in the structure in crack length orientation no instability is yet obtained at $2c_{krit}$.

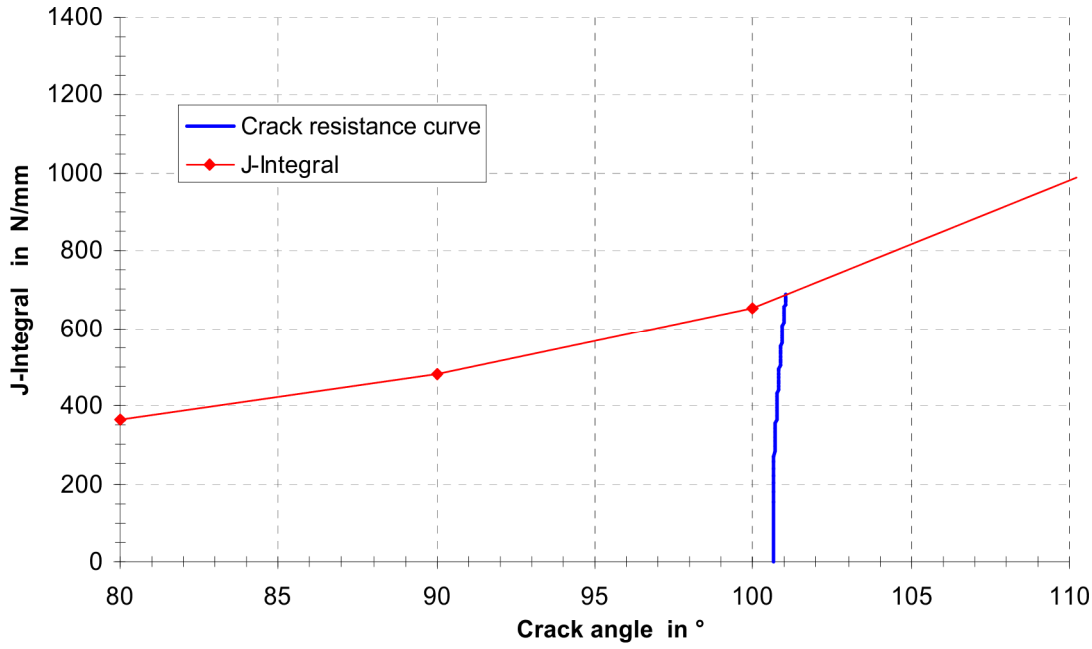

Figure D 2-11: Progression of J-integral and J-R curve

D 2.4.5 Two-criteria method

(1) The calculation in this example are made to [32] for point A acc. to **Figure D 1-12** with and without consideration of welding residual stresses.

Note:
The calculation for point A leads to higher crack loadings compared to point B and thus is conservative for this example.

(2) The determination of secondary stresses to Table R5 in connection with Table R1 in [32] results in a non-linear course across the wall thickness, see **Figure D 2-12**:

$$\sigma^S = 0.4246 \cdot R_{p0,2T} \cdot [1 + 3.8116\,(x \cdot s^{-1}) - 99.82 \cdot (x \cdot s^{-1})^2 + 339.97\,(x \cdot s^{-1})^3 - 404.59 \cdot (x \cdot s^{-1})^4 + 158.16 \cdot (x \cdot s^{-1})^5] \quad \text{(D 2.4-7)}$$

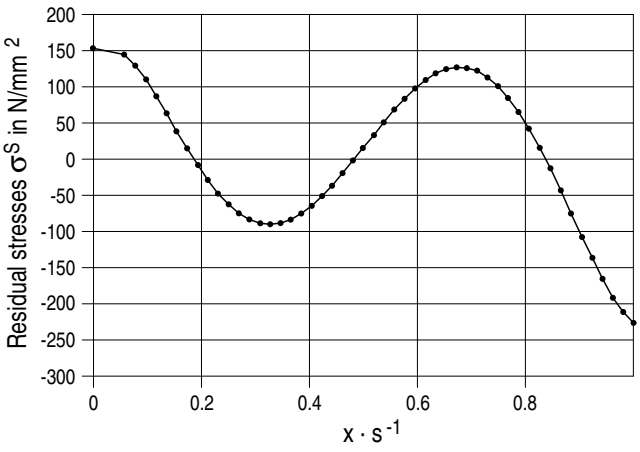

Figure D 2-12: Course of residual stresses across the wall thickness

(3) The critical through-thickness crack length $2c_{krit}$ and the critical crack depth a_{krit} of the surface crack shall be determined using the J-R curves of **Figure D 2-1**.

(4) The "Failure Assessment Curve" (FAC) is calculated acc. to the following relationship:

$$K_r \le f_{R6} = (1 - 0.14 \cdot L_r^2) \cdot [0.3 + 0{,}7\exp(-0.65 \cdot L_r^6)] \quad \text{(D 2.4-8)}$$

$$L_r \le L_r^{max} = \frac{\sigma_f}{R_{p0.2}} \quad \text{for materials without Lüders plateau} \quad \text{(D 2.4-9)}$$

Note:
The material 20MnMoNi5-5 does not show a Lüders plateau at the temperature used in the assessment.

$$\sigma_f = 2.4 \cdot S_m \quad \text{(D 2.4-10)}$$

(5) K_r is calculated for point A using the tabulated shape functions for K_I to Appendix K3.5.

(6) The calculation of L_r does not depend on the considered evaluation point and is performed according to Appendix L3.5.

(7) Determination of the critical crack depth a_{krit}

$a_{krit} > 0.75 \cdot s = 39$ mm, see **Figure D 2-13**.

$a_{zul} = 0.75 \cdot s = 39$ mm.

Note:
Since (a, 2c) = (0.75 · s, $2c_e$) is outside the range of application of the K solutions, a conservative calculation with a/2c = 1/6 = constant was made.

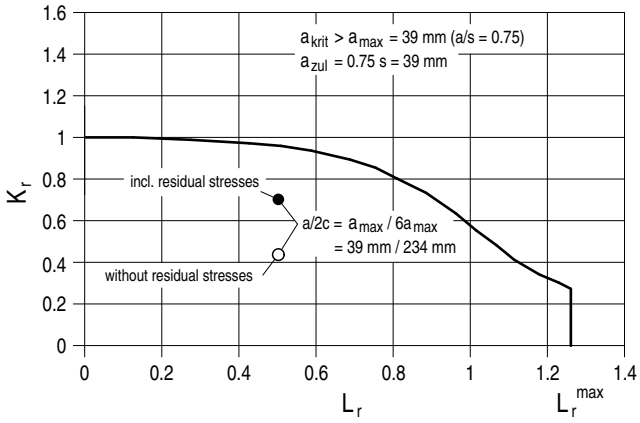

Figure D 2-13: Determination of allowable crack depth

(8) Determination of the critical through-thickness crack length $2c_{krit}$

Note:

Due to the limitation of the J-R curve to Δa_{max} no instability is yet obtained at $2c_{krit}$.

a) The critical through-thickness crack length without consideration of residual stresses results in $2c_{krit}$ = 627 mm, see **Figure D 2-14**.

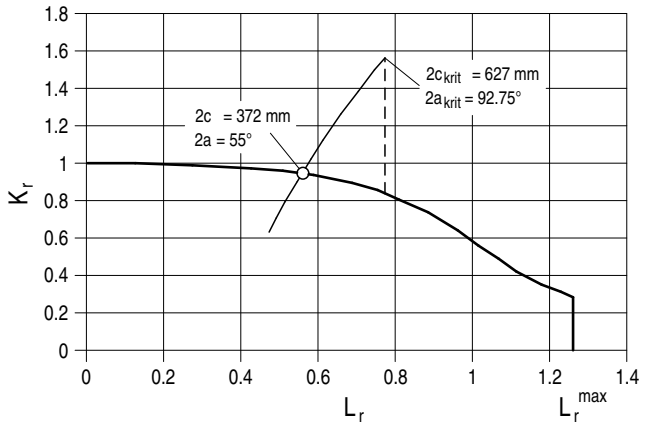

Figure D 2-14: Determination of critical crack length without consideration of residual stresses

b) The critical through-thickness crack length with consideration of residual stresses results in $2c_{krit}$ = 607 mm, see **Figure D 2-15.**

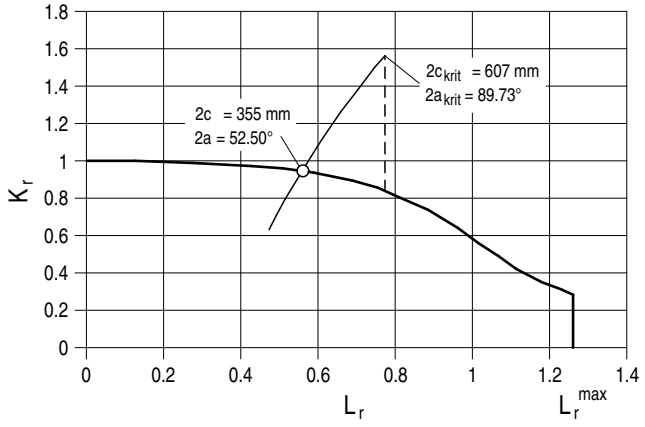

Figure D 2-15: Determination of critical crack length with consideration of residual stresses

D 2.5 Step 5 to Figure A-3: calculation of the detectable through-thickness crack length $2c_{LÜS}$

(1) Input values from D 2.1 and the following additional data:

a) crack surface roughness: R_Z = 10.0 µm

b) flow inlet loss: ζ_{Ein} = 0.5

c) flow outlet loss: ζ_{Aus} = 0.0

d) flow channel length: s = 57 mm (= wall thickness incl. 5 mm cladding)

e) fluid density: ρ_S = 669.7 kg/m^3 (saturation value to [74])

f) saturation pressure: p_0 = 11.13 MPa (at T_0 = 319 °C to [74])

g) detectable leak rate: $\dot{m}_{LÜS}$ = 200 kg/h

(2) Leakage area calculation depending on crack length 2c

The leakage area depending on the crack length 2c is shown in **Figure D 2-16**.

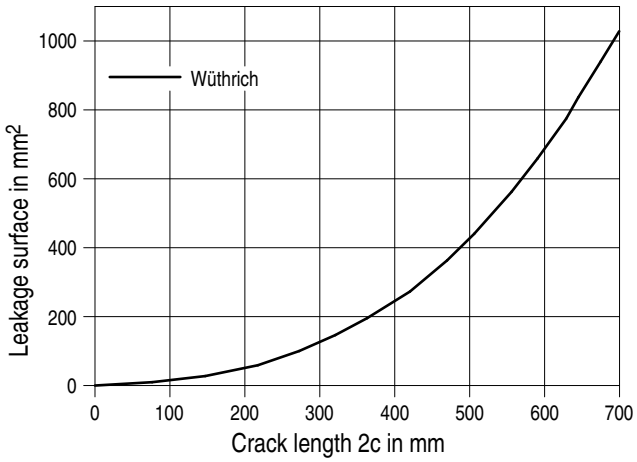

Figure D 2-16: Leakage area depending on crack length 2c for the considered ferriitic piping with circumferential crack

For the purpose of clarity only the individual results for the critical through-thickness crack length $2c_{krit}$ = 695.6 mm determined by the FSC/KWU method are given hereafter by means of formulas as example.

a) $\sigma = \sigma_p + \sigma_{Mb}$ = 136.0 N/mm^2

Note:
The consideration of the bending stress as membrane stress in the present example within the calculation procedure as per [55] is justified (see [65]).

b) $E' = E/(1-\nu^2)$ = 211.0 kN/mm^2

c) Leakage area for infinitely large plate:
A_0 = 489.9 mm^2 as per equation B 3.1-1

d) shell parameter:
λ = 4.2 as per equation B 3.1-5

e) buckling factor for circumferential crack:
$\alpha(\lambda)$ = 1.74 as per equation B 3.1-4

f) stress ratio:
$s = \sigma/\sigma_f$ = 136.0/[0.5 · (363+513)] = 0.31

g) plasticity correction factor:
$\gamma(s)$ = 1.07 as per equation B 3.1-7

h) leakage area for circumferential crack:
$A = \alpha(\lambda) \cdot \gamma(s) \cdot A_0$ = 916 mm^2 as per equation B 3.1-2.

(3) Leak rate calculation depending on crack length 2c

a) It is assumed that the leakage area can be modelled by a rhombus, therefore, the leakage area circumference is:
$U = \{4 \cdot A^2/c^2 + 16 \cdot c^2\}^{0.5}$ = 1390 mm

b) Hydraulic diameter:
$D_h = 4 \cdot A/U$ = 2.63 mm as per equation B 3.2-3

c) Acc. to clause B 3.2.2.5 the following applies:
$D_h/(2 \cdot R_z)$ = 131.7,
thus the resistance factor results in
λ = 0.095 as per equation B 3.2-13

d) Flow resistance:
$\zeta = \zeta_{Ein} + \lambda \cdot s/D_h + \zeta_{Aus}$ = 2.55 as per equation B 3.2-2

e) Mass flow density:

$$G = \sqrt{\frac{2 \cdot [p_0 - p_S(T_0)] \cdot \rho_S(T_0)}{1 + \zeta}} = 0.042 \text{ kg} \cdot \text{s}^{-1} \cdot \text{mm}^{-2}$$

as per equation B 3.2-1

f) Leak rate:

$\dot{m}_{LÜS} = G \cdot A = 38.43 \text{ kg/s} \geq 200 \text{ kg/h}$

At a crack length $2c_{LÜS}$ = 83 mm the leak rate of 200 kg/h detectable by the leakage monitoring system is already attained, see **Figure D 2-17**:

D 2.6 Step 6 to Figure A-3: Evaluation whether integrity is proved

In D 2.3 the possible crack growth as well as possible crack lengths and crack depths have been determined. In D 2.4 the critical crack length has been determined. The following evaluation shows that integrity has been proved:

a) flaw length: $2c_e = 31.25 \text{ mm} < 2c_{krit} = 695 \text{ mm}$

b) flaw depth: $a_e = 5.42 \text{ mm} < 0.75 \cdot s = 39 \text{ mm}$

Note:
a_{krit} has not been calculated here and will be greater than 0.75 · s acc. to the calculation in sub-clause D 2.4.5 (7).

D 2.7 Step 7 to Figure A-3: Evaluation whether leak-before-break is proved

In D 2.4 the critical crack length $2c_{krit}$ has been calculated. In D 2.5 the detectable crack length $2c_{LÜS}$ has been determined. The evaluation hereafter shows that leak-before-break behaviour has been proved:

$$2c_{LÜS} = 83 \text{ mm} < 2c_{krit} = 695 \text{ mm}$$

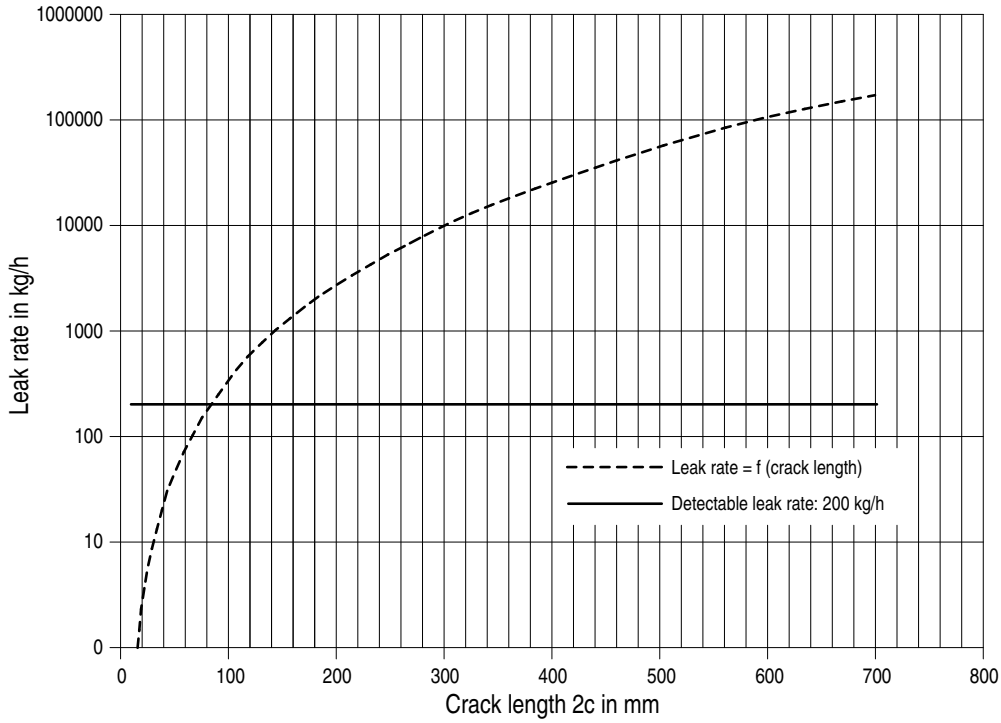

Figure D 2-17: Leak rate for the considered ferritic piping with circumferential crack

Annex E

Regulations and literature referred to in this safety standard

(The references exclusively refer to the version given in this annex. Quotations of regulations referred to therein refer to the version available when the individual reference below was established or issued.)

Atomic Energy Act (AtG)		Act on the Peaceful Utilization of Atomic Energy and the Protection against its Hazards (Atomic Energy Act) of December 23, 1959 (BGbl. I, p. 814) as Amended and Promulgated on July 15, 1985 (BGBl. I, p. 1565), last Amendment by article 5 of the Law dated 28th August 2013 (BGBl. I p. 3313)
StrlSchV		Ordinance on the Protection against Damage and Injuries Caused by Ionizing Radiation (Radiation Protection Ordinance) dated 20th July 2001 (BGBl. I p. 1714; 2002 I p. 1459), at last amended by article 5 para. 7 of the Law dated 24th February 2012 (BGBl. I p. 212)
SiAnf		Safety Requirements for Nuclear Power Plants (SiAnf) of November 22, 2012 (BAnz. of January 24th, 2013)
Interpretations on the SiAnf		Interpretations on the Safety Requirements for Nuclear Power Plants of November 29th 2013 (BAnz. of December 10th, 2013)
KTA 1401	(2013-11)	General Requirements Regarding Quality Assurance
KTA 1403	(2010-11)	Ageing Management in Nuclear Power Plants
KTA 3201.1	(1998-06)	Components of the Reactor Coolant Pressure Boundary of Light Water Reactors; Part 1: Materials and Product Forms
KTA 3201.2	(2013-11)	Components of the Reactor Coolant Pressure Boundary of Light Water Reactors; Part 2: Design and Analysis
KTA 3201.3	(2007-11)	Components of the Reactor Coolant Pressure Boundary of Light Water Reactors; Part 3: Manufacture
KTA 3201.4	(2010-11)	Components of the Reactor Coolant Pressure Boundary of Light Water Reactors; Part 4: Inservice Inspections and Operational Monitoring
KTA 3203	(2001-06)	Surveillance of the Irradiation Behaviour of Reactor Pressure Vessel Materials of LWR Facilities
KTA 3211.1	(2000-06)	Pressure and Activity Retaining Components of Systems Outside the Primary Circuit; Part 1: Materials
KTA 3211.2	(2013-11)	Pressure and Activity Retaining Components of Systems Outside the Primary Circuit; Part 2: Design and Analysis
KTA 3211.3	(2012-11)	Pressure and Activity Retaining Components of Systems Outside the Primary Circuit; Part 3: Manufacture
KTA 3211.4	(2013-11)	Pressure and Activity Retaining Components of Systems Outside the Primary Circuit; Part 4: Inservice Inspections and Operational Monitoring
DIN EN ISO 6892-1	(2009-12)	Metallic materials - Tensile testing - Part 1: Method of test at room temperature (ISO 6892-1:2009); German version EN ISO 6892-1:2009
DIN EN ISO 6892-2	(2011-05)	Metallic materials - Tensile testing - Part 2: Method of test at elevated temperature (ISO 6892-2:2011); German version EN ISO 6892-2:2011
ISO 12135	(2002-12)	Metallic materials - Unified method of test for the determination of quasistatic fracture toughness (Technical Corrigendum 2008-06)
ASME BPVC Section XI		ASME Boiler & Pressure Vessel Code, Section XI, Rules for the Inspection of Nuclear Power Plant Components, The American Society of Mechanical Engineers, New York, 2010
NUREG/CR-6176		W.J. Shack, T.F. Kassner, Review of Environmental Effects of Fatigue Crack Growth of Austenitic Stainless Steels, NUREG/CR-6176, May 1994
US NRC Reg.-Guide 1.161		Evaluation of Reactor Pressure Vessels with Charpy Upper-Shelf Energy Less Than 50 Ft-Lb, U.S. Nuclear Regulatory Commission, June 1995
ASTM-E 1820-11	(2011)	Standard Test Method for Measurement of Fracture Toughness

Literature

[1] Uhlmann, D., Herter K.-H.: „Erstellung eines Nachweisverfahrens für die Bewertung der Integrität von druckführenden Rohrleitungen“. MPA/VGB-Vorhaben 5.6, VGB Kennzeichen 05/98, Abschlußbericht 944 705 601, MPA Stuttgart, Dezember 1998
(Uhlmann. D.; Herter, K.-H.: Establishment of a verification procedure for assessing the integrity of pressure piping”, MPA-VGB project 5.6, VGB number 05/98, Final Report 944 705 601, MPA Stuttgart, December 1988)

[2] Blasset, S., Keim E., Tiete R.: „German Engineering Methods for Critical Crack Size Assessment in Ductile Regime based on Envelop Flow Stress“, 2010 ASME Pressure Vessel and Piping Division Conference, July 18-20, 2010, Bellevue, Washington, Proceedings of PVP 2010, PVP2010-25973.

[3] MPA/VGB - Forschungsvorhaben 3.2: "Untersuchungen zur Integritätsbewertung von Mischnähten in Rohrleitungen“, Abschlussbericht, SA AT 13/00, Materialprüfungsanstalt (MPA) Universität Stuttgart, Dezember 2007
(MPA/VGB – Research Project 3.2: “Investigations for the integrity assessment of dissimilar welds in piping”, Final Report, SA AT 13/00, Materialprüfungsanstalt (MPA) University of Stuttgart, December 2007)

[4] Folias, E.S.: „An axial crack in a pressurized cylindrical shell“, Int. Journ. of Fracture Mechanics, Vol. 1 (1965), pp. 104/113

[5] Hahn, G. T., M. Sarrata, A. R. Rosenfield: "Criteria for crack extension in cylindrical pressure vessels". Int. Journ. of Fracture Mechanics, Vol. 5 (1969), pp. 187/210

[6] Folias, E.S.: "On the theory of fracture of curved sheets". Engineering Fracture Mechanics, Vol. 2 (1970), pp. 151/164

[7] Kiefner, J. K., W. A. Maxey, R. J. Eiber, A. R. Duffy: "Failure stress levels of flaws in pressurized cylinders". ASTM STP 536 (1973), pp. 461/481

[8] Eiber, R. J., W. A. Maxey, A. R. Duffy, T. J. Atterburry: "Investigation of the initiation and extend of ductile pipe rupture". Battelle Memorial Institute, BMI 1866 (1969)

[9] Maxey, W. A.: "Fracture initiation, propagation and arrest". 5th Symposium on Line Pipe Research, 1974

[10] BMU Forschungsvorhaben SR 471: „Versagensanalyse von längsfehlerbehafteten Rohren und Behältern“, 22. Technischer Bericht, MPA Stuttgart, 01/1992
(BMU Research Project SR 471: “Failure analysis of piping and vessels with longitudinal defects”, 22nd Technical Report, MPA Stuttgart, 01/1992)

[11] Kanninen, M.F. et al.: "Mechanical fracture predictions for sensitized stainless steel piping with circumferential cracks". EPRI NP-192, September 1976

[12] Kanninen, M.F. et al.: "Instability predictions for circumferentially cracked type 304 stainless steel pipes under dynamic loading". EPRI Project T118-2, EPRI NP-2347, Vol. 1 and 2, April 1982

[13] Kastner, W. E., E. Röhrich, W. Schmitt, R. Steinbuch: „Critical crack sizes in ductile piping“. Int. Journal Pressure Vessel and Piping 9 (1981), pp. 197/219

[14] Bartholomé, G., W. Kastner, E. Keim: „Experimental and theoretical investigation on the behaviour of circumferential cracks in piping“. ASME PVP-Vol. 95/II (1984), pp. 189/197

[15] Kastner, W., E. Röhrich, W. Schmitt, R. Steinbuch: „Critical crack sizes in ductile piping“. Int. Journal Pressure Vessel and Piping 9 (1984), pp. 189/197

[16] Roos E., K.-H. Herter, G. Bartholomé, G. Senski: „Assessment of Large Scale Pipe Tests by Fracture Mechanics Approximation Procedures with regard to Leak-Before-Break“. Nuclear Engineering and Design 112 (1989), pp. 183/195

[17] Rice, J. R., „A Path Independent Integral and the Approximation Analysis of Strain Concentration by Notches and Cracks“, in J. Appl. Mech., Vol. 35, pp. 379-386, 1968

[18] Parks, D. M, „A stiffness derivative finite element technique for determination crack tip stress intensity factors“, Int. Journ. Of Fracture, 10, No. 4, 1974, 487-502

[19] pc-CRACK for Windows, Structural Integrity Associates, Inc., SIR-98-073, Rev. 0

[20] Paris, P.C., et al., „The Theory of Instability of the Tearing Mode of Elastic-Plastic Crack Growth“, Elastic-Plastic Fracture, ASTM STP 668, J.D. Landes, J.A. Begley, and G.A. Clarke, Eds., American Society for Testing and Materials, 1979

[21] Paris, P. C., et al., „A Method of Application of Elastic-Plastic Fracture Mechanics to Nuclear Vessel Analysis“, Elastic-Plastic Fracture: Second Symposium Volume II – Fracture Resistance Curves and Engineering Applications, ASTM STP 803, C. F. Shih and J. P. Gudas, Eds., American Society for Testing and Materials, 1983

[22] Kumar, V., et al., „An Engineering Approach for Elastic-Plastic Fracture Analysis“, EPRI Report NP-1931, Project 1237-1, Electric Power Research Institute, July 1981

[23] Zahoor A., „Ductile fracture handbook - Volume 3 - Chapter 8 - finite length, axial part-through wall flaw“ NP-6301-D, october 1990

[24] Zahoor A., „Ductile fracture handbook - Volume 2 - Chapter 6 - axial through wall crack“ NP-6301-D, october 1990

[25] Kumar, V., et al., „Advances in Elastic-Plastic Fracture Analysis“, EPRI Report NP-3607, Project 1237-1, Final Report, Electric Power Research Institute, July 1984

[26] Kumar, V., et al., „Estimation Technique for the Prediction of Elastic-Plastic Fracture of Structural Components of Nuclear Systems“, GE Report SRD-82-048, Combined Fifth and Sixth Semiannual Report, EPRI Contract RP 1237-1

[27] Shih, C. F., et al., „Fully Plastic Crack Problem: Part 1: Solution by a Penalty Method“, ASME Journal of Applied Mechanics, Vol. 51, 1984, pp. 48-56.

[28] Ainsworth R. et al., „Flaw analysis in the French RSE-M and RCC-MR code appendices” International Journal of Pressure Vessels and Piping 84 (2007) 590–696

[29] Kumar, V., and German, M.D., 1988, „Elastic-plastic fracture analysis of through-wall and surface flaws in cylinders: Final report”, EPRI/NP-5596

[30] R6: Assessment of the Integrity of Structures containing Defects, British Energy Generation Ltd (BEGL) Gloucester, U.K., Revision 4, 2010

[31] SINTAP: Structural Integrity Assessment Procedure, Final Revision, EU-Project BE 95-1462, Brite Euram Programme, Brüssel, 1999

[32] SSM: A Combined Deterministic and Probabilistic Procedure for Safety Assessment of Components with Cracks – Handbook RSE R&D Report No. 2008:01. Det Norske Veritas (DNV), 2008

[33] BS 7910:2013-12-31: Guide to methods for assessing the acceptability of flaws in metallic structures

[34] API 579: Recommended Practice for Fitness for Service, American Petroleum Institute (API), Washington, 2007

[35] Berger, C., Blauel, J.G., Hodulak, L., Pyttel, B., Varfolomeyev, I., Bruchmechanischer Festigkeitsnachweis für Maschinenbauteile, FKM Richtlinie, VDMA-Verlag, 3. überarbeitete Ausgabe, Stand 2009
(Berger, C., Blauel, J.G., Hodulak, L., Pyttel, B., Varfolomeyev, I., Fracture-mechanics strength verification for machine parts, FKM Guideline, VDMA-Verlag, 3rd revised edition, 2009)

[36] Ainsworth, R.A., The assessment of defects in structures of strain hardening material, Eng. Fract. Mech. 19, 633-642, 1984

[37] A. Needleman und V. Tvergaard, „An analysis of ductile rupture in notched bars“, J.Mech.Phys. Solids 32, 461-490, 1984

[38] A. L. Gurson, „Continuum theory of ductile rupture by void nucleation and growth: Part 1 – yield criteria and flow rules for porous ductile materials“, J. Engn. Mat. Tech. 99, 2-15 (1977)

[39] Rousselier, G., „Ductile fracture models and their potential in local approach of fracture“, Nuclear Engineering and Design, 105, 97-111 (1987).

[40] Abaqus Analysis User's Manual, Beschreibung des porösen Materialverhaltens (Formelwerk), “Porous metal plasticity,” Section 4.3.6 of the Abaqus Theory Manual
(Description of porous material behaviour (collection of formulae)

[41] Tvergaard, V., A. Needleman: Analysis of the Cup-Cone Fracture in a Round Tensile Bar, Acta Metallurgica, Vol. 32 (1984), 157-169

[42] Aifantis, C.: On the role of gradients in the localization of deformation and frac-ture, International Journal of Engineering Sience, Vol. 30 (1992), 1279-1299

[43] Bazant, P., T. Belytschko, T. P. Chang: Continuum Theory for Strain-Softening, Journal of Engineering Mechanics, Vol. 110 (1984), 1666-1692

[44] Leblond, J. B., G. Perrin, J. Deveaux: Bification Effects in Ductile Metals With Nonlocal Damage, Journal of Applied Mechanics, Vol.61 (1994), 236-242

[45] Seidenfuß, M., M. K. Samal, E. Roos: On critical assessment of the use of local and nonlocal damage models for prediction of ductile crack growth and crack path in various loading and boundary condition, Intern. Journal of Solids and Structures 48 (2011), p. 3365-3381

[46] Forman R. G., Kearney V. E., Engle R. M., Numerical analysis of crack propagation in cyclic loaded structures, J. Basic Engineering, Trans ASME 89, 1967

[47] Paris P. C., Erdogan F., A critical analysis of crack propagation laws, J. Basic Engineering, 85, 528-534, 1960

[48] ASME Boiler & Pressure Vessel Code Section XI Appendix C Article C-3000, Edition 2010

[49] ASME Boiler & Pressure Vessel Code Section XI Appendix A Article A-4000, Edition 2010

[50] ASME Boiler & Pressure Vessel Code Section XI Appendix C Article C-8000, Edition 2010

[51] W.J. Shack, T.F. Kassner, Review of Environmental Effects of Fatigue Crack Growth of Austenitic Stainless Steels, NUREG/CR-6176, May 1994

[52] W.J. Shack, Fatigue Crack Growth in SS, corrected pages for NUREG/CR-6176; Argonne National Laboratory, Telecopy Number 7-0-11-49-89-579-12070 send to: D. Beukelmann TÜV Bayern Sachsen, 5/11/95

[53] Itatani, et al., Fatigue Crack Growth Curve for Austenitic Stainless Steels in BWR Environment, Transactions of the ASME 166 / Vol. 123, May 2001

[54] D. Munz (Ed.), Leck-vor-Bruch-Verhalten druckbeaufschlagter Komponenten; Fortschr. Ber. VDI-Z. Reihe 18, Nr.14, VDI-Verlag, Düsseldorf (1984)
(D. Munz (Ed.), Leak-before-break behaviour of pressurized components; Fortschr. Ber. VDI-Z. Reihe 18, Nr.14, VDI-Verlag, Düsseldorf (1984))

[55] C. Wüthrich: Crack opening areas in pressure vessels and pipes; Eng. Fract. Mech. 18, Issue 5, 1049–1057 (1983)

[56] Round Robin Activities on the Calculation of Crack Opening Behaviour and Leak Rates for Small Bore Piping Components, NEA/CSNI/R(95)4

[57] Reimann, J., Vergleich von kritischen Massenstrom-Modellen im Hinblick auf die Strömung durch Lecks, in: Leck-vor-Bruch-Verhalten druckbeaufschlagter Komponenten (Hrsg. D. Munz), Fortschr.-Ber. VDI-Z. Reihe 18, Nr. 14, 1984, 63-95
(Reimann, J.: "Comparison of critical mass flow density models with regard to the flow through leaks", in: Leak-before-break behaviour of pressurized components, (edited by E. Munz), Fortschr.-Ber. VDI-Z. Reihe 18, Nr. 14, 1984, 63-95)

[58] Pana, P., Müller, M., Subcooled and two-phase critical flow states and comparison with data, Nucl. Engng. and Design 45, 1978, 117-125

[59] Moody, F.J., Maximum flow rate of a single component, two-phase mixture, J. of Heat Transfer 87, 1965, 134-142

[60] Fauske, H., Contribution to the theory of two-phase, one-component critical flow, report ANL-6633, 1962

[61] Henry, R.E., The two-phase critical discharge of initially saturated or subcooled liquid, Nucl. Sci. & Engng. 41, 1970, 336-342

[62] Estorf, M., Leckratenberechnung, Beitrag Vattenfall, Anlage 1 zur Niederschrift über die 16. Sitzung des Arbeitsgremiums KTA 3206 am 18.11.2011
(Estorf, M.: "Leak flow rate calculations", contributed by Vattenfall, Annex 1 to the minutes of the 16th meeting of KTA 3206 working group on 18th November 2011)

[63] ATHLET Models and Methods, Mod. 2.2 Cycle A, GRS-P-1/Vol. 3 Rev. 2, 2009

[64] Keim, E., Rippel, R., Bestimmung von Leckflächen, Rißöffnungen und Leckraten, KWU E121/91/058, 1991
(Keim, E., Rippel, R., Determination of leakage areas, crack openings and leak flow rates", KWU E121/91/058, 1991)

[65] Grebner, H., Heckmann K., Sievers, J., Berechnung von Leckflächen und Leckraten mit vereinfachten Methoden, Technischer Zwischenbericht der GRS zum Vorhaben 3613R01332, GRS-A-3720, Juni 2014
(Grebner, H., Heckmann K., Sievers, J., Calculation of leakage areas and leak flow rates by simplified methods", Technical Intermediate Report of GRS relating to the Project 3613R01332, GRS-A-3720, June 2014)

[66] Untersuchungen im Zusammenhang mit der Versuchsgruppe E22 an einem im Labor erzeugten Ermüdungsriss zur Ermittlung von Rissform und Topografie der Rissfläche. Werkstoff: X 10 CrNiMoTi 18 9. Prüfungsbericht der MPA Stuttgart, PHDR Bericht Nr. 20.030/90, 1990
(Investigations in connection with the test group E22 on a laboratory-generated fatigue crack to determine crack shape and topography of crack area: material X 10 CrNiMoTi 18 9, Test report of MPA Stuttgart, PHDR Report No. 20.020/90, 1990)

[67] Bartholomé, G., Kastner W., Keim E., Design and calibration of leak detection systems by thermal hydraulics and fracture mechanics analyses, Nuclear Engineering and Design 142 (1993) 1-13

[68] Bridgman, P. W.: Studies in Large Plastic Flow and Fracture. McGraw-Hill Book Company Inc., 1952

[69] Roos, E., U. Eisele, X. Schuler, H. Silcher: Design and Material Selection for Plants under Consideration of Fracture Mechanics Aspects. 35th MPA-Seminar, 9th October 2009

[70] BMWi Forschungsvorhaben 1501302: Anwendbarkeit technischer Ersatzkennwerte für duktile Rissinitiierung in Abhängigkeit von der Mehrachsigkeit des Spannungszustandes. Abschlussbericht, MPA Universität Stuttgart und IEHK RWTH Aachen, März 2009
(BMWi Research Project 1501302: Applicability of technical characteristic values for ductile crack initiation in dependence of multi-axial stress state, Final Report MPA University of Stuttgart and IEHK RWTH Aachen, March 2009)

[71] X. Schuler, D. Blind, U. Eisele, K.-H. Herter: Extension of fracture mechanics evaluation methods by consideration of multiaxiality of stress state for piping components. Nuclear Engineering and Design 158 (1995) 227-240

[72] MPA/VGB Forschungsvorhaben 6.1: Bauteilversuche Austenit mit Analytik. VGB Nr. 11/93, Abschlussbericht, 07/1997
(MPA/VGP Research Project 6.2: Component tests on austenitic materials with analysis, VGB No. 11/93, Final Report, 07/1997)

[73] ASME Boiler & Pressure Vessel Code Section XI, Appendix A, Article A-3000, Edition 2010

[74] Wagner W., Kretzschmar H.-J.: International Steam Tables; Properties of Water and Steam Based on the Industrial Formulation IAPWS-IF97; Second Edition, Springer-Verlag Berlin Heidelberg 2008